UNIVERSIDADE FEDERAL DE UBERLÂNDIA
INSTITUTO DE GENÉTICA E BIOQUÍMICA
PÓS-GRADUAÇÃO EM GENÉTICA E BIOQUÍMICA

Instabilidadde cromossômica e alterações na expressão da telomerase durante a carcinogênese

Robson José de Oliveira Júnior

Orientador: Professora Doutora Sandra Morelli

Co-Orientador: Professor Doutor Luiz Ricardo Goulart Filho

UBERLÂNDIA - MG
2012

UNIVERSIDADE FEDERAL DE UBERLÂNDIA
INSTITUTO DE GENÉTICA E BIOQUÍMICA
PÓS-GRADUAÇÃO EM GENÉTICA E BIOQUÍMICA

Instabilidadde cromossômica e alterações na expressão da telomerase durante a carcinogênese

Aluno: Robson José de Oliveira Júnior

Orientador: Professora Doutora Sandra Morelli

Co-Orientador: Professor Doutor Luiz Ricardo Goulart Filho

Tese apresentada à Universidade Federal de Uberlândia como parte dos requisitos para obtenção do Título de Doutor em Genética e Bioquímica (Área Genética)

UBERLÂNDIA - MG
2012

Dados Internacionais de Catalogação na Publicação (CIP)

Sistema de Bibliotecas da UFU, MG, Brasil.

O48i 2012 Oliveira Júnior, Robson José de, 1984-
Instabilidadde cromossômica e alterações na expressão da telomerase durante a carcinogênese/Robson José de Oliveira Júnior. -- 2012.
149 f. : il.

Orientadora: Sandra Morelli.
Coorientador: Luiz Ricardo Goulart Filho.
Tese (doutorado) - Universidade Federal de Uberlândia, Programa de Pós-Graduação em Genética e Bioquímica.
Inclui bibliografia.
Em inglês.

1. Genética - Teses. 2. Citogenética -Teses. 3. Carcinogênse -
Teses. 4. Câncer - Teses. 5. Peptídeos - Teses. I Morelli, Sandra.
II. Goulart Filho, Luiz Ricardo, 1962- . III. Universidade Federal
de Uberlândia. Programa de Pós-Graduação em Genética e Bioquímica. IV. Título.

CDU: 575

UNIVERSIDADE FEDERAL DE UBERLÂNDIA
INSTITUTO DE GENÉTICA E BIOQUÍMICA
PÓS-GRADUAÇÃO EM GENÉTICA E BIOQUÍMICA

Instabilidadde cromossômica e alterações na expressão da telomerase durante a carcinogênese

ALUNO: Robson José de Oliveira Júnior

COMISSÃO EXAMINADORA

Presidente: **Prof. Dra. Sandra Morelli** (Orientador)

Examinadores: **Prof. Dra. Ana Maria Bonetti - UFU**
Prof. Dra. Eloisa Amália Vieira Ferro – UFU
Prof. Dra. Mirian Machado Mendes – UFG
Prof. Dra. Elisângela de Paula Silveira Lacerda - UFG

Data da Defesa: 14 /11/2012

As sugestões da Comissão Examinadora e as Normas PGGB para o formato da Dissertação/Tese foram contempladas

_____
(Sandra Morelli)

Viver!
E não ter a vergonha
De ser feliz
Cantar e cantar e cantar
A beleza de ser
Um eterno aprendiz...!
(Gonzaguinha)

Dedicatória

Dedico essa tese aos meus pais, à minha irmã e a...:
Um anjo muito mais doce,
Muito mais meigo, muito mais puro e
Muito mais guerreiro, pois teve que lutar pela vida muito mais cedo.
Pouco tempo tivemos para desfrutar da alegria,
das gracinhas,
dos beijinhos e da “linguinha” que tão cedo aprendeu a mostrar.
Mas quem teve a chance de conhecer esse homenzinho,
Sabe que ele NUNCA será esquecido.
Obrigado João Pedro (Plin...) !!!

Agradecimentos

Agradeço primeiramente a Deus por estar sempre presente ao meu lado, guiando meus passos e abrindo meus caminhos. Obrigado senhor por nunca me desamparar.

Agradeço a meus pais Robson José de Oliveira e Rosemere Mendes de Oliveira por nunca terem medido esforços para que eu chegasse até aqui e por acreditar em mim e sempre me estimularem na conquista de meus ideais.

Agradeço à minha grande irmã e companheira, Danyele Mendes de Oliveira, por todo o apoio e carinho. Muito obrigado por ter nos dado o presente mais precioso que existe neste mundo.

Agradeço ao meu amado afilhado João Pedro Mendes Abalém por ter vindo a esse mundo e ter me ensinado tanto em tão pouco tempo.

Agradeço à minha grande tutora, professora, orientadora, chefe e porque não mãe, Doutora Sandra Morelli, por todas as oportunidades que me proporcionou. Com você aprendi muito mais do que ciência, aprendi lições de vida, amizade, confiança e carinho. Além de ter aprendido também a apreciar um bom vinho.

Agradeço também ao professor Dr. Luiz Ricardo Goulart Filho, por ter me adotado no grupo nanobios. Obrigado por sempre acreditar em minhas idéias e por estimular meu crescimento como pesquisador, mudando minha forma de pensar ciência. Sua contribuição foi fundamental.

Agradeço a todos os Professores do Instituto de Genética e Bioquímica, em especial ao Prof. Dr. Carlos Ueira Vieira, Prof. Dra. Rute Magalhães Brito, Prof. Dr. Mário Antônio Spanó, Prof. Dra. Ana Maria Bonetti e todos os demais professores por apoiar meus experimentos e por compartilhar conhecimentos.

Agradeço aos amigos e irmãos do laboratório de citogenética Sabrina, Nayara, Roberto, Alessandra, Priscila, Aurélio, José Clidenor, Luana, Carine, Luiz Paulo, Jayça, Ana Luiza, Boscolli, Edimar.

Agradeço a todos os meus alunos e companheiros Sofia, Makswell, Pedro, Dão Pedro, Lorena, Jéssica. Vocês também são grandes responsáveis por esta conquista.

Agradeço aos grandes amigos do laboratório de nanobiotecnologia Luciana Bastos, Juliana, Franco, Patrícia Tieme, Carolina Reis, Gauber, Karina, Mayara, Lara, Bruna, Cláudia, Léa, Emília, Thaise, Patrícia Terra, Angela, Fausto, Ana Carolina Siquieroli e Yara

Agradeço a todos os familiares e amigos que de forma direta ou indireta me apoiaram. Muito Obrigado Luciana Machado Bastos, Sabrina Vaz, Maildes, Tia Maria, Tia Lúcia, Elaine Dutra, Frank, Ana Cláudia, Ana Luiza, Marianna Crosara, Nívea, Rafael, Renata, João Augusto, Rodrigo Salviano, Érick, Lau, Dhiego, Weder, Carlos, Aline, Viviane, Wallace, Paula...

Agradeço a todos os animais que permitiram que essa pesquisa fosse realizada

Agradeço à Universidade Federal de Uberlândia e ao Instituto de Genética e Bioquímica por promoverem minha formação.

Agradeço à CAPES, FAPEMIG e CNPq pelo fomento à pesquisa.

Muito Obrigado a Todos...!

Sumário

Lista de abreviaturas e símbolos

aCGH - Array-based CGH

Ag-NOR - argyrophilic protein of NOR

ALT - alternative lengthening of telomeres

ATCC - American Type Culture Collection

BRP - bevacizumab-responsive peptide

CDKs - cyclin dependent kinasis

cDNA – complementar Desoxorribonucleic acid

CGH - Comparative Genomic Hybridization

DAB – diaminobenzidine

DEPC - diethylpyrocarbonate

DMSO - dimethylsulfoxide

DNA – Desoxorribonucleic acid

DSBs - Double Strand Breaks

ELISA - immunoessay

FCS - fetal calf serum

FISH - Fluorescence In Situ Hybridation

FITC - fluorescein isothiocyanate

H2O Agua

HIV – Human immunodeficiency virus

I-FISH - interphase cells

INGEB - Instituto de Genetica e Bioquimica

kDa – Kilodaltons

LC-MS/MS - Liquid Chromatography Tandem Mass Spectrometry

LEA - Animal Experimentation Laboratory

MEF - Murine Embryonic Fibroblasts

mFISH - Multicolor FISH

mg - Miligrams

MgCl2 - Magnesium cloride

mL - Mililiters

mM - Milimolar

mRNA – Messenger ribonucleic acid

MT1-MMP - membrane type 1 metalloproteinases

MTT - Malignant Triton Tumor

ng - Nanograms

nm – nanometer

NORs - Nucleolus Organizer Regions

OD - optical density

PBS - Phosphate buffered saline

PCR - Polymerase Chain Reaction

qRT-PCR - quantitative real time PCR

rRNAs - ribosomal RNAs

RT - Reverse transcription

siRNA – small interfering RNA

SKY - Spectral Karyotyping

VCAM-1 - vascular cell adhesion molecule-1

µg - Microgram

µL - Microliter

µM – Micromolar

APRESENTAÇÃO

A tumorigênese está inserida em uma paisagem genômica complexa e instável. Diversos trabalhos são publicados anualmente na tentativa de entender quais são os mais prováveis “hallmarkers” da carcinogênese. Existem duas teorias conflitantes que tentam explicar a origem das células tumorais. A teoria genocêntrica acredita que mutações pontuais em genes específicos são as grandes responsáveis pela transformação celular enquanto a teoria cromossômica diz que as aneuploidias são a grande força motriz de todas as alterações genéticas encontradas em uma célula tumoral. No presente trabalho, utilizamos diversas linhagens celulares murinas na tentativa de desvendar o papel das anomalias cariotípicas na carcinogênese e da influência da telomerase na manutenção dos balanços cromossômicos ideias, permitindo assim a progressão tumoral. A presente tese é composta por cinco capítulos, sendo que os dois primeiros são referentes à fundamentação teórica que foi realizada sob a forma de dois artigos de revisão. No terceiro e quarto capítulo, algumas linhagens tumorais murinas são submetidas a ferramentas de citogenética para analisar o papel das alterações cromossômicas numéricas e estruturais na biologia tumoral e a técnicas de biologia molecular, para entender as alterações gênicas decorrentes da instabilidade genética onipresente no câncer. No quinto capítulo a tecnologia de phage display é utilizada para selecionar peptídeos ligantes especificamente à linhagem celular TG180 para serem utilizados para a entrega seletiva do RNA de interferência contra a telomerase, entrega de drogas ou até mesmo para realização de imagem *in vitro* e *in vivo* de sarcomas. Paralelamente aos resultados aqui expostos, o presente grupo em parceria com outra universidade (UFPB), também descreveu um composto fitoterápico com atividade citotóxica contra o sarcoma murino TG180 (Anexo1). Assim, fomentamos para o futuro utilizar os peptídeos selecionados pela técnica do phage display, descritos no capítulo 5 do presente trabalho, para direcionar a entrega deste composto fitoterápico em células tumorais.

Capítulo 1: Fundamentação Teórica

“An old tool with new and promissory perspectives for cancer research”

Artigo de revisão submetido à revista Bioscience Journal

An old tool with new and promissory perspectives for cancer research

Robson José de Oliveira-Junior[1], Luiz Ricardo Goulart Filho[1], Luciana Machado Bastos[1], Dhiego de Deus Alves[2], Sabrina Vaz dos Santos e Silva[1], Sandra Morelli[1]

[1]Instituto de Genética e Bioquímica, Universidade Federal de Uberlândia, MG;
[2]Instituto de Biologia, Universidade Federal de Uberlândia, MG;
robson_junr@yahoo.com.br

Abstract

Cytogenetics is an important tool in the study of cancer biology. Following the molecular revolution, this area has been underexplored and represents just a small portion of cancer genetic studies. Recent studies have shown the importance of chromosome rearrangements to carcinogenesis. There are two models that attempt to explain carcinogenesis: the conventional genetic models, in which punctual mutations and epigenetic alterations are responsible for tumorigenesis and the model based on chromosomal changes, indicating that cytogenetic aberrations are responsible, by providing chromosomes with all necessary genes for carcinogenesis. Thus, more research must be done to clarify the importance of the chromosomal rearrangements in cancer, since evidences indicates that the correct chromosome balance is crucial to cancer development. Furthermore, many cytogenetic techniques can be used to help in the diagnosis, prognosis and direct the ideal treatment. The union between the cytogenetics, molecular cytogenetics and molecular genetics is essential. This can generate a vast amount of information, improving knowledge about cancer biology and help in the treatment of the disease.

Keywords: Tumor. Chromosomes. Karyotype. Chromosomal Aberrations. Cytogenetic Techniques.

Resumo

As duas visões conflitantes da tumorigênese que são amplamente discutidas são a hipótese da mutação gênica e a hipótese da aneuploidia. Nesta revisão vamos resumir as contribuições da citogenética no estudo das células tumorais e propor um modelo hipotético para explicar a influência dos eventos citogenéticos na carcinogênese, enfatizando o papel da aneuploidia. A teoria da mutação gênica estabelece que mutações específicas ocorrem e mantêm o fenótipo alterado das células de um tumor, enquanto a hipótese da aneuploidia estabelece que a aneuploidia é necessária e suficiente para a iniciação e progressão da transformação maligna. A aneuploidia é considerada um “hallmark” do câncer e esta desempenha um importante papel tanto na tumorigênese, quanto na progressão tumoral. Células aneuplóides são derivadas de células poliplóides, que podem surgir espontaneamente ou são induzidas por agentes ambientais ou compostos químicos. A instabilidade genética observada em células poliplóides leva a perdas ou rearranjos cromossômicos, resultando em cariótipos variavelmente aberrantes. Devido à grande quantidade de evidências indicando que um balanço cromossômico correto é crucial para o desenvolvimento do câncer, as técnicas citogenéticas são ferramentas importantes tanto para a pesquisa básica, tais como pesquisas para elucidar a carcinogênese, quanto pesquisas aplicadas, como no diagnóstico, prognóstico e escolha do tratamento. A combinação da citogenética clássica, citogenética molecular e genética molecular é essencial e pode gerar uma grande quantidade de dados, aumentando o nosso conhecimento da biologia do câncer, melhorando assim o tratamento desta doença.

Palavras-chave: Tumor. Cromossomos. Instabilidade cromossômica. Técnicas citogenéticas.

Introduction

Cytogenetics is a branch of genetics responsible for performing chromosome studies, a subject that has always been one of the most exciting areas of cytology. Cytogenetics is derived from the union of genetics and cytology and is a unique tool that allows viewing of the entire genome of a eukaryote in the form of condensed blocks of genetic material (GUERRA, 2002). The origin of human cytogenetics is attributed to Walther Flemming, who published the first illustrations of human chromosomes in 1882 and used, for the first time, the term mitosis. In 1888, Heinrich Wilhelm Gottfried von Waldeyer-Hartz first used the term chromosome, referring to the colored bodies observed during mitosis. Walter Stanborough Sutton and Theodor Boveri independently developed the chromosome theory of inheritance in 1902 and Sutton was responsible for the union of cytology and genetics, referring to the study of chromosomes as cytogenetics. The correct determination of the human diploid chromosome number as 46, by Joe Hin Tjio and Albert Levan occurred in December 1955, at the University of Lund, Sweden (GERSEN; KEAGLE, 2005).

Since its origin, cytogenetics has been used in many fields such as, taxonomy, plant breeding and clinical analysis, including cancer diagnosis and prognosis. With the advancement of molecular techniques, cytogenetics was somewhat forgotten over the years, but recent studies have shown the importance of cytogenetics as a tool to understand some aspects of tumor biology. Thus, the present paper reviewed diverse papers involving cancer cytogenetics in order to point the importance and evolution of this old tool for cancer studies.

1. Genetic instability and cancer

Cancer results from genetic alterations occurring in a single somatic cell. All the resulting cells from the first neoplasic clone acumulate a series of genetic and epigenetics alterations which cause changes in the gene activity, modifying its phenotype that is submitted to a selection process (PONDER, 2001). The genetic instability or changes in the chromosome number or structure are important factors in oncogenesis. The consequence of genetic instability can be changes in the copy number of one or more genes and changes in the gene expression or structure, modifying the corresponding protein structure. These genetic alterations

can cause an increase or decrease of the protein activity or can create a different protein with new function (SAUNDERS *et al*., 2000). The most important genetic alterations in the tumor cells occur in genes responsible by controlling the cellular proliferation (proto-oncogenes and tumor suppressors) resulting in uncontrolled growth, a characteristic of the disease. The tumor suppressor genes present diverse cellular functions, generally related to the control of cellular proliferation, but these genes are inactive in tumor cells, while the oncogenes present activator mutations, stimulating the cell growth (OJOPI; NETO, 2002).

When the neoplasic cells replicate into a unique cellular mass, the tumor is considered benign. A tumor is considered to be cancerous just if it presents with malignant properties, being capable of escape from the initial mass, through the blood or lymphatic vessels, invading the neighbor tissues and originating secondary tumors or metastasis (ALBERTS *et al*.,1994). According to Hanahan and Weinberg (2000), malignization depends on the acquiring of some characteristics by tumor cells. Initially it was proposed that transformation of normal cells in malignant cells depends on six mutations that provide insensitivity to anti-growth signals, sustained angiogenesis, evading apoptosis, self-sufficiency in growth signals, limitless replicative potential, tissue invasion and metastasis.

Additional features have been added to the list of cancer hallmarks, including evasion of immune surveillance (KROEMER *et al.*, 2008), DNA damage and several causative conditions of cellular stress such as DNA replication, mitosis and oxidative proteotoxic and metabolic processes (LUO *et al.*, 2009). Negrini *et al*. (2010) suggested the inclusion of genomic instability as one of the hallmarks since it is present in all stages of cancer. Hanahan and Weinberg (2011) revisited the hallmarks of cancer and proposed the next set, including in their initial proposal, the deregulating cellular energetic and avoiding immune destruction as emerging characteristics, and tumor-promoting inflammation and genome instability and mutation as enabling characteristics.

One important class of genome instability is the chromosome instability, generally designated as CIN. The term CIN is designated when cancer cells present an instable karyotype, generating a heterogeneous population of cells, and it is a very common feature exhibited by many tumor cancers. Although CIN can drive aneuploidy, not all aneuploid cell exhibits CIN, since it can be found aneuploid cells with a very stable cytotype (DAVID *et al*., 2012). The presence of

chromosomal abnormalities is ubiquitous in solid tumors, therefore cytogenetic analysis is very important to improve our understanding about the role of karyotypical abnormalities generated by CIN in cancer development and progression.

2. *Using classic cytogenetics to diagnosis, prognosis and treatment of cancer*

Cancer origin is closely linked with mutations and changes in the chromosome structure, making important such cytogenetics studies. Each genetic alteration observed in malignant cells, associated with the event of initiation or proliferation of a tumor, can be mediated by large chromosomal changes and thus it is cytogenetically visible. The cytogenetic rearrangements found in tumors are divided into three categories, based on the mechanism by which it promotes the growth of the tumor (Table 1) (CASARTELLI, 1993).

Table 1 – Types of cytogenetic rearrangements found in tumors and the influence of these aberrations in the tumor progression (CASARTELLI, 1993).

Cytogenetic rearrangements	**Mechanism by which it promotes the growth of the tumor**
Translocations, inversions and insertions;	These events affect genes in a limited distance from the point of breakage and can result in chromosomal deregulation of genes or chimeric oncogenes formation.
Chromosomal deletions and monosomies;	These alterations show that the loss of function of some genes is important for the initiation or progression of the tumor.
Polisomies, amplifications, isochromosomes, extrachromosomes, microchromosome, double-minutes, among other chromosome markers;	Such cytogenetic changes can alter the expression of hundreds or thousands of genes, and the physiological effects vary depending on the dosage of genes with altered expression.

Cytogenetic data indicates that chromosomal changes in a tumor can be used for classification, diagnosis and prognosis of it. Sometimes, the histological

features of a tumor coincide with the characteristics of other tumors, making their differentiation with histological methods almost impossible. For example, it is difficult to differentiate the myxoid liposarcoma from other types of liposarcomas. The discovery of the t (12, 16) facilitated the diagnosis of this type of sarcoma. Some types of leukemia, particularly the acute kinds, are often characterized by specific chromosomal events, enabling the differentiation in different subtypes (CASARTELLI, 1993; HAHN; FLETCHER, 2005).

Several studies have demonstrated the importance of gene fusions resulting from chromosomal translocations in cancer progression. These chromosome alterations were identified in leukemias, lymphomas and sarcomas and some examples are the fusions between BCR-ABL1 (Figure 1) found in Chronic Myeloid Leukemia (CML) and ETV6-NTRK3 (Figure 2) found in congenital fibro-sarcoma. In the alveolar soft tissue sarcoma, the translocation between chromosomes X and 17 causes *ASPL-TFE3* fusion, is present in more than 90% of tumor cells and have a great diagnostic utility (GERSEN; KEAGLE, 2005).These translocations are responsible for the juxtaposed portions of two genes, creating chimeric gene products with a different and specific role in cell proliferations or it can change the expression of involved genes (BARR, 1998).

According to the Catalogue of Somatic Mutations in Cancer (http://www.sanger.ac.uk/genetics/CGP/cosmic/), until June 2012, there was 7732 gene fusions related to human cancer described. This large number is additional evidence of the essential role of chromosomal rearrangements in cancer progression.

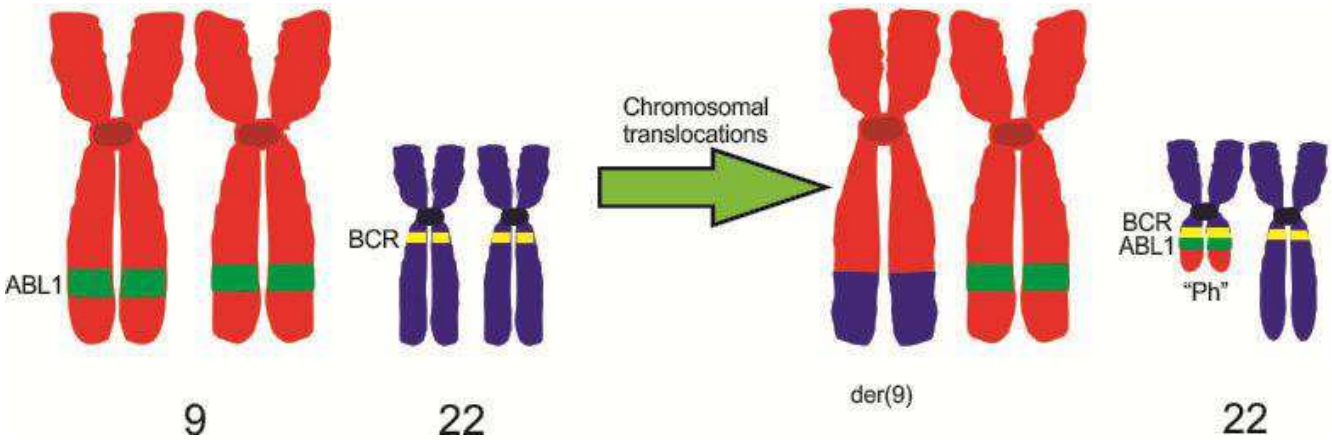

Figure 1 – Schematic representation of the translocation occurred between the chromosomes 9 and 22, originating the Philadelphia chromosome. (Source: author).

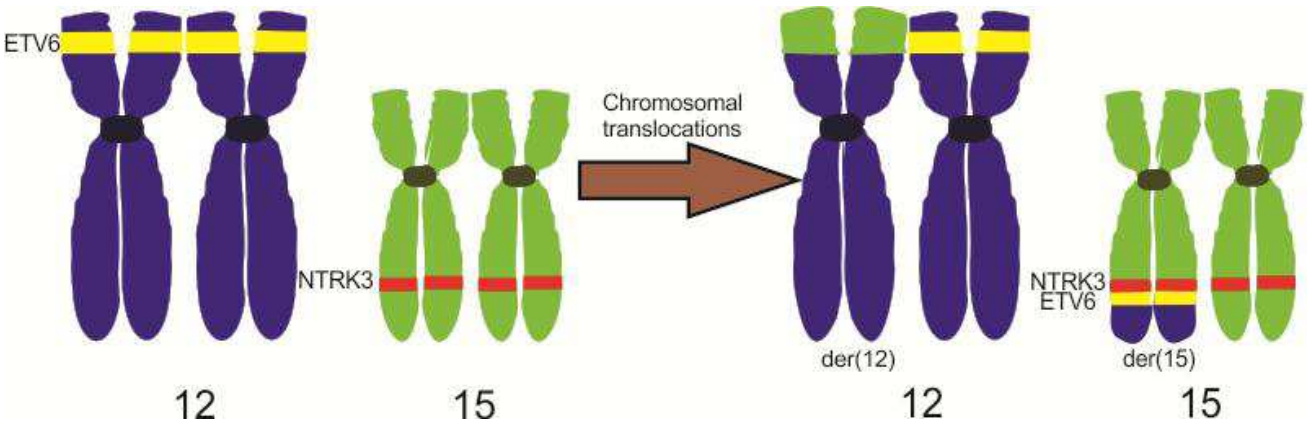

Figure 2 - Schematic representation of the translocation that occurred between the chromosomes 12 and 15. (Source: author).

Gene fusions mentioned thus far are associated with specific tumour types, thus cytogenetic studies of this kind of rearrangements can be a useful tool to identify specific tumors. For example, in Chronic Myeloid Leukemia (CML) patients, cytogenetic analysis plays an imperative function, since in addition to establishing diagnosis, it can predict clinical transformation of the chronic phase into accelerated phase or blast crisis and in CML the prescription of some drugs, as imatinib mesylate (STI571, Gleevec™), is based on cytogenetic analysis to identify the fusion BCR-ABL1 (GERSEN; KEAGLE, 2005).

Several clinical observations have shown that tumors with the same classification have a highly variable metastatic behavior. Some research groups have shown a correlation between the invasive ability and cytogenetic characteristics of tumor cells. The increase in the number of chromosome copies or the presence of some marker chromosomes can determine whether a cell line is more or less invasive to another, thereby directing the type of treatment to be adopted. Even cells that have similar ploidy may show specific rearrangements that increase their metastatic capacity (BERTRAND *et al*., 1999).

Different genetic subtypes of multiple myeloma (MM) were identified which presented different underlying biologic features and showed heterogeneity in clinical outcomes. In multiple myeloma, classic cytogenetics and FISH permits the identification of high risk genetic features and allows patients to be stratified nmnnninto the new risk-adapted therapies. For example, the hypodiploid group with t(4;14)(p16;q32) or t(14;16)(q32;q23) is considered a high-risk group, while the hyperdiploid patients with t(11;14)(q13;q32) are considered to have a better

prognosis. A big challenge to future researches will be to integrate data from conventional cytogenetics, Fluorescence In Situ Hybridization (FISH), Interphasic Fluorescence In Situ Hybridization (I-FISH), Gene Expression Profiling (GEP), Comparative Genomic Hybridization (CGH), Array Comparative Genomic Hybridization (aCGH), and Single-Nucleotide Polymorphism (SNP) arrays into improved diagnostic and prognostic tools to guide the therapy of multiple myeloma. (SAWYER, 2011)

Prior data indicates that the applications of cytogenetics in tumor classification and in the measure of its invasiveness, indicate the importance of the cytogenetic studies. Since its origin, cytogenetics passed by advances that allowed its application in cancer and other genetic diseases.

3. Cytogenetic techniques applied to cancer study

Cytogenetics has an essential role in the detection of human diseases, considering that numerical abnormalities, poliploidy and aneuploidy, and structural, translocation, inversion, deletion and duplication are easily observed using this technique. The first advances in cytogenetics were the application of colchicine and hypotonic solutions for cell treatment and represents a milestone in cytogenetic studies. Treatment with these solutions allowed improved quality of mitotic chromosomes and consequently the analysis of them. Colchicine is an alkaloid derived from a plant called *Colchicum autumnale,* capable of binding to tubulin dimers, preventing microtubules polymerisation. In addition to its action in the polymerization, colchicine disrupts dimers previously associated preventing the mitotic spindle formation and consequently the segregation of sister chromatids (WILSON; MEZA, 1973).

The treatment of the biological material with hypotonic salt solutions is an important step for obtaining good quality metaphases, a prerequisite for subsequent cytogenetic analyzes. The exposure to hypotonic solution of metaphases promotes chromosomes dispersing once they chromosomes leave the central region and disperse throughout the cytoplasm (CLAUSSEN et al, 2002).

A way to visualize numerical and structural karyotypic alterations is by producing chromosomal markers, called bandings. Among the procedures for

banding, the G-banding (Giemsa) is the most widely used method for recognition of the chromosome pairs. The effectiveness of the G band becomes widely used in oncology research and clinical analysis. For example, when metaphases of tumor cells from patients with congenital fibrosarcoma underwent the procedure of G banding it revealed trisomy of chromosome 15 and structural abnormalities as the translocation t(12; 15) (p13, q25) (SANDBERG, MELONI-EHRIG, 2010).

According to Buwe et al., (2003), cytogenetic analysis is frequently required to investigate the causative genetic defects and neoplastic cells often show complex chromosome aberrations and in many different marker chromosomes. Less pronounced differences in banding patterns make it difficult to assign genetic abnormalities to certain chromosomes by conventional banding techniques. One important event in cytogenetics was when classic cytogenetic and molecular biology together emerged as molecular cytogenetics, a technique which involves the manipulation of genetic material. Molecular cytogenetics started with in situ hybridization, another milestone of cytogenetic evolution, described by Gall and Pardue in 1969 (BUWE *et al.*, 2003).

With the continuous advancement of molecular cytogenetics, the development of Fluorescence In Situ Hybridation (FISH), Comparative Genomic Hybridization (CGH) and Spectral Karyotyping (SKY) was made possible. These techniques are excellent tools for genetic analysis and the banding patterns obtained by molecular cytogenetics represents the central theme for any cytogenetics laboratory of clinical analysissince technical difficulties as low quality chromosomes or few tumor cells are overcome more easily with the help of advanced cytogenetic techniques.

One of the first molecular cytogenetic techniques used was FISH. It is a useful technique for the detection of chromosome abnormalities because it enables the analysis of interphase cells (I-FISH), the characterization of marker chromosomes, the screening of a large number of cells within a short period of time, and the ability to study samples with few or poorly assessable metaphases (OUDAT *et al.*, 2001)

The FISH technique can be used for mapping specific chromosomal loci and for the detection of numerical and structural cytogenetic aberrations. FISH allows the visualization of the genomic target using metaphases, interphasic nucleus or tissue sections. Its application is particularly important for the detection

of translocations, inversions, insertions and microdeletions, as well as identification of chromosome marking and in the characterization of chromosome break points (LE SCOUARNEC; GRIBBLE, 2012). FISH is considered the best method for the detection of v-myc (myelocytomatosis viral oncogene, also called MYCN) in neuroblastoma where t (8, 14) (q24; q32) causes its uncontrolled expression, as well in other tumors as medulloblastoma, rhabdomyosarcoma and Wilms tumor where this gene can be found amplified. In hematological cancers as in CML loss of DNA in translocation break points can be observed through FISH. Because of its sensitivity, this technique should be considered for monitoring cancer post-treatment. The FISH procedure is a sensitive, fast and indispensable complement to conventional cytogenetic techniques (WAN, MA, 2011).

Despite its effectiveness in detecting several chromosomal rearrangements, using just FISH or chromosome banding alone, cannot characterize comprehensively a disturbingly high number of chromosomal aberrations (GARINI *et al.*, 1996). One important advance in the FISH technique is the emerging of Spectral Karyotyping (SKY), an imaging technique for the analysis of FISH experiments. The SKY technique was developed by Schrock et al. in 1996 and allows easy visual interpretation during the analysis of results. It is based on the simultaneous hybridization of 24 combinatorialy labelled human chromosome painting probes and the visualization of all human chromosomes in different colors is achieved by spectral imaging. This technique can be used to characterize translocations evolving non-homologous chromosomes; however, this procedure does not allow the detection of structural abnormalities such as inversion, deletion and duplication on the same chromosome, because each chromosome has a unique color (WAN; MA, 2011; GARINI *et al.*, 1996).

According to Bayani and Squire (2002), SKY has been used to identify various tumor groups. This includes hematological malignancies, sarcomas, carcinomas and brain tumors. The intent of using SKY is in identifying specific chromosomal abnormalities that may provide insight into genes involved in the disease process as well as identifying recurrent cytogenetic markers for clinical diagnosis and prognostic assessment. Rare tumors such as alveolar soft tissue sarcomas have also been studied using SKY. The literature cites chromosome 17q25 as a site of frequent cytogenetic classification of an soft tissue sarcomas with the sole abnormality of an add(17)(q25) to der(17)t(X;17)(p11.2;q25) following

SKY analysis (BAYANI; SQUIRE, 2002). Using SKY and other cytogenetic techniques, Holland *et al.*,(2012) found 169 structural chromosomal aberrations most frequently involving chromosomes 1, 2, 3, 4, 10, and 12, including two not previously described alterations, a nonreciprocal translocation t(3;11)(p12;q13), and one interstitial chromosomal deletion del(2)(q21q31). In addition to cytogenetics, Holland *et al.*,(2012) used other molecular genetic techniques and the authors emphasized the necessity of combining complementary methods to obtain comprehensive information and understanding about tumorigenic aberrations.

Another technique used as a complementary tool to classical cytogenetics is the CGH. This technique detects unbalanced chromosomal changes (loss/gain) using small amount of DNA. In CGH, normal DNA (called reference) and tumor DNA are marked with different fluorochromes and after labeling, both DNAs are co-hybridized to normal human metaphase chromosomes, and fluorescence ratios along the length of chromosomes provide a cytogenetic representation of the relative DNA copy-number variation. If the chromosome or its sub-regions have the same copy number of the target DNA control sample, fluorescence is observed with an equal contribution soft tissue sarcomas from tumor DNA and normal DNA. If there are deletions in tumor sample, the marking will be found with the color of reference sample and in cases of gains, tumor fluorescence will be predominant (PINKEL et al., 1998). The advantage of CGH is that only the tumor DNA is required for molecular cytogenetic analysis and tumor DNA can be easily obtained from micro dissection of tumor samples and this feature turned the CGH in to one of the most used techniques in research and molecular diagnostics (WAN; MA, 2011).

According to Wada et al (2002) chromosomal gains detected using CGH on 5p, 7, 12p, 12q, 19p, 19q, 20p and 20q in Hurthle cell carcinomas are associated with tumor recurrence and such chromosomal aberrations may be predictive for the recurrence of the disease. Studies with CGH in a patient affected with rare bone tumor called Malignant Triton Tumor (MTT) revealed amplification in several chromosomes (1p, 6p, 16p, 16q, 17p, 17q, 19p, 19q, and 20p 22q) coinciding with previous data, where was described recurrent genomic aberrations at the chromosomes 1, 16, 17, 19, and 22 suggest the involvement of several oncogenes in the genesis of MTT (KOUTSIMPELAS et al., 2011). Yeh et al. (2012) presented

a case that highlights the use of two maneuvers useful in the diagnosis of spindle cell melanoma, CD34 Fingerprint and CGH. In this study, a shave biopsy from the cheek of a 58-year-old man demonstrated a thin invasive melanoma and CGH demonstrated gain of chromosome 6p, loss of 6p and gain of 7, supporting the diagnosis of spindle cell melanoma.

An adaptation of CGH is the Array-based CGH (aCGH). According to Harvell et al (2004), aCGH is a method that combines traditional CGH and microarray technology. In this technique, tumor and normal genomic DNAs are differentially fluorescently labeled and co-hybridized onto an array containing mapped DNA sequences, providing measurements of tumor copy number changes at high resolution across the genome. In their study, Harvell et al (2004) used aCGH as a diagnostic test in distinguishing Spitz nevus and melanoma using DNA isolated from formalin-fixed and paraffin-embedded samples, showing the effectiveness of using the method as a diagnostic tool in differentiating Spitz nevus from melanoma.

4. Cytogenetic events related to Cancer Progression

4.1 Polyploidy and Cancer

Eukaryotic organisms generally have a diploid number of chromosomes. The diploid state is preferred and evolutionarily maintained. It allows for the sexual reproduction and facilitates genetic recombination. However, there are a surprising number of exceptions. There are organisms that have more than one diploid chromosome complement, as observed by Morelli et al. (1983) in a fish specimen, or even less than the diploid complement. Moreover, the chromosome complement may differ within the same organism, depending on the cell type and the increased chromosome number is widely observed in tumor cells (STORCHOVA; PELLMAN, 2004).

There are two different classes of polyploidy, the allopolyploid which combine two or more related but not identical genomes and autopolyploid which combine two or more identical genomes. Polyploidy cells can be formed by three different mechanisms: an abortive cell cycle, cell fusion and endoreduplication (STORCHOVA; PELLMAN, 2004).

According to Larizza and Schirrmacher (1984), tumor cells that have metastatic properties often have higher gene dosage than the original cells. This fact is seen by the increased ploidy level, chromosomal duplication and gene amplification. The acquisition of a large chromosome number observed in tumor cells may be the result of endoreduplication or somatic hybridization (cell fusion). In some cell types, the cell fusion is part of the normal development, producing terminally differentiated cells such as muscle cells and osteoclasts. The cell fusion causes an intracellular disorder with changes in the genetic structure of the cell and consequent instability. This fact can cause the emergence of aneuploid clones. These clones may have neoplastic characteristics and have an unstable or relatively stable chromosome complement, ranging from triploid to tetraploid (HESELMEYER, 1997; STORCHOVA; PELLMAN, 2004; DUELLI; LAZEBNIK, 2007).

The endoreduplication, observed in many tumor cell lines, is a common event in arthropods and is well characterized in the drosophila salivary glands (forming the politenic chromosomes) and in megakaryocytes, which are mammal cells responsible for the platelets formation (STORCHOVA; PELLMAN, 2004). The process of endoreduplication results in diplochromosomes, consisting of four chromatids grouped side by side, instead two. Endoreduplication occurs when the cells go through two rounds of DNA replication without the chromatid separation (SUMNER, 1998).

Endoreduplication happens when some mechanisms that drive the sequential progression of G1, S, G2 and mitotic phase (M) of the cell cycle are modified. Usually the chromosomes only replicate once per cell cycle and the mitosis progression (M phase) is required for the releasing of other points of replication origin, starting the next round of chromosomal duplication (LARKINS *et al*., 2001). The normal mitotic cycle consists of periods of DNA synthesis (S phase) and chromosome segregation (M phase), preceded by intervals: G1 and G2 respectively. During the cell cycle, the orderly progression of events that cause the duplication and chromosome separation is governed by cyclin dependent kinasis (CDKs). These cyclins were found in all studied eukaryotes and are encoded by a large number of genes. Human CDK1 interacts with the mitotic cyclins A and B and promotes the transition from G2 to M phase (also called factor promoter of mitosis). CDK2 interacts with the cyclins D, E, and A and functions

during G1 and S. In the normal cell cycle, the progression of S phase needs a complete M phase, but in the process of endoreduplication this dependency is turned off and chromatin is re-licensed even if does not complete mitosis. These mechanisms are regulated by the concentration of CDKs and the use of inhibitors of these proteins results in polyploidy (LARKINS *et al*., 2001)

In many cancer cells the number and structure of chromosomes can be highly variable, which is known as aneuploidy, which is a consequence of initial polyploidy. The aneuploidy is the situation where the number of chromosomes is not an exact multiple of the species characteristic haploid number. The aneuploidy is often observed in tumor cells, primarily in solid tumors. The correlation between cancer and aneuploidy has been known for decades, however the answer to the central question has not been answered yet: is aneuploidy a contributing cause or a mere secondary consequence of the malignant transformation? (LENGAUER; KINSLER; VOLGELSTEIN, 1997; (STORCHOVA; PELLMAN, 2004).

4.2 Aneuploidy: cause or consequence of tumorigenesis?

Two conflicting visions on tumorigenesis are widely discussed: the one which says that gene specific mutations start and maintain the altered phenotype of tumor cells and another that says that aneuploidy is necessary and sufficient for the initiation and progression of malignant transformation. Aneuploidy, although observed in cancerous cells nearly a century ago, and until 1960s considered the cause of malignant transformation, remained forgotten for the past 25 years, primary because the technology of the time failed to identify specific patterns of chromosomal rearrangements in different types of cancer. However, a growing list of articles demonstrates the role of aneuploidy as genetic support for the cancer development (STOCK; BIALY, 2003).

The role of intra-genic punctual mutations in cancer is well established. However, the contribution of massive genomic changes collectively known as aneuploidies is less certain. Many works suggest that aneuploidy is required for carcinogenesis in mice and that it can work with intra-genic mutations during tumorigenesis. The genomic plasticity provided by aneuploidy could facilitate changes in gene dosage that would promote tumorigenesis and accelerate the oncogenes accumulation and the loss of tumor suppressor genes. These discoveries stimulate revising the basic concepts of cancer pathogenesis and has

significant implications for the diagnosis and treatment of the disease (PIHAN; DOXSEY, 2003).

The theories based on genic mutations ("genocentrics") defends that cancer is caused by the clonal expansion of cells, which accumulate specific mutations to the development of the disease, but at the same time, how do the normal cells of the body remain without mutations? According to Duesberg et al. (2005 and 2007) the conventional genetic model and the epigenetic events cannot explain the carcinogenesis properties listed below, which are explained by chromosomal theory of cancer:

(1) Most tumors are not heritable and thus, are extremely rare in infants and are a senile disease. According to the genocentric theory, the cancer should be a common disease in infants, since they could inherit mutant genes of the father and mother, accumulating mutations needed for carcinogenesis. According to the chromosomal theory aneuploidy is the trigger cause of cancer and this event is not heritable, because it corrupts development programs, which would be fatal in the development of the embryo;

(2) Carcinogenic non-mutagenic agents may cause cancer. The carcinogens are physical or chemical agents that accelerate the carcinogenesis and can be classified into mutagenic and non-mutagenic. The agents that accelerate the carcinogenesis, also called promoters of tumor, are not mutagenic or do not directly induce mutations as the tar, asbestos, aromatic hydrocarbons, nickel, arsenic, lead, certain dyes, uretan and dioxin. According to the chromosomal theory, carcinogens act more as aneuploidy inductors than as mutagens. The gene mutation theory cannot explain how non-mutagenic carcinogens cause cancer. In fact the mutagenic agents may lead to aneuploidy through direct destruction or fragmentation of chromosomes, such as radiation, but non mutagenic carcinogens can cause aneuploidies by different mechanisms, such as causing a microtubule dysfunction;

(3) The tumors develop only years or decades after initiation by carcinogens. Many carcinogens, that are mutagens, act quickly, causing instantaneous changes in DNA such as the X-ray and Ultra Violet light. However, all carcinogens, mutagens or not, have a slow action, which presents results in the long-term, causing cancer only after a period of "cancer latency."

According to the chromosomal theory, cancer latency would be the time needed for the cells that have an initial aneuploidy to develop any specific chromosomal changes to become cells with malignant characteristics;

(4) The genocentric theory does not offer an exact correlation between cancer and aneuploidy because the omnipresence of aneuploidies in cancer are not postulated or even predicted. Studies of gene expression in tumor cells through "micro-arrays" identified abnormal expression of thousands of genes, corresponding to the abnormal ploidy of the chromosomes corresponding to these genes;

(5) Pre-neoplasic aneuploidies are found in some tissues. These cells are often observed following exposure to carcinogens. These cells are also found inheritable diseases that predispose to high rates of aneuploidy systemic such as xeroderma, Werner Syndrome, Fanconi anemia among others and also in congenital aneuploidies as Down syndrome that increase the predisposition of individuals to cancer. The chromosomal theory of cancer predicts that the pre-neoplasic aneuploidies are an intermediary phase in the evolution that generates the chromosomal aneuploidies specific of cancer;

(6) The karyotypic and phenotypic variation observed in tumor cells is much higher than the rate of conventional mutations. This karyotypical variability observed in tumor cells is the reason cancer consists of a non-clonal or partially clonal heterogeneous population of cells. However, one in every thousand aneuploid tumor cells generate a new specific phenotype by cellular generation, at levels considerably higher than the conventional mutation;

(7) Despite the high karyotypical variability found in tumor cells, it has been identified since 1960 that several cancer-specific chromosome alterations (not randomic alterations), also known as aneusomies. In some cases marker chromosomes that are generated from rearrangements are observed. Aneusomies were linked to different specific events of carcinogenesis such as the malignant transformation, invasiveness, metastasis, drug resistance, ability to be transplanted into other hosts, cellular morphology, abnormal metabolism and cancer-specific viral receptors. Such characteristics are correlated with the changed expression

of thousands of genes, which corresponds to the presence or absence of specific chromosomes, generated by aneuploidy. Random chromosomal changes or non-cancer-specific changes are not predicted or postulated by the mutational theory of cancer.

(8) The tumor cells phenotype is too complex to be explained by the mutational theory. For example, when the cells are exposed to some drugs, the tumor can acquire resistance to the chemotherapy used, but it is also observed that the cells become resistant to several other drugs, causing the MDR phenotype (multi-drug resistance), characterizing a multigenic event. According to the chromosomal theory, carcinogenesis is not dependent on mutation because the carcinogenesis initiation is much more probable via the aneuploidization route than via mutation. The phenotypic variation observed in the aneuploidization pathway is 4 to 11 times faster than via mutation. The mutations observed in malignant cells may be a result of aneuploidy and even the tumors observed in heritable syndromes can be generated by aneuploidy;

(9) The conventional genetic theory explains the tumor evolution through specific mutations and Darwinian selections. But this model cannot explain the presence of notselective phenotypes in tumor cells. The presence of metastasis cannot be explained because it is not present at the site of origin of the disease, so it is not positively selected. The multi-drug resistance would be interesting only in the presence of chemotherapy.

(10) Several genic mutations have been observed in cancer since 1980, but none of them are a cancer-causing gene primarily because the mutations found in cancer are not cancer specific. When this information is available, most of the mutations are not clonal. The expression of hypothetical cancer-causing genes, are not detectable without methods of amplification. Despite many efforts, using a mutant gene or even combinations of mutant genes researchers were unable convert a diploid cell into a cancer cell.

(11)

4.3 Increase in the Nucleolus Organizer Regions (NORs) activity as a proliferation marker

NORs are chromosomal regions in which the ribosomal genes (rDNA) are clustered together, from which are transcribed ribosomal RNAs - rRNAs. These regions are associated with the nucleoli and are responsible for its reorganization in the end of cell division. There is a group of specific argyrophilic proteins associated with active NORs and these proteins becomes visible in the nucleus and chromosomes by a silver-nitrate staining technique under a light microscope and it has been called argyrophilic protein of NOR (Ag-NOR) (MILLER *et al*., 1976).

The silver nitrate impregnation technique can be used to visualize the activity at the site of rDNA genes. The silver impregnation does not occur in all rDNA sites; just those which are transcriptionally active or who have been active and still have residues of proteins associated with rRNA attached around condensed rDNA cistrons (SCHWARZACHER *et al*., 1978).

AgNORs counting is frequently used to measure the proliferative activity of several tumor types, since these regions are linked to high protein synthesis and, consequently, to the tumor aggressiveness, making its conservation in malignant cells interesting (OSHIMA; FORONES, 2001; KANEKO *et al.*, 1991; ISHIDA *et al.,* 1993). This cell cycle kinetics information is used to measure proliferation potential of a tumor, a very important feature for its diagnosis and prognosis (KANEKO et al., 1991; ISHIDA et al. 1993; AHMED et al., 2011; DE-MORAES et al., 2012).

According to Hanemann et al. (2011), AgNOR staining techniques can be a useful diagnostic tool in the different types of oral squamous cell carcinoma, since differences in AgNOR numeric values can be identified and can be largely used in histopathology due to its low cost and can be easily performed. Aiming to determine the diagnostic accuracy of Silver stained Nucleolar Organizer Regions (AgNOR) staining in brush biopsies taken from suspected oral lesions for early detection of oral cancer, Rajput et al. (2010) concluded that brush biopsy in conjunction with AgNOR staining is an easily practicable, non-invasive, safe and accurate screening method for the detection of macroscopically suspicious oral cancerous lesions. According to these authors, NOR detection can be used as an adjunct to other routine cytological diagnoses for the early detection of oral cancer.

4.4 Telomere damage and its influence in carcinogenesis

The telomeres are structures present in the end of linear chromosomes, maintaining the chromosome integrity. These structures are essential to ensure an appropriate chromosome structure and function, maintaining the genetic stability of the cell. In mammals, as well as in all vertebrates, the telomeres consist of many kilo-bases of tandem repetitions of the TTAGGG sequence and of the specific telomere associated protein and telomeres end in a large duplex T-loop (Figure 3) (GRIFFITH *et al.*, 1999). Among many proteins associated with telomere, TRF1 and TRF2 are important. TRF1 regulates the telomere length and TRF2 maintains its integrity (KARLSEDER et al., 1999). The length of the TTAGGG repetitions varies from one species to another. In the human germ line cells telomeres have been identified to be between 15 to 20 Kb in length, while in mice (*Mus musculus*) the telomeres are much longer, ranging from 30 to 50 Kb. In addition to this inter-species variation, the telomere length may vary intra-species and individually, depending on the genotype, the examined cell type and the replicative history of the cell. The telomeres are responsible for the control of cell division, so that after a certain number of divisions the cells get in the replicative senescence pathway (LIJNINE; MAKAROV; LANGMORE, 1995; BLACKBURN; GREIDER, 1995; FYHRQUIST; SAIJONMAA, 2012; RAMPAZZO *et al.*, 2012).

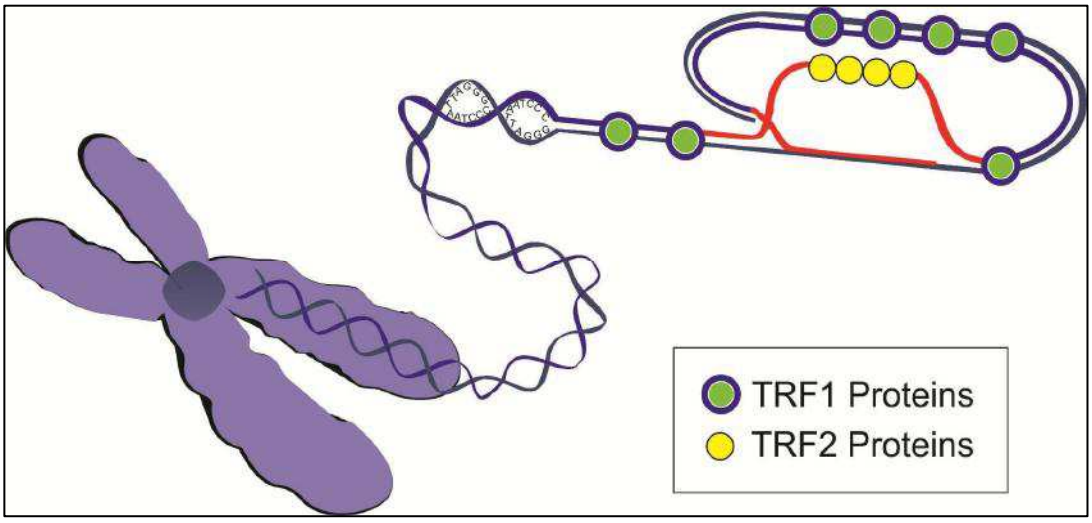

Figure 3: Schematic representation of mammalian telomeres, constituted by TTAGGG nucleotide repetitions and many associated proteins, being represented TRF1 in green and TRF2 in yellow (GRIFFITH *et al.*, 1999, adapted). (Source: author)

The replication of linear chromosomes presents a difficulty, which is the inability of DNA polymerase to complete the synthesis of the end of the linear chromosomes. Since the synthesis occurs only in the 5' => 3' sense, and requires RNA priming for its initiation, the telomeres are not completely replicated by the conventional complex of DNA polymerase. Thus, when the cell divides, the replication difficulty at the end of chromosome results in telomere reduction (GILLEY; TANAKA; HERBERT, 2005). When the telomeres reach a critical length, it induces the activation of checking points very similar from those initiated by damage to DNA. In human cells, short telomeres result in the senescence activation and the cell doesn't replicate anymore (MASER; DEPINHO, 2002).

The progressive shortening of telomeres causes senescence, cell death or genetic instability. Evidences suggest that telomeric shortening contributes to the initiation and progression of malignant tumors in several ways. The genetic instability caused by telomere dysfunction is one of the main factors that predispose the cells to the malignant transformation (CAMPISI *et al*., 2001). According to Martinez-delgado *et al.*, (2012) shorter telomere length is associated with increased ovarian cancer risk in both familial and sporadic cases, being a risk factor for early onset ovarian cancer. In a study performed by Zhou *et al.*, (2012), telomere length variation in normal epithelial cells adjacent to tumor is significantly associated with breast cancer and can be used as a potential biomarker for breast cancer local recurrence.

One prominent hypothesis is that the telomere dysfunction is one of the key processes behind the genomic instability observed in primary malignant lesions (Figure 4). The hypothesis of the telomere dysfunction indicates that telomeric protection is lost in a small group of normal precursor cells. This loss of telomeric protection results in the fusion between the telomeric regions of different chromosomes, causing genetic instability through cycles of fusion, with bridge and chromosomal breaks. Thus the telomeric dysfunction can generate various cytogenetic changes, so that the cells acquire the combinations of genetic material necessary to start carcinogenesis. The genetic instability provides the initial cancer cells with chromosome changes that disable the suppression of growth and apoptosis, allowing the engagement in metabolic pathways, essential for immortal growth (MASER; DEPINHO, 2002). The telomeric dysfunction can be caused by

aberrant length of the telomeric DNA sequence (telomere shortening) and/or loss of function of a protein linked to telomere (GILLEY; TANAKA; HERBERT, 2005).

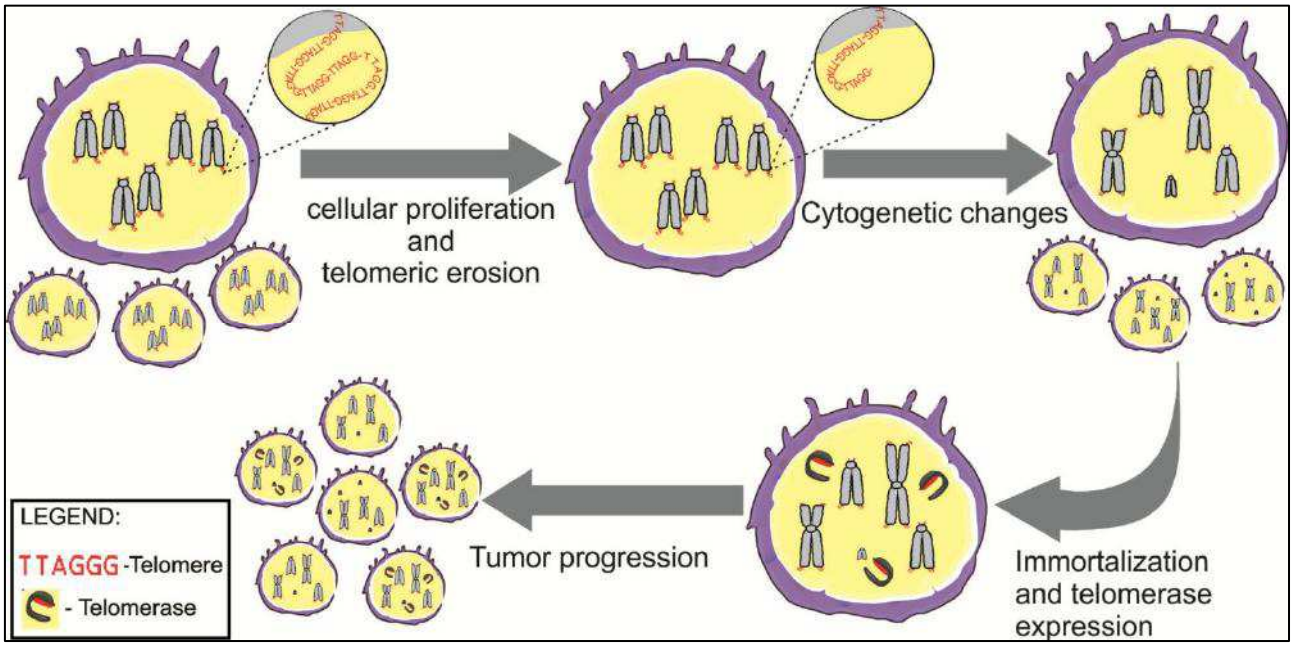

Figure 4 – Schematic representation of the role of telomeres in carcinogenesis. A small group of cells lose telomere protection due to telomere erosion. Telomere instability initiate a state of crisis, in which the chromosomes are submitted to cycles of fusion-bridge-breaks and the cells acquire many chromosome markers and become aneuploid. The cytogenetic changes can provide advantageous characteristics such as deletion of tumor suppressor genes and activation or over-expression of oncogenes. The telomerase over-expression stabilizes the chromosome markers originated during the crisis state, enabling cell immortalization and tumor progression. (Source: author)

When cells are kept in culture, their telomeres reach a critical length, which results in the activation of the Hayflick limit (mortality stage 1 or senescence) and the cells stop dividing. However, the Hayflick limit can easily be broken by inactivation of the growth inhibitory pathways induced by the genes Rb and p53. The continued proliferation of cells after the Hayflick limit causes the exacerbated telomeric erosion and high genomic instability, culminating in a period of massive cell death or cell crisis (stage of mortality 2). Although the crisis is an important barrier to cell immortalization, the massive genetic instability in this stage may be the mechanism by which few survivor cells acquire the large number of genetic changes required for malignant transformation. These rare cells emerge from crisis through the activation of mechanisms for telomeric maintenance, most commonly by increased expression of telomerase (MASER; DEPINHO, 2002).

The telomerase is a ribonucleoprotein complex, consisting of a catalytic subunit (TERT), which regulates the activity of telomerase, and has reverse transcriptase action whereby a RNA chain (TR) provides the template to add the telomeric sequence (TTAGGG) to the chromosome ends (GILLEY, 2005). In humans telomerase is expressed only in some cells, such as embryogenic cells and active lymphocytes, while in tumors, this enzyme activity is detected in 90% of cases, while the other 10% maintains their telomeres through an alternative lengthening of telomeres (ALT) (KIM *et al*.; 1994).

The telomerase plays an important role in the growth of tumors and cell immortalization. The reactivation of this enzyme may be a critical event that promotes the tumor proliferation by removing the barrier of telomeric shortening (CHANG; KHOO; DEPINHO, 2001). One example is the study performed by Takahashi et al. (2003), in which a translocation occured between the chromosomes 11 and 22 in Ewing's sarcoma that causes the fusion of genes EWS and ETS, producing a chimeric protein responsible for the telomerase activation in this sarcoma. Chang et al. (2005), in a classic work, also demonstrated the importance of telomerase over-expression when they immortalized an endothelial cell line through transfection and ectopic expression of the telomerase hTERT catalytic subunit. These observations and the frequency and intensity of telomerase expression in human tumors, suggest that telomeric maintenance is essential for the cell immortalization and that it may be possible to inhibit the growth of cancer by interfering with the action of telomerase (LI *et al*., 2005). Thus, many strategies have been developed to inhibit telomerase, such as antisense nucleotides, ribozymes and interference RNA to use the inactivation of this enzyme as a therapeutic approach (GUO *et al*., 2005).

5. A hypothetical model to explain the influence of cytogenetic events in carcinogenesis

By combining data on cell transformation with the hypothesis of other authors, it is possible to propose a model that explains chromosome changes in tumors which present a complex karyotypes, as the near-tetraploid ones. We hypothesize that initially a normal cell has a faulty mechanisms of replication or checkpoint controls, due to physiological or genetic factors or exposition to chemical agents, becoming polyploid. Extra copies of chromosomes can be

generated by endoreduplication, an event frequently observed in tumor cells (BOTTURA; FERRARI, 1963; LIMA *et al.*, 2004). Additional evidence about the importance of endoreduplication in the carcinogenesis process is that when exposed to chemotherapeutic drugs which inhibit mitosis, cancer cells also utilize endoreduplication in order to evade apoptosis and the presence of endoreduplication is associated with development of secondary malignancies (CORTÉS; PASTOR, 2003; CANTERO *et al.*, 2006; PUIG *et al.*, 2008). Davoli and De Lange, (2012) also report that endoreduplication and mitotic failure occur during telomere crisis in human cells and promotes transformation of mouse cells.

After increasing the chromosome number of the tumor-initiating cell, the next step to malignization would be aneuploidy acquisition. According to Mayer and Aguilera (1990), polyploidy *per se* appears to dramatically increase chromosome loss, presumably due to increasing genome instability and to the inability of polyploid cell to undergo proper chromosome segregation. Another event that can be responsible to generate aneuploidy is Double Strand Breaks (DSBs) in the DNA molecule. When a DSB happens, the chromosome turns instable and needs to be repaired. A way to solve this problem is by joining the damaged chromosomes, but erroneous rejoining of broken DNA may occur, resulting in deletion or amplification of chromosome material and even translocations (KHANNA et al., 2001; JACKSON, 2002). DSBs can be caused by telomere erosion after several rounds of mitotic cycles or oxidative stress resulting from inflammation, which cause, among other effects, an increasing in free radicals at tumor site (represented in the Figure 5).

As a result of Double Stranded Breaks (DSBs), chromosomes destabilize and may have suffered several structural alterations such as fusions, bridges and chromosome breakages. Genetic instability is responsible for generation of important chromosome malignant markers, which are ubiquitous in the karyotype of solid tumors. The genetic instability and chromosomal aberrations may provide some advantageous phenotypic changes, enabling cells to evade apoptosis by retaining its proliferation. Thus, some rare cells with ideal chromosomal combinations may achieve a malignant phenotype. However, the chromosomes of these tumor cells still present unstable replication and segregation, probably due to telomere dysfunction. This obstacle is overcome by reactivation or over-expression of telomerase.

After the chromosomal stabilization by telomerase, cancer cells are able to divide indefinitely, establishing the tumor. During tumor progression, many changes occur and only the advantageous genotypes are positively selected. Although there is a cellular heterogeneity among tumor population, only cells that have the ideal chromosome combination are responsible for cancer perpetuation and they are called tumor stem-cells.

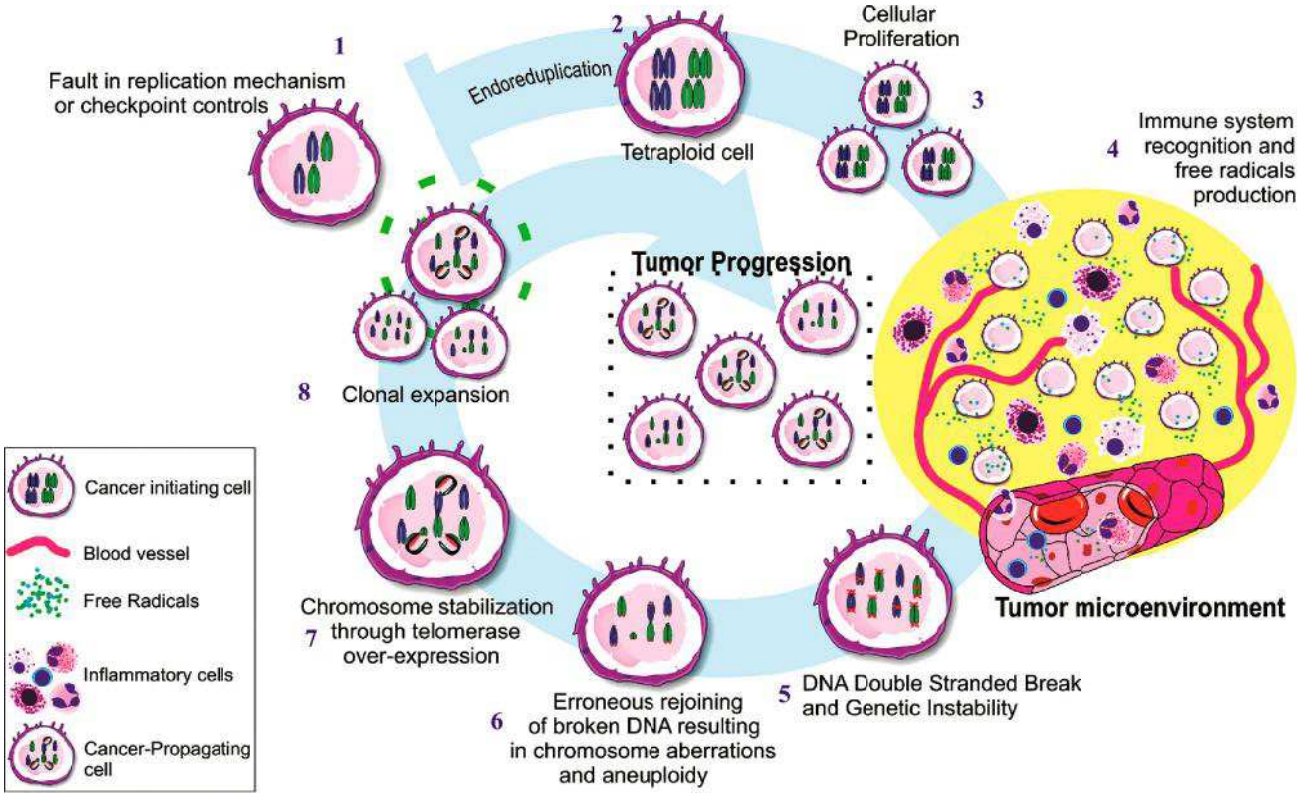

Figure 4 - **A proposed model for the karyotype evolution of a cancer cell.** Due to faults in the replication mechanism or check-point controls, a normal cell becomes polyploid through endoreduplication. After many mitotic cycles, the resulting cells are recognized by the immune system, which tries to eliminate the abnormal cells by producing cytotoxic mediators such as free radicals. These reactive compounds attack DNA, causing double-strand breaks (DSBs) and genetic instability. Attempts to stabilize the DSBs result in the erroneous rejoining of broken DNA, giving rise to aneuploidy. A rare cell with an advantageous near-tetraploid karyotype may possess a better proliferative potential when the chromosomes are stabilized by telomerase over-expression. These specific proliferating cells promote tumor progression through clonal expansion.

Conclusion

Given the data presented in this review, it is possible to percept the importance of chromosomal rearrangements in tumor evolution since this event is ubiquitous in the malignant cells of most patients. More effort should be directed to cytogenetic studies, since evidence indicates that correct chromosome balance is crucial to cancer development and this technique is a valuable tool to diagnose and direct cancer treatment. The union between the classic cytogenetics, molecular cytogenetics and molecular genetics must be exploited, in order to generate a great amount of information, improve knowledge about the cancer biology.

6. Acknowledgments

The authors are thankful to the Federal University of Uberlândia, Genetic and Biochemistry Institute and to CAPES, CNPq and FAPEMIG by the financial support given to the pos graduation program and INGEB.

8. REFERENCIAS BIBLIOGRÁFICAS

AHMED, H.G.; AL-ADHRAEI, M.A.; ASHANKYTY, I.M. Association between AgNORs and Immunohistochemical Expression of ER, PR, HER2/neu, and p53 in Breast Carcinoma. **Pathology Research International**, v. 2011, 6p., 2011.

ALBERTS, B. Câncer. In: ALBERTS, B; BRAY, D; LEWIS, J; RAFF, M; ROBERTS, K; WATSON, J. D. 3ª edição. **Biologia molecular da célula.** Porto Alegre: Artes Médicas, 1994, p. 1255-1291.

BARR, F. G. Translocations, cancer and the puzzle of specificity. **Nature Genetics**, v.19, p.121-124, 1998.

BAYANI, J. M.; SQUIRE, J. A. Applications of SKY in cancer cytogenetics. **Cancer investigation**, v. 20, n. 3, p. 373-86, jan 2002.

BERTRAND, V.; COUTURIER-TURPIN, M.H.; LOUVEL, A.; PANIS, Y.; COUTURIER, D. Relation between cytogenetics characteristics of two human colonic adenocarcinoma cell lines and their ability to grow locally or metastasize or both: an experimental study in the nude mouse. **Cancer genetics and cytogenetics**, v.113, p.36-44, 1999.

BLACKBURN, E. H.; GREIDER, C. W. **Telomeres**, New York: Cold Spring Harbor, 1995. 396p.

BLASCO, M. A.; LEE, H.W.; HANDE, M.P.; SAMPER, E.; LANSDORP, P.M.; DEPINHO, R.A.; GREIDER, C.W. Telomere shortening and tumor formation by mouse cells lacking telomerase RNA. **Cell,** v.91, p.25-34, 1997.

BOTTURA, C.; FERRARI, I. Endoreduplication in acute leukemia. **Blood**, v. 21, p. 207-12, 1963.

BUWE, A; STEINLEIN, C.; KOEHLER, M. R. *et al.* Multicolor spectral karyotyping of rat chromosomes. **Cytogenetic and genome research**, v. 103, n. 1-2, p. 163-8, jan 2003.

CAMPISI, J.; KIM, S.; LIM C.; RUBIO, M. Cellular senescence, cancer and aging: the telomere connection. **Experimental Gerontology**, v.36, p. 1619-1637, 2001.

CASARTELLI, C. Câncer and cytogenetics. **Revista Brasileira de Genética,** v.4, p. 1109-1131, 1993.

CANTERO, G.; PASTOR, N.; MATEOS, S.; CAMPANELLA, C.; CORTÉS, F. Cisplatin-induced endoreduplication in CHO cells: DNA damage and inhibition of topoisomerase II. **Mutation research**, v. 599, n. 1-2, p. 160-166, 2006.

CHANG, M.W.F.; GRILLARI, J.; MAYRHOFER, C.; FORTSCHEGGER, K.; ALLMAIER, G.; MARZBAN,G.; KATINGER, H.; VOGLAUER, R. Comparison of early passage, senescent and hTERT immortalized endothelial cells. **Experimental Cell Research,** v.309, p.121-136, 2005.

CHANG, S.; KHOO, C.; DePINHO, R.A. Modeling chromosomal instability and epithelial carcinogenesis in the telomerase-deficient mouse. **Cancer biology**, v.11, p.227-238, 2001.

CLAUSSEN, U.; MICHEL, S.; MÜHLIG, P.; WESTERMANN, M.; GRUMMT, U.-W.; KROMEYER-HAUSCHILD, K.; LIEHR, T. Demystifying chromosome preparation and the implications for the concept of chromosome condensation during mitosis. **Cytogenet Genome Res** v. 98, p.136–146, 2002.

CORTÉS, F.; PASTOR, N. Induction of endoreduplication by topoisomerase II catalytic inhibitors. **Mutagenesis**, v. 18, n. 2, p. 105-112, 2003.

DAVID, J.; GORDON, B. R.; PELLMAN, D. Causes and consequences of aneuploidy in cancer. **Nature reviews Genetics,** v. 13, p. 189-203, 2012.

DE-MORAES, M.; MONTEIRO-MAIA, C.A.D.; DE ALMEIDA-FREITAS, R.; GALVÃO, H.C. Cell proliferation markers in oral squamous cell carcinoma. **Journal of Molecular Biomarkers & Diagnosis** S2:006. doi:10.4172/2155-9929.S2-006, 2012.

DEV, V.G.; TANTRAVAHI, R.D.A.; MILLER, O.J. Nucleolus organizers in Mus musculus subspecies and in the RAG mouse cell line. **Genetics**, v.86, p.389-398, 1977.

DUELLI , D.; LAZEBNIK, Y. Cell-to-cell fusion as a link between viruses and cancer. Nature reviews cancer. **Nature Reviews Cancer**, v.7**,** p.968-976, 2007.

DUESBERG, P.; Li, R.; FABARIUS, A.; HEHLMANN, R. The chromosomal basis of cancer. **Cellular oncology**, v.27, p.293-318, 2005.

DUESBERG, P.; Li, R.; SACHS, R.; FABARIUS, A.; UPENDER, M.B.; HEHLMANN, R. Cancer drug resistance: The central role of the karyotype. **Drug Resistance Updates**. v.10, p.51–58, 2007.

FYHRQUIST, F.; SAIJONMAA, O. Telomere length and cardiovascular aging. **Annals of medicine**, v. 44, p. 138-142, 2012.

GARINI, Y.; MACVILLE, M.; MANOIR, S. *et al.* Spectral karyotyping. v. 4, p. 65-72, 1996.

GERSEN, S. L.; KEAGLE, M. B. **The principles of clinical cytogenetics** Totowa, NJ: Humana Press, 2005.

GILLEY, D.; TANAKA, H.; HERBERT, B.S. Telomere dysfunction in aging and cancer. **The International Journal of Biochemistry and Cell Biology,** v.37, p.1000-1013, 2005.

GRIFFITH, J. D.; COMEAU, L.; ROSENFIELD, S. *et al.* Mammalian telomeres end in a large duplex loop. **Cell**, v. 97, n. 4, p. 503-14, 14 maio 1999.

GUERRA, M. **Como observar cromossomos.** Ribeirão Preto: FUNPEC, 2002.

GUO, B.; DA, W.; HAN, X. The Application of Spectral Karyotyping in Leukemia. **Chinese Journal of Clinical Oncology**, v.3, p.254-257, 2006.

GUO, Y.; LIU, J.; LI, Y.; SONG, T.; WU, J.; ZHENG, C.; XUE, C. Effect of vector-expressed shRNAs on hTERT expression. **World journal of gastroenterology**, v.11, p.2912-2915, 2005.

HAHN, H.P.; FLETCHER, C.D.M. The role of cytogenetics and molecular genetics in soft tissue tumor diagnosis – a realistic appraisal. **Current diagnostic pathology,** v.11, p.361-370, 2005.

HANAHAN, D.; WEINBERG, R.A. Hallmarks of cancer: the next generation. **Cell,** v.144, p.646-674, 2011.

HANAHAN, D.; WEINBERG, R.A. The Hallmarks of Cancer. **Cell**, v.100, p.57–70, 2000.

HANEMANN, J. A. C.; MIYAZAWA, M.; SOUZA, M. S. G. S.. Histologic grading and nucleolar organizer regions in oral squamous cell carcinomas. **Journal of Applied Oral Science,** v. 19, p. 280-285, 2011.

HARVELL, J.D.; KOHLER, S.; ZHU, S.; HERNANDEZ-BOUSSARD, T.; POLLACK, J.R.; VAN DE RIJN, M. High-Resolution Array-Based Comparative Genomic Hybridization for Distinguishing Paraffin-Embedded Spitz Nevi and Melanomas. **Diagnostic Molecular Pathology**, v.13, p.22-25, 2004.

HESELMEYER, K. MACVILLE, M.; SCHROCK,E.; BLEGEN, H.; HELLSTROM,A.C.; SHAH, K.; AUER, G.; RIED, T. Advanced-stage cervical carcinomas are defined by a recurrent pattern of chromosomal aberrations revealing high genetic instability and a consistent gain of chromosome arm 3q. **Genes Chromosomes Cancer,** v.19, p.233–240, 1997.

HOLLAND, H.; AHNERT, P.; KOSCHNY, R. *et al.* Detection of novel genomic aberrations in anaplastic astrocytomas by GTG-banding, SKY, locus-specific FISH, and high density SNP-array. **Pathology, research and practice**, v. 208, n. 6, p. 325-30, 15 jun 2012.

IMATAKA, G.; ARISAKA, O. Chromosome Analysis Using Spectral Karyotyping (SKY).**Cell Biochem Biophys**, v.62, p.13–17. 2012

ISHIDA, T.; KANEKO, S.; AKAZAWA, K.; TATEISHI, M.; SUGIO, K.; SUGIMACHI. K. Proliferating Cell Nuclear Antigen Expression and Argyrophilic Nucleolar Organizer Regions as Factors Influencing Prognosis of Surgically Treated Lung Cancer Patients **Cancer Research,** v.53, p.5000-5003, 1993.

JACKSON, S.P. Sensing and repairing DNA double-strand breaks. **Carcinogenesis,** v.23, p687-696, 2002.

KANEKO, S.; ISHIDA, T.; SUGIO, K.; YOKOYAMA, H.; SUGIMACHI. K. Nucleolar Organizer Regions as a Prognostic Indicator for Stage I Non-Small Cell Lung Cancer. **Cancer Research,** v.51, p.4008-4011, 1991.

KHANNA K.K.; JACKSON S.P. DNA double-strand breaks: signaling, repair and the cancer connection. **Nat Genet,** v.27, p.247-254, 2001.

KARLSEDER, J.; BROCCOLO, D.; DAI, Y.; HARDY, S.; LANGE, T. p53- and ATM-dependent apoptosis induced by telomeres lacking TRF2. **Science**, v.283, p.1321-1324, 1999.

KIM, N.W.; PIATYSZEK, M.A.; PROWSE, K.R.; HARLEY, C.B.; WEST, M.D.; HO, P.L.; COVIELLO, G.M.; WRIGHT, W.E.; WEINRICH, S.L.; SHAY, J.W. Specific association of human telomerase activity with immortal cells and cancer. **Science**, v.266, p.2011-2015, 1994.

KOUTSIMPELAS, D.; BRIEGER, J.; HEINRICH, U.; TORZEWSKI, M.; SOMMER, C.; MANN, W. J. Cytogenetic analysis of a malignant triton tumour by comparative genomic hybridization (CGH) and review of the literature. **Eur Arch Otorhinolaryngol**. v.268, p.1391–1396, 2011.

KROEMER, G.; POUYSSEGUR, J. Tumor cell metabolism: cancer's Achilles' heel. **Cancer Cell** v.13, p.472-482, 2008.

LARIZZA, L.; SCHIRRMACHER, V. Somatic cell fusion as a source of genetic rearrangement leading to metastatic variants. **Cancer Metastasis Reviews**. v.3, p.193–222, 1984.

LARKINS, B.A.; DILKES, B.P.; DANTE, R.A.; COELHO, C.M.; WOO, Y.; LIU, Y. Investigating the hows and whys of DNA endoreduplication. **Journal of Experimental Botany**, v.52, p.183-192, 2001.

LE SCOUARNEC, S.; GRIBBLE, S. M. Characterising chromosome rearrangements: recent technical advances in molecular cytogenetics. **Heredity,** v.108, p.75–85, 2012.

LEJNINE S.; MAKAROV, V.L.; LANGMORE, J.P. Conserved nucleoprotein structure at the ends of vertebrate and invertebrate chromosomes. **Proc Natl Acad Sci** v.92, p.2393–2397, 1995.

LENGAUER, C.; KINSLER, K.W.; VOLGELSTEIN, B. Genetic instability in colorectal cancers. **Nature**, v.386, p.623-627, 1997.

LI, S.; CROTHERS, J.; HAQQ, C.M.; BLACKBURN, E.H. Cellular and gene expression responses involved in the rapid growth inhibition of human cancer cells by RNA interference-mediated depletion of telomerase RNA. **The journal of biological chemistry**, v.280, p. 23709-23717, 2005.

LIMA E.M.; RISSINO, J.D.; HARADA, M.L.; ASSUMPCAO, P.P.; DEMACHKI, S. Conventional cytogenetic characterization of a new cell line, ACP01, established from a primary human gastric tumor. **Braz J Med Biol Res**, v.37, p.1831-1838, 2004.

LUO, J.; SOLIMINI, N.L.; ELLEDGE, S.J. Principles of cancer therapy: oncogene and non-oncogene addiction. **Cell, v.**136, p.823-837, 2009.

MARTINEZ-DELGADO, B.; YANOWSKY, K.; INGLADA-PEREZ, L. Shorter telomere length is associated with increased ovarian cancer risk in both familial and sporadic cases. **Journal of medical genetics**, v. 49, p.341-4, 2012.

MASER, R.S.; DEPINHO, R.A. Connecting chromosomes, crisis, and cancer. **Science**, v.297, p.565-569, 2002.

MAYER, V. W.; AGUILERA, A. High levels of chromosome instability in polyploids of Saccharomyces cerevisiae. **Mutation research**, v. 231, n. 2, p. 177-86, 1990.

MILLER, O.J.; MILLER, D.A.; DEV, V.G.; TANTRAVAHI, R.;CROCE, C.M. Expression of human and suppression of mouse nucleolus organizer activity in mouse–human somatic cells hybrids. **Proc. Natl Acad. Sci**. v.73, p.4531–4535, 1976.

MORELLI, S.; BERTOLLO, L.A.C; MOREIRA FILHO, O. Cytogenetics considerations on the genus Astyanax (Pisces, Characidae). II. Occurrence of natural triploidy. **Caryologia**, v.36, p.245-250, 1983.

NEGRINI, S.; GORGOULIS, V.G.; HALAZONETIS, T.D. Genomic instability--an evolving hallmark of cancer. **Nat Rev Mol Cell Biol,** v.11, p.220-228, 2010.

OJOPI, E.P.B.; NETO, E.D. Genes e câncer, alguns eventos moleculares envolvidos na formação de um tumor. **Biotecnologia Ciência e Desenvolvimento**, v.27, p.28-38, 2002.

OSHIMA, C.T.F.; FORONES, N.M. AgNOR em câncer gástrico. **Arq Gastroenterol***,* v.38, p.89-93, 2001.

PARDUE, M.L.; GALL, J. G. Molecular hybridization of radioactive DNA to the DNA of cytological preparations. **Proc Natl Acad Sci** USA 64:600-604. 1969

PIHAN, G.; DOXSEY, S.J. Mutations and aneuploidy: Co-conspirators in cancer? **Cancer cell,** v.4, p.89-94, 2003.

PINKEL, D.; SEGRAVES, R.; SUDAR, D.; CLARK, .;, POOLE, I.; KOWBEL, D.; COLLINS, C.; KUO. W. L.; CHEN, C.; ZHAI, Y.; DAIRKEE, S. H.; LJUNG, B.

M.; GRAY, J. W.; ALBERTSON, D. G. High resolution analysis of DNA copy number variation using comparative genomic hybridization to microarrays**. Nat Genet.** v.20, p.207-211, 1998.

PONDER, B. A. J. Câncer genetics. **Nature,** v.411, p.336-341, 2001.

PUIG, P.-E.; GUILLY, M.-N.; BOUCHOT, A. *et al.* Tumor cells can escape DNA-damaging cisplatin through DNA endoreduplication and reversible polyploidy. **Cell biology international**, v. 32, n. 9, p. 1031-43, 2008.

RAJPUT DV, TUPKARI JV. Early detection of oral cancer: PAP and AgNOR staining in brush biopsies. **Journal of oral and maxillofacial pathology,** v. 14, p. 52-58, 2010.

RAMPAZZO, E.; BONALDI, L.; TRENTIN, L. *et al.* Telomere length and telomerase levels delineate subgroups of B-cell chronic lymphocytic leukemia with different biological characteristics and clinical outcomes. **Haematologica**, v. 97, p.56-63, 2012.

SANDBERG, A. A.; MELONI-EHRIG, A. M.Cytogenetics and genetics of human cancer: methods and accomplishments. **Cancer Genetics and Cytogenetics.** v.203, p.102-126, 2010.

SAUNDERS WS, SHUSTER M, HUANG X, GHARAIBEH B, ENYENIHI AH, PETERSEN I, GOLLIN SM. Chromosomal instability and cytoskeletal defects in oral cancer cells. **Proc. Natl Acad. Sci**, v.97, p.303-308, 2000.

SAWYER, J.R. The prognostic significance of cytogenetics and molecular profiling in multiple myeloma. **Cancer Genetics**, v.204, p.3-12, 2011.

SCHWARZACHER, H. G.; MIKELSAAR, A. V. & SCHNEDL, W. The nature of the Ag-staining of nucleolus organizer regions. Electron and light microscopic studies on human cells in interphase, mitosis and meiosis. **Cytogenetic and Cell Genetics,** v.20, p.24-39, 1978.

STOCK, R.P.; BIALY,H. The sigmoidal curve of cancer. **Nature biotechnology,** v.21, p.13-14, 2003.

STORCHOVA, Z.; PELLMAN, D. From polyploidy to aneuploidy, genome instability and cancer. **Molecular cell biology**, v.5, p.45-54, 2004.

SUMNER, A.T. Induction of diplochromosomes in mammalian cells by inhibitors of topo II. **Chromosoma,** v.107, p.486–490, 1998.

TAKAHASHI, A.; HIGASHINO, F.; AOYAGI, M.; YOSHIDA, K.; ITOH, M.; KYO, S.; OHNO, T.; TAIRA, T.; ARIGA, H.; NAJAJIMA, K.; HATTA, M.; KOBAYASHI, M.; SANO, H.; KOHGO, T.; SHINDOH, M. EWS/ETS Fusions activate telomerase in Ewing`s tumor. **Cancer research**, v.63, p. 8338-8334, 2003.

WAN, T.S.K.; MA, E.S.K. Molecular Cytogenetics: An Indispensable Tool for Cancer Diagnosis.Chang Gung Med J. v.35, p.96-110, 2012.

WILSON, L.; MEZA, I. The mechanism of action of colchicine. **The Journal of cell biology**, v. 58, n. 3, p. 709-19, set 1973.

YEH, I. ; VEMULA, S. S.; MIRZA, S.A.; MCCALMONT, T.H. Neurofibroma-Like Spindle Cell Melanoma: CD34 Fingerprint and CGH for Diagnosis. **American Journal of Dermatopathology**, v.34, p 668–670, 2012.

ZHOU, X.; MEEKER, A. K.; MAKAMBI, K. H. Telomere length variation in normal epithelial cells adjacent to tumor: potential biomarker for breast cancer local recurrence. **Carcinogenesis**, v.3, p.113-8, 2012

ZUCKERBERG, C. Ultrastructure of Sarcoma 180. **Cancer Research,** v.33, p.2278-2282, 1973.

Capítulo 2: Fundamentação teórica

“Phage display and its prospects of uses in imaging and drug delivery”

Artigo de revisão formatado de acordo com as normas da revista

Molecules

Phage display and its prospects of uses in imaging and drug delivery

Oliveira-Júnior, RJ[1]; Santos, FAA[1]; Souza, MI[1]; Goulart, LR[1]; Morelli, S[1].
[1]Instituto de Genética e Bioquímica, Universidade Federal de Uberlândia, MG;
[2]Instituto de Biologia, Universidade Federal de Uberlândia, MG;
robson_junr@yahoo.com.br

Abstract

Therapy and diagnosis of cancer are major goals of many research centers around the world. Among available strategies, the phage display subtractive proteomic technology has provided important information for putative therapeutic and diagnostic targets. The technology involves the screening of ligands randomly displayed in the surface bacteriophage libraries, which consists of successive cycles of selection, washing, elution and amplification, resulting in high affinity peptide/antibody markers to any given target. These ligands can be used to recognize specific cancer markers or cells, either as direct therapeutic molecules to malignant cells or as sensing molecules for imaging analysis. Prominent examples of peptide phage display uses for imaging, diagnosis and drug delivery will be presented in the present review, in order to evidence the importance of this technology which has had a major impact on immunology, cell biology, drug discovery and pharmacology

Key-words: Bioactive peptides; tumor homing; diagnosis**.**

1. Introduction to phage display

Phages are viruses that infect bacterial cells, also called bacteriophages. This microorganism is largely used in genetic research as a vector to perform recombinant DNA research. Most phages used as vectors are the ones that infect the *Escherichia coli*, the standard host bacterium. Recombinant DNA vectors, including phages, accommodate segments of foreign DNA selected by researchers [1]. The filamentous phage particles used in phage display (strain M13, fd and f1), which infect E. coli via F pilus consist of a single stranded DNA enclosed in a protein capsule composed by five proteins (pIII, PVI, pVII, pVIII and pIX) (Figure 1). From these proteins there are approximately 2800 copies of the protein expressed by gene 8 (g8 or pVIII, a protein of 50 amino acid

residues) and 3 to 5 copies of gene 3 protein (g3 or pIII protein of 406 amino acids) [2]. The possibility of expressing a fusion protein on the capsid of bacteriophages, displayed in immunologically accessible form on the infectious particle, was demonstrated in 1985 by George Pieczenik Smith, to achieve expression of the restriction enzyme EcoRI by three fusion protein (pIII) of phage capsid [1].

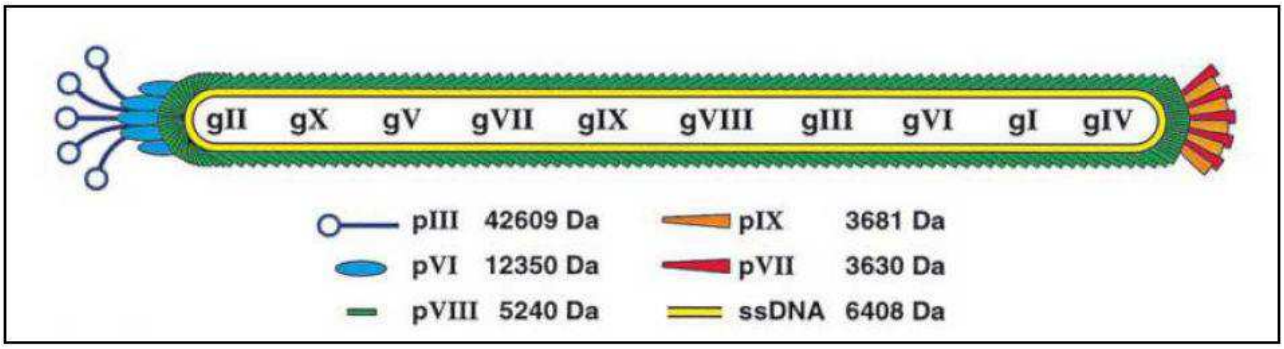

Figure 1: Filamentous phage scheme [3].

Phage display is an efficient technique for identifying peptides or proteins that bind to other molecules with different purposes. Since its inception in 1985, many thousands of peptides have been isolated and investigated using phage display. Such peptides are being explored in vaccine development, enzyme inhibition, inflammation, plant pathology, cardiovascular disease, cancer, etc. [4]. The technology is based on the principle that polypeptides can be expressed on the surface of filamentous bacteriophage. In case of phage display, the recombinant DNA of bacteriophage vector programs machinery of the *E. coli* host cell to synthesize a foreign peptide whose amino acid sequence is determined (*via* the genetic code) by the nucleotide sequence of the insert, establishing a physical linkage between phenotype and genotype. The DNA insert is spliced into the gene for one of the phage coat proteins, so that the foreign amino acid sequence is genetically fused to the endogenous amino acids of the coat protein to make a hybrid “fusion” protein or peptide. The hybrid coat protein is incorporated into phage particles (“virions”) as they are released from the cell, so that the foreign peptide or protein domain is displayed on the outer surface [1][5][6][7].

Phage display is a powerful technology for selecting and engineering polypeptides with novel functions. Highly diverse libraries can be constructed by fusing degenerate DNA to a coat protein gene, and library members with

desired binding specificities can be isolated by binding to an immobilized receptor *in vitro*. The sequences of selected polypeptides can be determined from the sequence of the encapsulated, encoding DNA and synthesized artificially [5].

This technology has had a major impact on immunology, cell biology, drug discovery and pharmacology. Its utility lies principally in generating molecular probes against specific targets and for the analysis and manipulation of protein/ligand interactions. Using phage display, libraries of variant nucleotide sequences with diversities of millions or billions may be converted into populations of displayed variant proteins which can then be conveniently screened for desirable properties [8].

In phage display system, the gene encoding the peptide or protein of interest is generally fused to a gene of two capsule proteins [9][10][6]. The peptide is typically expressed at the N-terminal of pIII or pVIII. The pIII protein is related to the infectivity of phage for binding to f pilus of bacteria. Due to the low representation of pIII in relation to pVIII in the virus coat, libraries using pIII fused synthetic peptides are more suitable for discovering ligands with high affinity, compared with the libraries of synthetic peptides fused in pVIII [10]. An advantage of the use of bacteriophage is that they do not generate a lytic infection in *Escherichia coli*, but rather, they induce a state in which the infected bacterium produces and secretes phage particles without undergoing lysis.

Infection is initiated by the coupling of the phage pIII protein in the f pilus of male *E. coli*. Only the single-stranded circular DNA of the phage penetrates the bacterium, where it is converted by bacterial replication machinery into a double stranded plasmid DNA, becoming replicative. This double stranded plasmid form undergoes constant replication to generate single-stranded DNA and also serve as a template for phage proteins expression. Phage progeny is assembled by packaging the single stranded DNA into protein capsids and after assembled, virions are released through bacteria membrane to extracellular medium [11].

Libraries of peptides generated by phage display are extensively applied to the discovery of a wide variety of polypeptides including antibodies, receptors, hormones, protease inhibitors, enzymes and proteins [12]. Antigenic determinants or epitopes (antigen regions recognized by antibodies) also can

be identified by this methodology, which has been extremely important for the identification and characterization of novel high-affinity ligands and its receptors in a multitude of diseases, including cancer, infectious, cardiovascular and autoimmune diseases [13].

The peptide libraries comprise a huge number of phages displaying random peptides of a given length, where their sequences are generated randomly for a variety of amino acid residues at each position. Construction of these libraries is mainly done by inserting degenerated oligonucleotides randomly chemically synthesized in the gene encoding the capsid protein. These libraries can be commercially purchased which ensures better maintenance of variability and can be easily used to select and purify specific phage particles bearing sequences with desired binding specificities [11].

The selection of peptides sequences based on the binding affinity of the phage to a target molecule is made by an *in vitro* or *in vivo* selection process called biopanning [14]. The biopanning is performed by incubating the peptide library exposed in phages against the chosen target. The target can be immobilized on a solid support which can be ELISA plates, magnetic microspheres or affinity resins and cell membranes. Phages that did not bind to the target are removed by successive washes and phages that bind in a specific way to the target remain bound for subsequent elution. The pool of specific phages is amplified for the next cycles of biological selection or biopanning (cycles of binding, elution and amplification) to ensure the enrichment of phages with specific sequences against the target. After three or four passages individual clones are characterized by DNA sequencing, western blotting and ELISA [15]. To better understand the selection process, a schematic illustration of biopanning immobilized on a solid support is represented below (Figure 2).

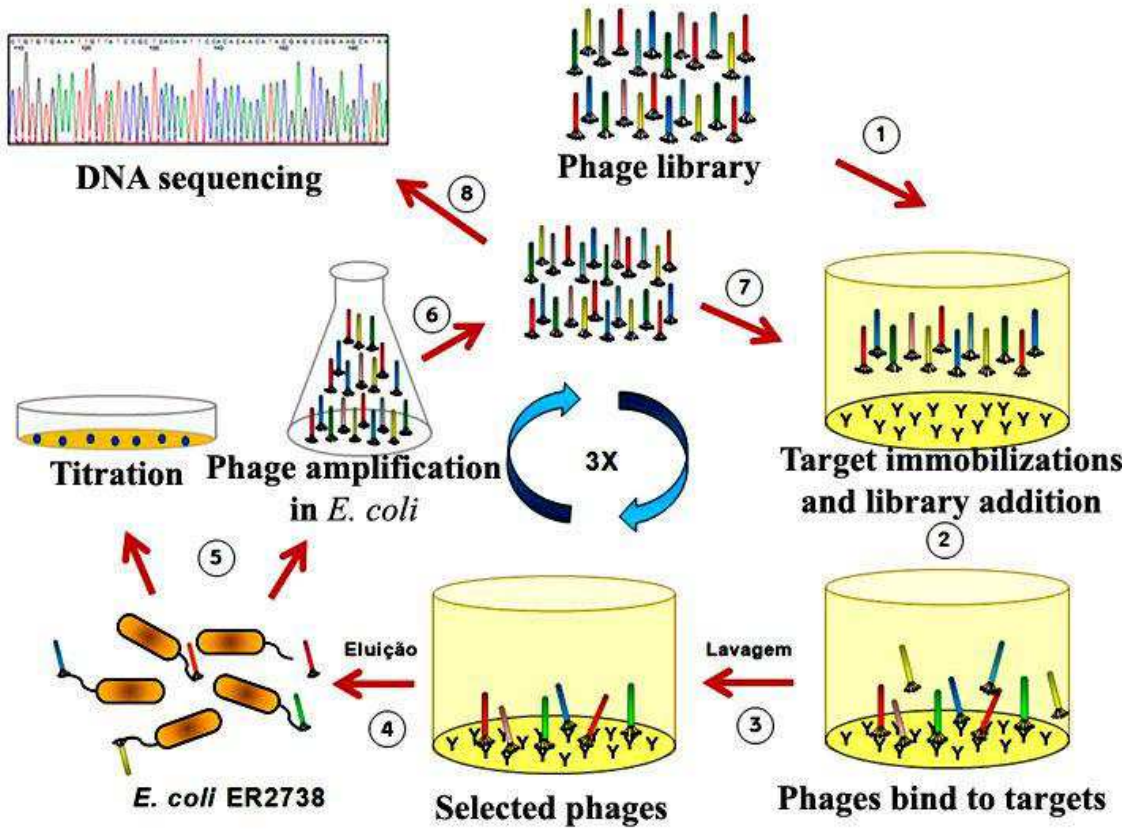

Figure 2: Schematic representation of biopanning process. The target is immobilized in a solid support and phage library is added. After incubation period, unbound phages are removed by successive washings. The bound phages are eluted, amplified in *E. coli* ER2738 an titrated. This cycle repeats for three rounds and after the last one, eluted phages are amplified and sequenced. Phage clones which express a peptide with the highest affinity for the target are selected [16].

Using the genetic code, the results of DNA sequencing are traduced to a peptide sequence, which is aligned with protein sequences of the target organism in order to analyze the possible protein that interact with the selected peptide. The selection of peptides for biological affinity with the use of random peptide libraries often reveals unexpected ligands that do not line up in linear epitopes of the target and do not have known sequences. This primarily occurs when the natural receptor epitopes are not from protein source, are discontinuous or even dependent on protein conformation [6]. Compared with small molecules and antibodies, peptides have often been neglected as potential drugs; although they are capable of binding their target proteins with

high affinity and unsurpassed specificity, and are thus attracting increasing attention as therapeutics and imaging diagnosis [17].

2. Phage display as a source of imaging peptides

The concepts of biomarkers have been summarized by the NIH Definitions Working Group as a characteristic that is objectively measured and evaluated as an indicator of normal biological processes, pathogenic processes, or pharmacologic responses to a therapeutic intervention [18].

Biomarkers can be used in many scientific fields and have great value in early efficacy and safety evaluations, disease diagnosis/staging, indicating disease prognosis, and prediction/monitoring of clinical response to a given intervention. Recently, molecular imaging with biological markers has emerged to provide valuable information at the structural/functional and/or molecular level [19].

In vivo molecular imaging has been identified by the National Cancer Institute as an extraordinary opportunity for studying diseases noninvasively and, in many cases, quantitatively at the molecular level. It is a growing research discipline aimed at developing and testing novel tools, reagents, and methods to image specific molecular pathways in vivo, particularly those that are key targets in disease processes. Target identification and validation with high-affinity probes is one of the key prerequisites for interrogation of specific molecular targets in living systems. Such probes can be small molecules—for example, receptor ligands or enzyme substrates. Alternatively, higher molecular weight affinity ligands (“biotechnology drugs”) are often utilized (eg, monoclonal antibodies, recombinant proteins). Although the design of potential affinity ligands against thousands of targets may appear daunting at first glance, recent advances in drug discovery technology (combinatorial techniques, rational design, high-throughput testing, robotics, target identification, and validation through genomic sciences) have helped move this process forward rapidly [20].

Molecular imaging requires multiple functional components, though in practice more than one function can be integrated into a single element. Localization and retention at the site of interest is typically via a *ligand* with both affinity and specificity for the target, for example antibody fragment or peptide. A contrast or *signaling element*, for example fluorochromes or quantum dots, may

be incorporated directly into the ligand or may be conveyed by a *carrier vehicle*, as nanoparticles or liposomes [21].

New peptide-based probes to facilitate the molecular imaging of disease are rapidly evolving due to implementation of combinatorial chemistry and bacteriophage (phage) display [4]. The use of phage as selfreplicating biological nanoparticles is a very safe, simple and attractive solution for the development and implementation of in vivo imaging modalities [22]. Compared with relatively large biomolecules, such as antibodies and proteins, small peptides have advantages as potential probes for molecular imaging. The display of peptide libraries on the surface of bacteriophage (phage) offers a way of searching for peptides with specific binding properties. Phage display peptide libraries are commonly used to obtain defined peptide sequences that interact with a particular molecule. The strength of this technology is its ability to identify interactive regions of proteins and other molecules without preexisting notions about the nature of the interaction. Especially, *in vivo* phage display selection procedures offer an advantage over *in vitro* screening protocols in that phages can be selected based on desired pharmacokinetic properties, including delivery and tumoral accumulation [19]. In this context, phage display can be an excellent tool to select ligands to any kind of desired *in vivo* imaging.

2.1 Using phage display for developing imaging markers for cancer

In a recent study, Chen et al. (2011) used phage display technique to select a peptide called GX1 which binds specifically to endothelium of solid tumors. They labeled this peptide with ^{64}Cu to turns it a radiotracer against a U87MG tumor xenografted mouse model and used the positron emission tomography (PET) to visualize the targeted tumor vasculature. They concluded that this radiolabeled peptide can be a promising radiotracer for imaging tumor vasculature and offers a noninvasive method for early detection of tumor angiogenesis and efficient monitoring of response to anti-tumor vasculature therapy [23].

According to Cao et al. (2011), early evaluation of cancer response to a therapeutic regimen can help increase the effectiveness of treatment schemes and, by enabling early termination of ineffective treatments, minimize toxicity, and reduce expenses. Looking for develop a class of novel molecular imaging to predict tumor early response to an antiangiogenic drugs, through six rounds

of biopanning Cao´s group selected a 12-mer peptide from a phage-display library which is able to bind to tumors treated with the humanized vascular endothelial growth factor antibody bevacizumab. The selected bevacizumab-responsive peptide (BRP) may be potentially useful pre-clinically and clinically for monitoring treatment response [19].

In a study using the xenografic human tumor model PC-3 prostate carcinoma, Newton-Northup et al. (2009), found a phage called G1, which was capable to extravasate the vasculature and bind directly to human PC-3 prostate carcinoma tumor cells in vivo, a fact demonstrated via immunocytochemical analysis. The authors developed two different pretargeting strategies. The two-step strategy used the biotinylated phage and ^{111}In-labeled DTPA conjugated to streptavidin, while the three-step pretargeting system involved, first, administration of biotinylated G1 phage, followed by injection of avidin and, finally, ^{111}In-labeled DOTA-biotin injection. Their results indicated that in the use of a phage-based tumor-targeting scheme for the *in vivo* imaging of cancer, the three-step pretargeting method is likely the most effective form described to date, once that in vivo SPECT/CT imaging of xenografted PC-3 tumors in SCID mice with the three-step pretargeting method was superior to that of the two-step pretargeting method, and, importantly, blocking studies demonstrated specificity of tumor uptake of ^{111}In-labeled biotin in the three-step pretargeting scheme [22].

The membrane type 1 metalloproteinases (MT1-MMP) is highly expressed in different cancers and plays an essential role in pathological processes as arthritis, tumorigenesis, tumor growth, invasion, metastasis and angiogenesis. Zhu et al. (2011) used a Ph.D.-12™ phage display peptide library and selected a peptide called MT1-AF7p, which showed high MT1-MMP binding affinity. This peptide was conjugated with the near-infrared fluorescent (NIRF) dye Cy5.5 for tumor imaging and they concluded that it can be used to mediate imaging of MT1-MMP expression in tumor sites and this MT1-MMP affinity peptide can be also explored in peptide mediated drug delivery that targets MT1-MMP. This strategy can be used to selectively target and kill tumor cells that overexpress MT1-MMP or newly formed neovasculature [24].

Sun et al (2012) performed a phage display–based screening from the Ph.D.-12 phage display peptide library, for selecting peptide sequences that

bind specifically to 143B osteosarcoma cells. The cell line 293T human embryonic kidney was used as negative control to eliminate phages that binds to normal cells. From biopanning, after four rounds of *in vitro* selection, they obtained the enrichment of peptides with the dominant sequence ASGALSPSRLDT, which was named as OSP-1. They suggested that the selected peptide is osteosarcoma specific, and the binding site of OSP-1 might be related to heparan sulfate proteoglycans. The OSP-1 peptide can be labeled to serve as a probe for osteosarcoma imaging *in vivo* and *in vitro*, helping in the diagnosis, or can be coupled to radioactive isotopes or even other drugs to treatment of osteosarcomas [25].

2.2 Using phage display for developing imaging markers for other diseases

Staniszewska et al. (2012), observed that the surface of abnormal neovessels expresses epitopes that are absent from normal neovessels using phage display technology. They induced abnormal retinal neovascularization in rats and screened a phage library over the surface of flat-mounted retinas and obtained specific phage called SH which expresses a peptide that has the potential to image and/or deliver payloads to abnormal neovessels. For instance, as an imaging tool, it could be used to assess the likelihood that patients with nonproliferative diabetic retinopathy will progress to the proliferative stage of the disease. Similarly, such an imaging tool would be invaluable to assess the efficacy of anti-angiogenic therapies. A reagent that targets neovessels could also be used as a vehicle to deliver cytotoxic agents with the overall intent of eliminating the neovessels [26]

Molecular and cellular processes of atherosclerosis, thrombosis, and vascular inflammation have identified new targets for imaging. The common goals of molecular imaging approaches are to accelerate and refine diagnosis, provide insights that reveal disease diversity, guide specific therapies, and monitor the effects of those therapies. In this context, peptides selected through phage display have been used as a source of ligands to direct specific therapies and imaging diagnostic to cardiovascular diseases [21].

As example it can be cited peptides which binds to vascular cell adhesion molecule-1 (VCAM-1), selected to target atherosclerotic plaques. Kelly, et al.

(2005), selected a peptide with one specific sequence containing the VHSPNKK motif, which binds to VCAM-1 and block leukocyte–endothelial interactions. This peptide was conjugated with iron nanoparticles and a fluorescent reporter and after injected into a mice model. These specific probes accumulate within endothelial cells at sites that develop atherosclerosis appearing intensely marked [27]. The group of Nahrendorf et al. (2009) also developed and validated a ligand labeled peptide called ^{18}F-4V which has affinity and specificity for VCAM-1. In their study, they concluded that the selected peptide allows noninvasive PET-CT imaging of VCAM-1 in inflammatory atherosclerosis, has the dynamic range to quantify treatment effects, and correlates with inflammatory gene expression [28]

Kolodziej et al. (2012) selected three classes of cyclic peptides (cyclized via disulfide bond between two Cys residues) that that bind to two unique sites of fibrin but not to fibrinogen or serum albumin. These peptides can be used as targeting moieties for thrombus molecular imaging probes, representing useful building blocks to create conjugates for fibrin-targeted imaging or therapy [29].

Inflammation is one of the major signs indicating the presence of either exogenous or endogenous danger signals in one of the body's tissues or organs. A non-invasive molecular imaging, aimed at tracking cellular and molecular events in their native environment in the intact living subject, has grown to be a powerful technique to help in the refined monitoring of inflammation [30].

Considering that injured intestine is responsible for significant morbidity and mortality after severe trauma and burn, Costantini, et al. (2012) used a Ph.D-12 Phage Display Peptide library to perform an *in vivo* biopanning using an animal model of burn injury, to select clones that express peptides which bind to the intestinal epithelium after severe burn injury. The group identified 3 gut-targeting peptide sequences which are internalized into both the normal and injured intestine. In the future the identified peptides may be used to the delivery of biotherapeutics [31].

3. Using phage display as a source of peptides to direct the drug delivery.

There is a growing interest in peptides that can direct drug molecules with specificity to target any site where it is needed. In this context, phage display technology has emerged as an important method to select peptides able to bind to any desired target molecule.

Peptides possess favorable pharmacokinetic properties through their small size, such as rapid clearance from blood, while lacking the immunogenic potential of antibodies [30]. However, the biodistribution, stability, and internalization efficiency of these homing peptides needs to be considerably improved [31][32][33][34]. Numerous structural modifications can be introduced into peptides to further broaden the chemical space and develop analogues with improved pharmacokinetic and/or pharmacodynamic characteristics [35][36][37].

Identification of peptides with specific targeting abilities and tumor affinity is a major challenge in cancer-related peptide research [34]. Phage display techniques have also been used to obtain novel peptides with a high specificity for cancers, and the isolation of homing peptides that recognize tumor-type-specific differences has also been reported [31]. Numerous peptides that target specific tissues, including both normal and cancerous tissues, have been discovered using this technology [38]

Viruses, such as M13 phage, have the unique advantage of structural uniformity and their chemical and conformational structures can be produced precisely and in large quantities. The versatile hierarchical assembly of viral coat protein subunits provides a natural and easy way for drug packaging [39].

Filamentous bacteriophages (phages) are the workhorse of antibody engineering and are gaining increasing importance in nanobiotechnology. Recently, an efficient integrated phage/virus system was developed where tumor targeting and molecular genetics imaging were merged into an integrated platform [40]

Conjugated cargos that have been selectively delivered to tumors include compounds such as doxorubicin, Taxol and apoptotic peptides, and these have been successfully used to reduce tumor growth while allowing the treatment of

recurrent malignant tumors in clinical trials. Some peptides such as somatostatin, and bombesin, which target receptors that are overexpressed in tumors have direct applications in diagnosis, radiopeptide therapy, and targeted delivery have been reported [31]. Some examples are the peptide CaIX-P1 is a promising candidate for the development of new ligands targeting human carbonic anhydrase IX, a cancer biomarker [30][34] and the peptide ZS-1, a potential candidate of biomarker ligands used for targeted drug delivery in therapy of lung cancer [41]. In general, combined with rational drug design, the screening of combinatorial peptide libraries against membrane receptors is a powerful tool for discovering novel pharmacologically active receptor agonists and antagonists or small peptide ligands for the targeted delivery of drugs, genes and diagnostics [35].

4. Final considerations

Phage display is a powerfull technology in which utility lies principally in generating molecular probes against specific targets and for the analysis and manipulation of protein/ligand interactions. The success in obtaining peptides with high affinity and specificity to its targets depends on biopanning selection strategy. Bioactive peptides can be screened to inumerous purposes, since imaging, diagnosis, and prognosis until drug delivery and even as a source of therapeutic molecules.

5. References

1. Smith, G. P.; Petrenko, V. a. Phage Display. *Chemical reviews* **1997**, *97*, 391–410.

2. Russel, M. Filamentous phage assembly. **1991**, *5*.

3. Deutscher, S. L. Phage Display in Molecular Imaging and Diagnosis of Cancer. **2011**, *110*, 3196–3211.

4. Francisco, S. S. Phage display in pharmaceutical biotechnology Sachdev S Sidhu. **2000**, 610–616.

5. Barbas, C. F. I.; Burton, D. R.; Scott, J. K.; Silverman, G. J. *Phage Display: A Laboratory Manual*; first.; Cold Spring Harbor Laboratory Press: New york, 2001; p. 736.

6. Smith, G. P. Filamentous fusion phage: novel expression vectors that display cloned antigens on the virion surface. *Science (New York, N.Y.)* **1985**, *228*, 1315–7.

7. Willats, W. G. T. Phage display: practicalities and prospects. *Plant molecular biology* **2002**, *50*, 837–54.

8. Phizicky, E. M.; Fields, S. Protein-protein interactions : methods for detection and analysis. **1995**, *59*.

9. Brígido, M.D.M. & Maranhão, A. . Bibliotecas Apresentadas em FAGOS. *Biotecnologia Ciência e Desenvolvimento* **2002**, *26*, 44–51.

10. Azzazy, H. M. E.; Highsmith, W. E. Phage display technology: clinical applications and recent innovations. *Clinical biochemistry* **2002**, *35*, 425–45.

11. de Haard, H. J.; van Neer, N.; Reurs, a; Hufton, S. E.; Roovers, R. C.; Henderikx, P.; de Bruïne, a P.; Arends, J. W.; Hoogenboom, H. R. A large non-immunized human Fab fragment phage library that permits rapid isolation and kinetic analysis of high affinity antibodies. *The Journal of biological chemistry* **1999**, *274*, 18218–30.

12. Stephen, C. W.; Helminen, P.; Lane, D. P. Characterisation of epitopes on human p53 using phage-displayed peptide libraries: insights into antibody-peptide interactions. *Journal of molecular biology* **1995**, *248*, 58–78.

13. Parmley, S. F.; Smith, G. P. Antibody-selectable filamentous fd phage vectors: affinity purification of target genes. *Gene 73*, 305–318.

14. Benhar, I. Biotechnological applications of phage and cell display. *Biotechnology advances* **2001**, *19*, 1–33.

15. Sun, N.; Aileen, S.; Willbold, D. Mirror image phage display – Generating stable therapeutically and diagnostically active peptides with biotechnological means. *Journal of Biotechnology* **2012**, *161*, 121–125.

16. Abstracts of the NIH-FDA Conference " Biomarkers and Surrogate Endpoints : Advancing Clinical Research and Applications ."**1998**, *14*, 187–334.

17. Cao, Q.; Liu, S.; Niu, G.; Chen, K.; Yan, Y.; Liu, Z.; Chen, X. Phage display peptide probes for imaging early response to bevacizumab treatment. **2011**, 1103–1112.

18. Weissleder, R. Molecular Imaging. **2000**.

19. Choudhury, R. P.; Fisher, E. A. Molecular Imaging in Atherosclerosis, Thrombosis, and Vascular Inflammation. *Arteriosclerosis, Thrombosis, and Vascular Biology* **2009**, *29*, 983–991.

20. Newton-Northup, J. R.; Figueroa, S. D.; Quinn, T. P.; Deutscher, S. L. Bifunctional phage-based pretargeted imaging of human prostate carcinoma. *Nuclear medicine and biology* **2009**, *36*, 789–800.

21. Chen, K.; Sun, X.; Niu, G.; Ma, Y.; Yap, L.-P.; Hui, X.; Wu, K.; Fan, D.; Conti, P. S.; Chen, X. Evaluation of 64Cu labeled GX1: a phage display peptide probe for PET imaging of tumor vasculature. *Molecular imaging and biology : MIB : the official publication of the Academy of Molecular Imaging* **2012**, *14*, 96–105.

22. Zhu, L.; Wang, H.; Wang, L.; Wang, Y.; Jiang, K.; Li, C.; Ma, Q.; Gao, S.; Wang, L.; Li, W.; Cai, M.; Wang, H.; Niu, G.; Lee, S.; Yang, W.; Fang, X.; Chen, X. High-affinity peptide against MT1-MMP for in vivo tumor imaging. *Journal of Controlled Release* **2011**, *150*, 248–255.

23. Sun, X.; Niu, G.; Yan, Y.; Yang, M.; Chen, K.; Ma, Y.; Chan, N. Phage Display − Derived Peptides for Osteosarcoma Imaging Phage Display – Derived Peptides for Osteosarcoma Imaging. *Clinical Cancer Research* **2010**, *16*, 4268–4277.

24. Staniszewska, M.; Gu, X.; Romano, C.; Kazlauskas, A. A phage display-based approach to investigate abnormal neovessels of the retina. *Investigative ophthalmology & visual science* **2012**, *53*, 4371–9.

25. Kelly, K. A.; Allport, J. R.; Tsourkas, A.; Shinde-patil, V. R.; Weissleder, R.; Josephson, L. Detection of Vascular Adhesion Molecule-1 Expression Using a Novel Multimodal Nanoparticle. **2005**, 327–336.

26. Zhang, H.; Hembrador, S.; Figueiredo, J.; Aikawa, E.; Kelly, K.; Libby, P.; Weissleder, R. 18F-4V for PET–CT Imaging of VCAM-1 Expression in Atherosclerosis. *JACC: cardiovascular imaging,* **2009**, *2*, 1213–1222.

27. Kolodziej, A. F.; Nair, S. A.; Graham, P.; Mcmurry, T. J.; Ladner, R. C.; Wescott, C.; Sexton, D. J.; Caravan, P. Fibrin Specific Peptides Derived by Phage Display: Characterization of Peptides and Conjugates for Imaging. *Bioconjugate Chemistry* **2012**, *23*, 548−556.

28. Schoonooghe, S.; Laoui, D.; Ginderachter, J. A. V.; Devoogdt, N.; Lahoutte, T.; Baetselier, P. D.; Raes, G. Novel applications of nanobodies for in vivo bio-imaging of inflamed tissues in inflammatory diseases and cancer. *Immunobiology* **2012**.

29. Costantini, T. W.; Eliceiri, B. P.; Putnam, J. G.; Bansal, V.; Baird, A.; Coimbra, R. Peptides Intravenous phage display identifies peptide sequences that target the burn-injured intestine. *Peptides* **2012**, *38*, 94–99.

30. Askoxylakis, V.; Garcia-Boy, R.; Rana, S.; Krämer, S.; Hebling, U.; Mier, W.; Altmann, A.; Markert, A.; Debus, J.; Haberkorn, U. A new peptide ligand for targeting human carbonic anhydrase IX, identified through the phage display technology. *PloS one* **2010**, *5*, e15962.

31. Nakase, I.; Konishi, Y.; Ueda, M.; Saji, H.; Futaki, S. Accumulation of arginine-rich cell-penetrating peptides in tumors and the potential for anticancer drug delivery in vivo. *Journal of controlled release : official journal of the Controlled Release Society* **2012**, *159*, 181–8.

32. Liu, S. Radiolabeled cyclic RGD peptides as integrin alpha(v)beta(3)-targeted radiotracers: maximizing binding affinity via bivalency. *Bioconjug. Chem.* **2009**, *20*, 2199–2213.

33. Pool, S. E.; Krenning, E. P.; Koning, G. A.; Van, C. H.; Eijck, J. J.; Teunissen, B.; Kam, R.; Valkema, D.J. Kwekkeboom, M. Preclinical and clinical studies of peptide receptor radionuclide therapy. *Semin. Nucl. Med.* **2010**, *40*, 209–218.

34. Askoxylakis, V.; Zitzmann-Kolbe, S.; Zoller, F.; Altmann, A.; Markert, A.; Rana, S.; Marr, A.; Mier, W.; Debus, J.; Haberkorn, U. Challenges in optimizing a prostate carcinoma binding peptide, identified through the phage display technology. *Molecules* **2011**, *16*, 1559–1578.

35. Molek, P.; Strukelj, B.; Bratkovic, T. Peptide Phage Display as a Tool for Drug Discovery: Targeting Membrane Receptors. *molecules* **2011**, 857–887.

36. Lien, S.; Lowman, H. B. Therapeutic peptides. *Trends Biotechnol.* **2003**, *21*, 556–562.

37. Funke, S. A.; Willbold, D. Mirror image phage display - a method to generate D-peptide ligands for use in diagnostic or therapeutical applications. *Mol. Biosyst.* **2009**, *5*, 783–786.

38. Svensen, N.; Walton, J. G. a; Bradley, M. Peptides for cell-selective drug delivery. *Trends in pharmacological sciences* **2012**, *33*, 186–92.

39. Ma, Y.; Nolte, R. J. M.; Cornelissen, J. J. L. M. Virus-based nanocarriers for drug delivery. *Advanced drug delivery reviews* **2012**, *64*, 811–25.

40. Bar, H.; Yacoby, I.; Benhar, I. Killing cancer cells by targeted drug-carrying phage nanomedicines. *BMC biotechnology* **2008**, *8*, 37.

41. Zang, L.; Shi, L.; Guo, J.; Pan, Q.; Wu, W.; Pan, X.; Wang, J. Screening and identification of a peptide specifically targeted to NCI-H1299 from a phage display peptide library. *Cancer letters* **2009**, *281*, 64–70.

Capítulo 3:

“Murine sarcoma development: from chromosome instability to highly stable phenotypes mediated by telomerase over-expression”

Artigo submetido à revista DNA and Cell Biology

Murine sarcoma development: from chromosome instability to highly stable phenotypes mediated by telomerase over-expression

Robson J. de Oliveira-Júnior[1*], Carlos Ueira-Vieira[1], Angela A. S. Sena[1], Carolina F. Reis[1], José R. Mineo[2], Luiz R. Goulart[1,3†], Sandra Morelli[1†]

[1] Institute of Genetics and Biochemistry, Federal University of Uberlândia, Uberlândia, MG, Brazil; [2] Institute of Biomedical Sciences, Federal University of Uberlândia, Uberlândia, MG, Brazil; [3] Department of Medical Microbiology and Immunology, University of California Davis, Davis, CA, USA. [†] **Co-senior authors.**

[*]**Corresponding author:** Robson J. Oliveira-Junior. Institute of Genetics and Biochemistry, Federal University of Uberlândia, Lab. of Nanobiotechnology, Campus Umuarama, Bloco 2E, Sala 248, Uberlândia, MG, Brazil. E-mail: robson_junr@yahoo.com.br

Abstract

Tumor initiation presents a complex and unstable genomic landscape; one of the earliest hallmark events of cancer, and its progression is probably based on selection mechanisms under specific environments that lead to functional tumor cell speciation. We hypothesized that viable tumor phenotypes possess common and highly stable karyotypes and their proliferation is facilitated by an attuned high telomerase activity. Very few investigations have focused on the evolution of common chromosomal rearrangements associated molecular events that result in functional phenotypes during tumor development. We have used cytogenetic, flow cytometry, and cell culture tools to investigate chromosomal rearrangements and clonality during cancer development using the murine sarcoma TG180 model, and also molecular biology techniques to establish a correlation between chromosome instability and telomerase activity, since telomeres are highly affected during cancer evolution. Cytogenetic analysis showed a near-tetraploid karyotype originated by endoreduplication. Specific chromosome aberrations and activated regions (NOR and rDNA) were ubiquitous in the karyotype, suggesting that the conservation of these patterns may be advantageous for tumor progression. High telomerase expression was also correlated with the chromosomal rearrangements stabilization. Our data reinforce the notion that the sarcoma cell evolution converges from a highly unstable karyotype to relatively stable and functional chromosome rearrangements, which are further enabled by telomerase overexpression.

Key words: Sarcoma cell line, tumor development, karyotyping, chromosome instability, telomerase activity.

1. Introduction

The hallmarks of cancer were recently revisited, and included cellular energetics' deregulation that avoids immune destruction as an emerging characteristic, and tumor-promoting inflammation, genome instability, and mutations as enabling characteristics[1]. Multiple genomic mutations are considered responsible for the malignant transformation of normal cells, which includes: capacity of tissue invasion and metastasis, insensitivity to antigrowth signals, sustained angiogenesis, ability to evade apoptosis, self-sufficient growth signals, limitless replication potential[1], evasion of immune surveillance[2], DNA damage and several causative conditions of cellular stress such as DNA replication, mitosis, and oxidative proteotoxic and metabolic processes[3]. However, an interesting emphasis has been given to the genomic instability as one of the most important hallmarks because of its presence in all cancer stages[4]. However, mathematical models of cancer progression present contrasting views of the complex processes involved in the carcinogenesis, and assume that tumor phenotypes are driven by mutations in only a few genes[5].

There are two conflicting views on carcinogenesis; one proposes that favorable gene mutations and epigenetic alterations ("genocentrics") are early events in cancer, leading to altered cell phenotypes and clonal expansion[6,7]. A second view is explained by the chromosomal theory of cancer based on aneuploidy[8], which is considered a solid cancer hallmark[9]. Aneuploidy may be required for tumor establishment in mice, and it may work in conjunction with intragenic mutations during tumorigenesis[10]. This is corroborated by observations that some genetic alterations associated with tumor initiation or proliferation events can be mediated by large chromosomal changes[11]. The presence or absence of specific chromosomes from the chromosome set, the increasing number of copies or the presence of some marker chromosomes can determine whether a cell line is more or less invasive, thereby directing the type of treatment to be adopted. Even cells with similar ploidy may show specific rearrangements that increase their metastatic ability[12].

Telomerase expression has also an important role in tumor growth and cell immortalization, and its neofunctionalization may be associated with

chromosomal rearrangements. Its reactivation is a critical event that promotes the tumor proliferation by removing the barrier of telomeric shortening[13], and telomeric maintenance is essential for the cell immortalization[14].

We have performed a detailed analysis of chromosomal rearrangements during tumor development of the murine cell line derived from sarcoma 180 (TG180) under *in vivo* and *in vitro* conditions, and demonstrated that equilibrium of the chromosomal architecture could be established in cell culture as opposed to *in vivo* conditions. Furthermore, the karyotypic stabilization was followed by an increase in the telomerase activity. Our results corroborate the chromosomal theory of cancer, by evidencing that viable tumor phenotypes possess common and highly stable karyotypes and their proliferation is facilitated by an attuned high telomerase activity.

2. Materials and Methods

2.1 Animals, Cells and culture conditions

TG180 cells were purchased from American Type Culture Collection (ATCC, Manassas, USA) and grown *in vitro* using RPMI-1640 medium, with 10% fetal calf serum (FCS), 25 mM HEPES, 1% penicillin-streptomycin, and 2 mM L-glutamine. The *in vivo* maintenance of the cells was done by the inoculation of 300 µL of cells (1.0 x 10^7 cells cells) in the peritoneum of three Balb-c male mice, weighting ± 20 grams. Animals were kept in the Animal Experimentation Laboratory (LEA) of the Federal University of Uberlândia under controlled conditions. Animals were housed under standard conditions (22±1^{o}C, humidity 60±5%, 12 h light/12 h dark cycle) with food and water *ad libitum*. All procedures for the handling, use and euthanasia of these animals followed the rules of the Brazilian Society for Laboratory Animals Science, and was approved by the Ethics Committee in Animal Research of the Federal University of Uberlândia, Brazil (CEUA/UFU N. 039/09), and every effort was made to minimize suffering.

2.2 Cell line cytogenetic characterization

Karyotypic analysis of cells was conducted in the Animal Cytogenetic Laboratory of the Federal University of Uberlândia. The mitotic chromosomes were obtained using the method described elsewhere[15]. The constitutive heterochromatin was revealed using the C-Band[16] and the staining with the fluorochromes chromomycin A3 and Hoechst 33258[17]. Chromosomes banding patterns were obtained by C- and G-banding[18], and by *Dde*I- and *Bam*HI-restriction enzyme digestions[19]. The Nucleolus Organizing Regions (NORs) were detected by the Ag-NOR impregnation[20]. Chromosomes characterizations were performed as described elsewhere[21] through conventional optical microscopes, epifluorescence microscope and AMG EVOS® fl Digital Inverted Fluorescence Microscope.

2.3 Ploidy analysis by flow cytometry

TG180 cells were collected and washed twice with PBS followed by fixation in 1% formaldehyde for 1 h and permeabilization with 70% ethanol overnight at 4°C. Cells were spun down, resuspended, and incubated in 1 mL solution containing 40 µg/mL of propidium iodide (PI) and 100 mg/mL RNase A at 37°C in the dark for 30 min. Under these staining conditions, signal due to residual double-stranded RNA is negligible and relative intensity of red fluorescence corresponds to DNA content[22]. Chicken erythroid nuclei were used as reference cells to determine the position of the diploid peak (2n). Cell fluorescence intensity and size were measured using AccuriC6 flow cytometer (BD Biosciences, San Diego, CA). Data were analyzed using FlowJo 7.6.1 (Tree Star Inc, Ashland, OR). The established criterion for ploidy of TG180 cells was based on 2n control cells peak/plot, subsequently the horizontal right displacement in the graphs represented a proportional increase of ploidy.

2.4 Clonogenic assay

To perform clonal expansion cells were maintained in 96-well culture microplates containing 200 µL of complete medium. The viability of cells grown in bottles of 25 cm^2 was verified by the Trypan blue exclusion test[23]. Subsequently these cells were resuspended in medium and diluted to a ratio of

1 cell/µL. An aliquot of 1 µL per well was transferred and examined under an inverted microscope (Olympus). The wells with only one cell were identified and cell growth was monitored to obtain an adequate number of cells for chromosomal analysis and for inoculation of tumor cells into mice.

2.5 Total RNA extraction and reverse transcription

Total RNA was extracted from TG180 and normal mice cells using the Trizol reagent according to the manufacturer's instructions (Invitrogen, Inc.). Reverse transcription (RT) was accomplished by adding 1 µg of total RNA from each sample to a final volume of 20 µL (completed with diethylpyrocarbonate (DEPC) treated water) containing 10 units of RNase inhibitor, 40 units of MMLV reverse transcriptase (RT), 1x MMLV-RT buffer, 200 µM of each dNTP and 6 µM of random hexamer primers and the solution incubated at 37 °C for 1 h and then 95 °C for 5 min.

2.6 RT-PCR of the samples

The cDNA was co-amplified in the same PCR reaction for the target (*M-Tert*) and control (*actin*) genes. For the *M-Tert* gene (accession number NM_009354.1) the primers were: sense 5'–GGATTGCCACTGGCTCCG–3'; antisense 5'-TGCCTGACCTCCTCTTGTGAC–3'. The actin constitutive gene (accession number NM_007393.2) was used as an internal positive control to normalize the products of the amplification reactions, and the primers were: sense 5'–GGCACCACACCTTCTACAATG–3' e antisense 5' – GTGGTGGTGAAGCTGTAG – 3'. Primers were designed for selective amplification of RNA, in which both primer ends (5' and 3') belonged to two adjacent exons. To check for genomic DNA contamination PCR reactions were also performed using total RNA as template, but no amplification was observed, demonstrating that all samples had no contaminant genomic DNA.

Amplification was carried out by adding 2 µL of primary cDNA to a 25 µL PCR mixture consisting of 200 µM of each dNTP, 0.4 µM of the primer pair for *M-Tert* or *Actin*, 2.0 mM MgCl2, 1.5 unit of Taq DNA polymerase and 1x buffer. The reactions were incubated at 95 °C for 3 min, followed by 35 (*M-Tert*) or 27 (*Actin*) cycles at 95 °C for 30 s, 59 °C (*M-Tert*) or 55ºC (*Actin*) for 40 s and 72 °C for 40 s, with a final extension of 10 min at 72 °C. The ideal number of PCR

cycles (35 and 27) was determined when the co-amplification of both genes reached the exponential phase.

2.7 Relative levels of gene expression

The *M-Tert* and *Actin* gene amplicons obtained were analyzed and quantified based on the staining intensities of the corresponding bands as assessed using the ImageMaster VDS software program, version 2.0 (Amersham Biosciences). The relative levels of *M-Tert* were obtained for each sample by normalizing the densitometric readings using the ratio *M-Tert*/*Actin*.

2.8 Statistical analysis

The statistical analysis concerning the distribution of chromosome numbers was performed by using a confidence interval for proportions by Student *t* test. The graphics and the statistical analysis for the telomerase expression were performed in the Statview for Windows version 4.57 (Abacus Concepts, Inc., Copyright 1992-1996). P values <0.05 were considered significant.

3. Results

3.1 Classic cytogenetic analysis reveals cell heterogeneity, near-tetraploidy and conservation of specific chromosomes

Chromosome counting revealed that TG180 is an heterogeneous cell line, with chromosome number ranging from 16 to 142 in the ascitic tumor, with a modal number of 68 chromosomes (Table 1). Conventional Giemsa karyotype suggested a near-tetraploid complement and revealed the constant presence of tree metacentric and four micro-chromosomes that were considered markers of the cell line (Fig. 1 A). Restriction enzyme banding with *Dde*I and *Bam*HI, and G-banding (Figs. 1B, 1C and 1D, respectively) produced specific transversal banding patterns, which allowed the determination of the appropriate chromosome pairing and karyotype assembly. Tetrasomy was frequently observed in several chromosomes, confirming the near-tetraploid complement. Metacentric chromosomes were strictly observed in single copies, suggesting that its origin occurred after polyploidization.

Table 1. Distribution of the number of chromosomes per cells in TG180 ascite tumor.

Ploidy	Percentage of cells
Haploid (n)	**0,7**
Diploid (2n)	**3,4**
Triploid (3n)	**9,1**
Tetraploid (4n)	**84,6**
Pentaploid (5n)	**0,1**
Hexaploid (6n)	**0,7**
Heptaploid (7n)	**1,4**
VCN	16-142
MN	68
Nº MN	59
TMA	353

The data in the table are based on the observation of chromosome number per cells. VCN = variation in chromosome number; MN = Modal number; Nº MN = number of metaphases with the modal number of chromosomes; TMA = total number of metaphases analyzed.

The metaphases of normal cells from mice were impregnated with silver nitrate and NORs were shown on one chromosome of six different homologous pairs (12, 15, 16, 17, 18 and 19). However, in TG180 cell metaphases at least 11 chromosomes with active NORs were observed (Fig. 1E). In addition to the six chromosome pairs with active NORs observed in normal cells, TG180 cells also presented them on chromosomes 2 (with a large telomeric amplification), 4, 8, 10, 11, and in the centromeric region of two metacentric markers. The TG180 cells presented highly active nucleoli (Fig. 1F) that were markedly disorganized and abundant when compared to normal cells (Fig. 1G).

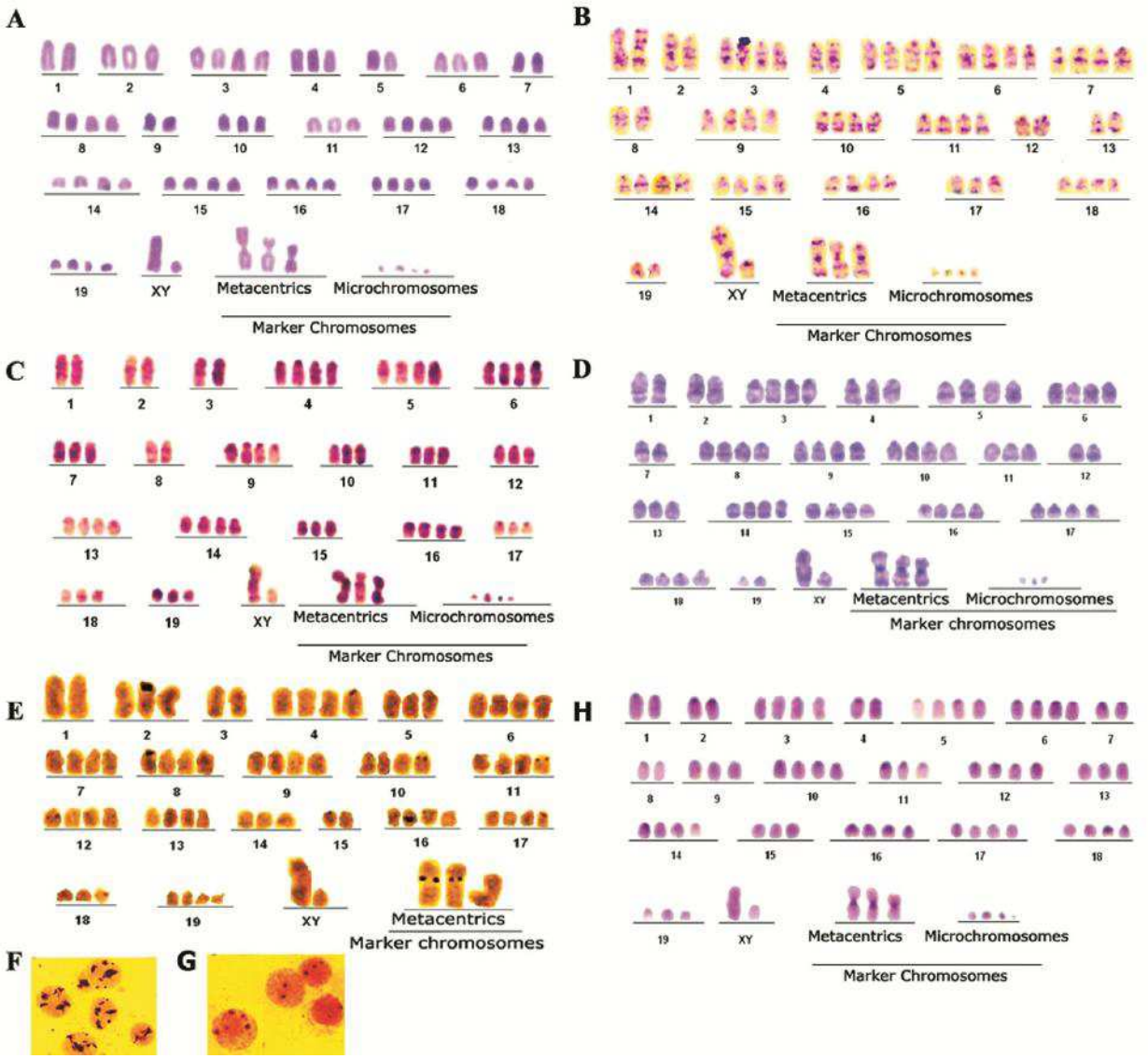

Figure 1. TG180 representative karyotypes under different staining and banding techniques. A conventional Giemsa staining. **B** Restriction enzyme *Dde* I. **C** Restriction enzyme *Bam* HI. **D** G-Banding. **E** Silver nitrate impregnation, evidencing Nucleolus Organizer Regions (darker regions on chromosomes). **F** TG180 nuclei impregnated with silver nitrate, evidencing the nucleoli (darker regions on nuclei). Note the greater amount and disorganization of tumor cells nucleoli. **G** Nuclei of mice bone marrow cells (normal cells). Note the presence of a constant organization. **H** C-Banding.

Constitutive heterochromatin blocks (C-band) were shown to be pericentromeric in most chromosomes, except in metacentric markers, which showed large centromeric blocks (Fig. 1H). Concerning to heterochromatin composition, no GC-rich island was evidenced using CMA3, even when counter-stained with Distamycin A (Fig. 2A). These heterochromatic blocks were AT-rich, since they were positively stained with Hoechst 33258 (Figure 2B).

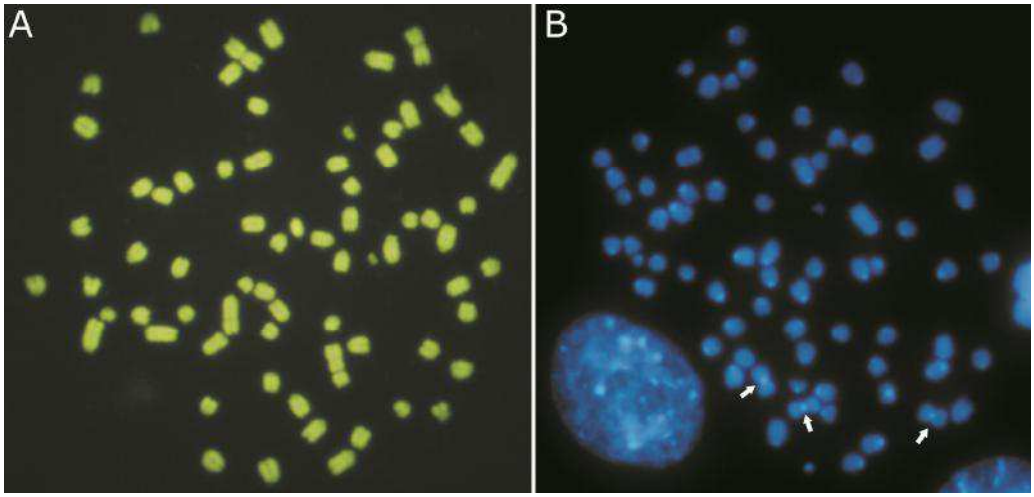

Figure 2. Photomicrographs of TG180 chromosomes stained with different fluorochromes. A TG180 metaphase stained with Chromomycin A_3, note that there are no fluorescent blocks, indicating that heterochromatin is not "rich" in GC bases. **B** TG180 metaphase stained with Hoechst 33258. Arrows indicate fluorescent heterochromatin blocks "rich" in AT.

As evidenced by cytogenetic analysis, flow cytometry also revealed a heterogeneous cell line, with a higher amount of cells with near-tetraploid characteristics. Dot-plots revealed that TG180 cells exhibited a remarkable shift in DNA content compared to 2n reference cells (chicken erythrocytes) (Fig. 3A, B). Also, the histograms showed wider distribution of nuclear sizes (Fig. 3C) and broader range of DNA contents (Fig. 3D) in the TG180 cells, represented by 76.4% of cells ranging 3-4n, which is consistent with the variation of chromosomal numbers and aneuploidy. A fluorescence image displays the propidium iodide-stained nuclei characterized by different sizes (Fig. 3E).

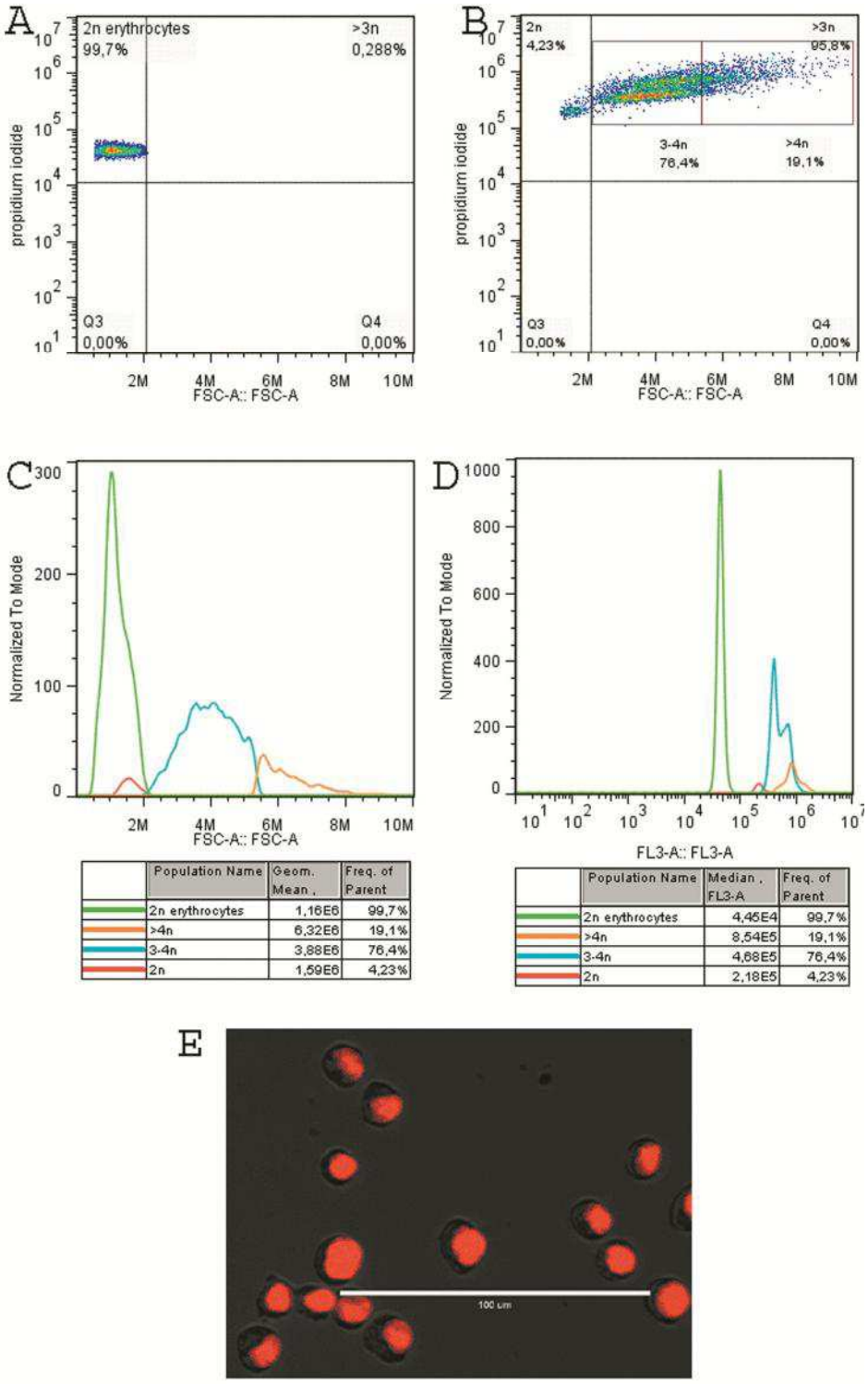

Figure 3. Analysis of TG180 cell population by flow cytometry. A and **B** Dot plots showing the ploidy distribution of TG180 cell population compared to the pattern of 2n chicken erythrocytes, respectively. Histogram of TG180 cell population subdivided according to its size in **C**, and to its DNA amount **D**, using PI staining. **E** Fluorescence micrograph of TG180 cells evidencing different nucleus size (red color) using PI staining.

3.2 Overexpression of telomerase in TG180

Semi-quantitative expression of the telomerase (RT-PCR) was analyzed in TG180 cells, and expression was compared among four normal mice tissues (peritoneal cells, blood, testicle and mesentery) as controls, which were normalized with actin gene expression. The telomerase expression in TG180 cells was much higher than those found in normal tissues with the same embryonic origin of the cell line as peritoneal cells, blood and mesentery. Even when compared to testicle, a tissue with intense proliferative activity, TG180 cell line presented *mTert* RNA levels at least twice higher (Fig. 4A and 4B). Although this cell line was composed by a heterogeneous population, it is probable that the telomerase overexpression was primarily produced by 68-chromosome cells, which were the most prevalent (~80%) cell sub-population.

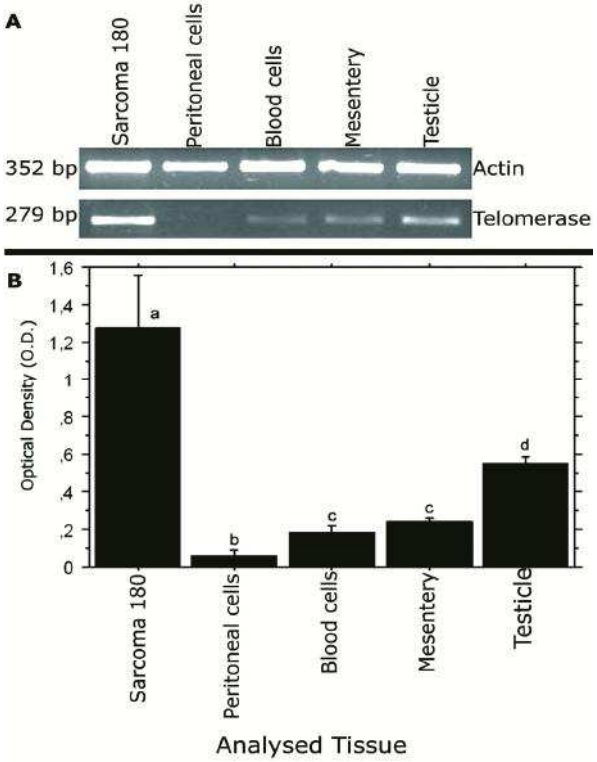

Figure 4. Analysis of telomerase expression by RT-PCR. A Agarose gel of RT-PCR products of the genes telomerase and actin of TG180 and normal tissues of mice. **B** Representative graphic of the RT-PCR semi-quantitative analysis of telomerase expression. The results represent the mean ± standard deviation of three independent experiments. It was used the t-student test and p values <0.05 were considered statistically significant. Bars with the same letter have no statistical difference.

3.3 In vitro, but not *in vivo*, microenvironment induces chromosomal alterations during cell line maintenance

In order to verify the microenvironment influence in the chromosome balance, chromosome counting was performed on three different maintenance cell line types: intraperitoneal inoculation (ascitic tumor), intramuscular inoculation (solid tumor) and cell culture (Fig. 5A). Three stages of *in vivo* tumor progression (7 days, 14 days and 21 days of tumor development) have been compared in ascites (Fig. 5B) and solid tumors (Fig. 5C). There were no significant differences in chromosomal number distribution among ascites and solid tumor maintenance and among days during tumor progression ($P>0.05$). A total of 1050 metaphases were analyzed and most of them (over 80%) showed a near-tetraploid chromosome complement (modal number of 68 chromosomes) in all stages of tumor progression in ascitic and solid tumor. In contrast, despite the higher percentage of tetraploid cells, the *in vitro* maintenance showed a wider distribution of ploidy, with an increment in the number of diploid and triploid cells, when compared with cell types of *in vivo* tumor maintenance. It was also observed an increased number of chromosomal aberrations in cells under *in vitro* maintenance, with several chromosome breaks, associations and even chromosome pulverization (Fig. 6A and B).

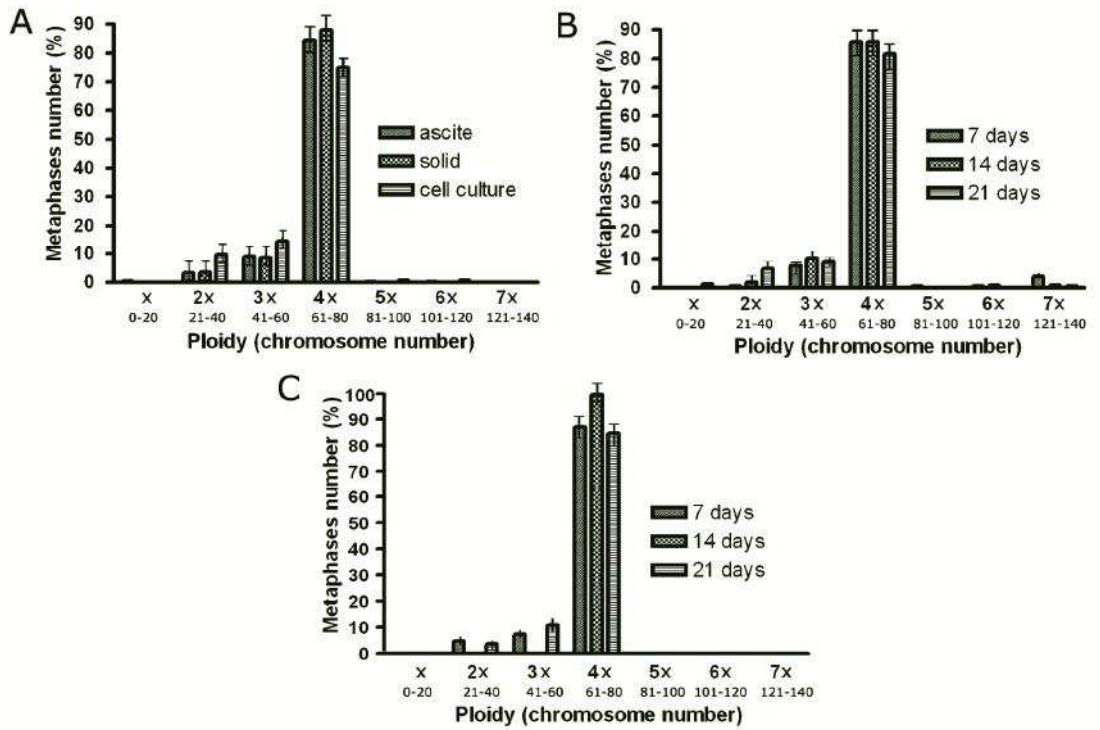

Figure 5. Chromosome number distribution of TG180 according to types of cell line maintenance and tumor progression time. A type of cell line maintenance. **B** Progression Time of ascites tumor. **C** Progression time of solid tumor. Confidence interval for proportions by t-student test at 0.05 significance level. Bars represent ± SEM.

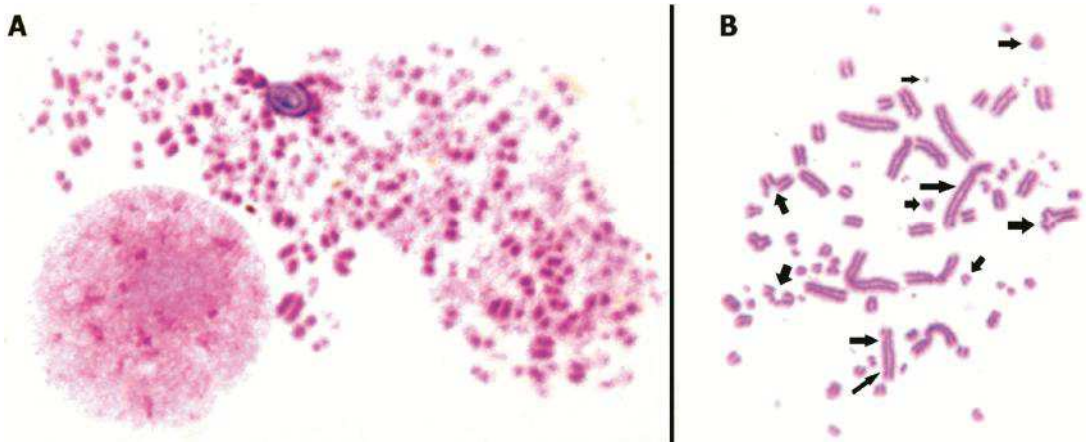

Figure 6. Giemsa stained metaphases of TG180 kept in culture. A chromosome pulverization. **B** Metaphase showing diverse chromosome aberrations such as chromatid breaks, chromosome fragmentation and microchromosomes, rings, dicentric chromosomes, triradials and chromosome amplification. Black arrows indicate chromosomal aberrations.

Seeking to analyze the chromosome inheritance pattern of TG180, a clonogenic assay was performed. Single cells were distributed in 50 wells of a cell culture microplate. Only one out of these 50 cells showed clonogenic capacity. Development was monitored and photographed (Fig. 7A-F). When culture reached an appropriated number of cells (after a month of culture maintenance), an amount of the cell culture was used to perform cytogenetic analysis, which revealed that i*n vitro* clonogenic expansion changed the chromosome balance of TG180. Clonogenic expansion also resulted in a heterogeneous cell population with a smaller sub-population presenting a near-tetraploid karyotype state (32%) and a main sub-population (52% of analyzed metaphases) presenting a heptaploid cytotype, with chromosome number ranging from 121 to 140 (Fig. 7G).

A sample of cells derived from the clonal culture (1.0 x 10^7 cells) was inoculated in the peritoneum of three animals and after ascitic tumor development, cells were harvested for cytogenetic analyses. Surprisingly, the original near-tetraploid main sub-population was recovered after *in vivo* progression. It was observed that the cells returned to their original near-tetraploid state, evidenced by 91.6% of analyzed metaphases that presented chromosome number ranging from 61 to 80 (Fig. 7G). Clonogenic heptaploid cells were generated by a mechanism called endoreduplication, since diplochromosomes were observed in many metaphases of the clonal cell culture (Fig. 8A and B). This event may also have happened in the initial origin of the tumor cell line.

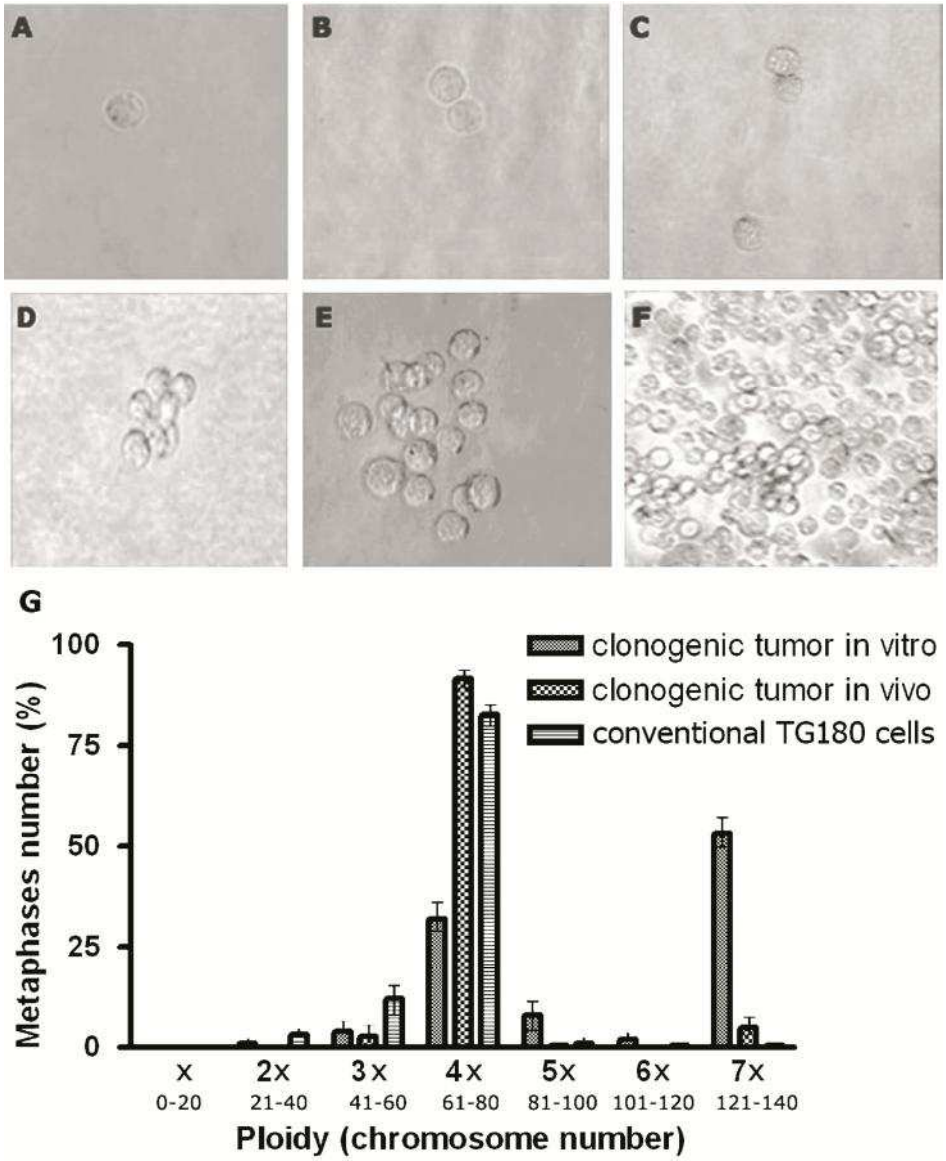

igure 7. Photomicrographs and Chromosome number distribution TG180 cells submitted to clonogenic assay. A-F Different stages of the clonogenic assay, in which a cell was individualized (A) and its development was monitored on an inverted microscope. **G** Representative graphic of chromosome number distribution from tumor cells obtained by clonal expansion kept *in vitro* and *in vivo* in comparison with conventional TG180 cell line. 400 X magnification.

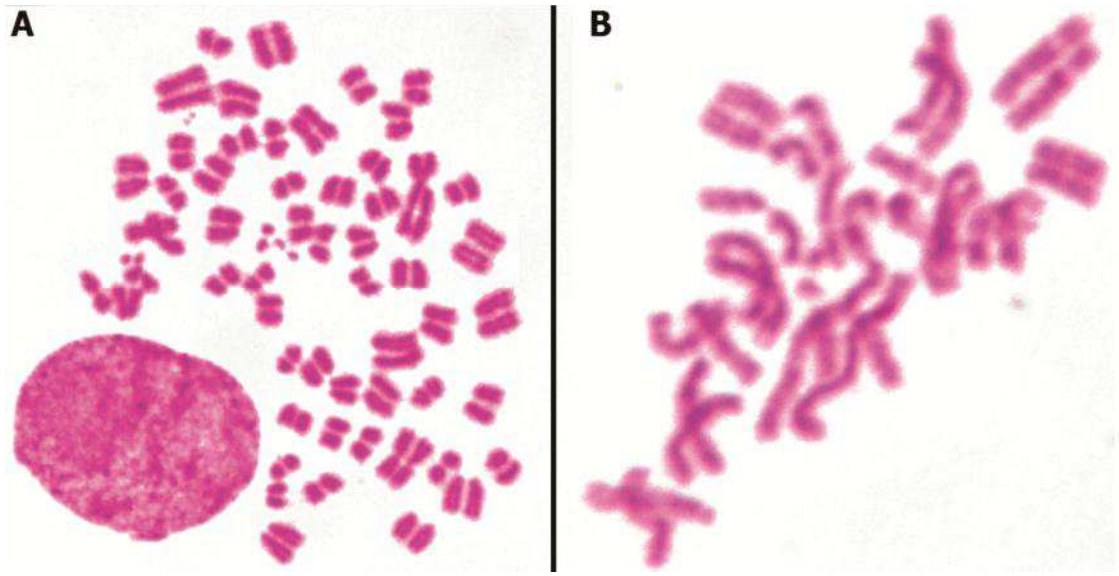

Figure 8. Giemsa stained metaphases of TG180*. **A** and **B** TG180 metaphases showing endoreduplication.*

4. Discussion

Aneuploidies characterized by complex karyotypes are the most prominent and common feature of tumors. This chromosomal instability predisposes cells to tumor development, and has become a very intense research focus, because the mechanisms that drive tumor growth in whole chromosome aneuploidy are less well understood[24-26]. Although animal models and human cancer syndromes have been exploited to understand cancer development, very few cancer studies have used concomitant *in vivo* and *in vitro* settings to observe chromosomal behavior under different environmental conditions. We have chosen multiple *in vitro* and *in vivo* strategies, using a murine sarcoma cell line, an *in vivo* animal model, and *in vitro* cell culture, to investigate chromosomal aneuplody during tumor development and telomerase expression.

We have shown that the karyotype of the TG180 cell line is highly unstable, and this chromosome instability is highly associated with tumor initiation, but as tumor becomes established *in vivo*, it tends to stabilize its numerical and structural chromosomal abnormalities followed by telomerase up-regulation. We corroborate the notion that there is a strong link among chromosomal instability, telomere dysfunction, and excessive telomerase

activity[27], and it is possible that cells' survival during evolution might have occurred due to the increased telomerase activity, which maintains the telomere lengthening mechanism, stabilizes existing telomeres, and possibly alleviates chromosome instability.

Cellular mechanisms that sustain tumor heterogeneity is an unsolved question in cancer biology[28]. We have shown that the TG180 tumor cell line was a highly heterogeneous population of cells related to chromosome number in all stages of tumor development and forms of tumor maintenance. Chromosomal differences were observed between *in vivo* and *in vitro* maintenance settings, suggesting that environmental changes can alter chromosomal configuration, especially when considering that animal cells were exposed to low O_2 concentrations *in vivo* (1 to 10 mmHg), while the in vitro cell culture was kept under high O_2 concentrations (150 mm Hg), which may have caused oxidative stress in cells, leading to ROS generation and impairment of antioxidant cellular defenses[29], resulting in a greater chromosome instability.

Increased rate of chromosome instability in tumors generates karyotypical diversity[30], a striking feature for the maintenance of the tumor. During tumor evolution, the variable phenotypes are then subjected to clonal selection through Darwinian competition[31]. The great variability of cell phenotypes and chromosome balance may explain the survival and replication of tumor cells during therapies. Therefore, resistance to treatments is an adaptive response to the high selective pressure in any specific environment, where few cells with proper chromosome balance may lead to clonal propagation and proliferation.

Many chromosomes with four homologous containing the same chromosomal banding pattern were observed in the TG180 karyotyping, revealing for the first time the presence of tetraploidy in this cell line. Many evidences support the idea of tetraploidy as a link to aneuploidy. Several tetraploid or near-tetraploid cells have been described in the premalignant condition (Barrett's oesophagus)[32], early-stage (cervix)[33], and even some mature cancers have near-tetraploid karyotypes[34]. Furthermore, in the present work it was detected diplochromosomes thus, it is reasonable to suggest that the standard karyotype of TG180 could be a result of an initial tetraploidy via endoreduplication, an event that drives tumor cells to acquire higher

chromosome numbers[35]. Endoreduplication occurs when the cells pass through two rounds of DNA replication without chromatid separation. In this case chromatin is re-licensed even if complete mitosis does not occur[36].

In TG180, the endoreduplication probably occurred before the formation of metacentric chromosomes, because they have been observed strictly as single copy. These three metacentric chromosomes and four microchromosomes, considered as marker chromosomes, were frequently observed in cytogenetic analysis. Probably, they provide some beneficial effects and adaptive characteristics to the tumor cell line growth, thus explaining its maintenance. In this context, we suggest that these metacentric chromosomes are probably derived from Robertsonian translocation between two acrocentric chromosomes (Fig. 9), generating micro-chromosomes as a result of arm breaks.

Analyzing the banding pattern generated by the restriction enzyme *Dde* I (Fig. 9A) and G-Banding (Fig. 9B), we propose that the largest metacentric chromosome was originated from the fusion of two chromosomes 11 or between one chromosome 11 and one 15. The second metacentric chromosome may be a result of the translocation between the chromosome 19 and 9, while the third metacentric chromosome could be derived from the union of the chromosomes 13 and 19 or 13 and 17. It is reasonable to associate the origin of metacentric and microchromosomes as a result of double-stranded breaks (DSB) caused by free radicals present in tumor site during an inflammation process. Erroneous rejoining of broken DNA DSBs may occur, resulting in deletion or amplification of chromosome material and even translocations[37,38]. These genetic changes are very important in tumor progression, once the resulting genomic instability can generate malignant phenotypes. In the present work, we have indirectly shown the possible influence of ROS in chromosome integrity, because cells kept in culture showed several chromosomal disorders.

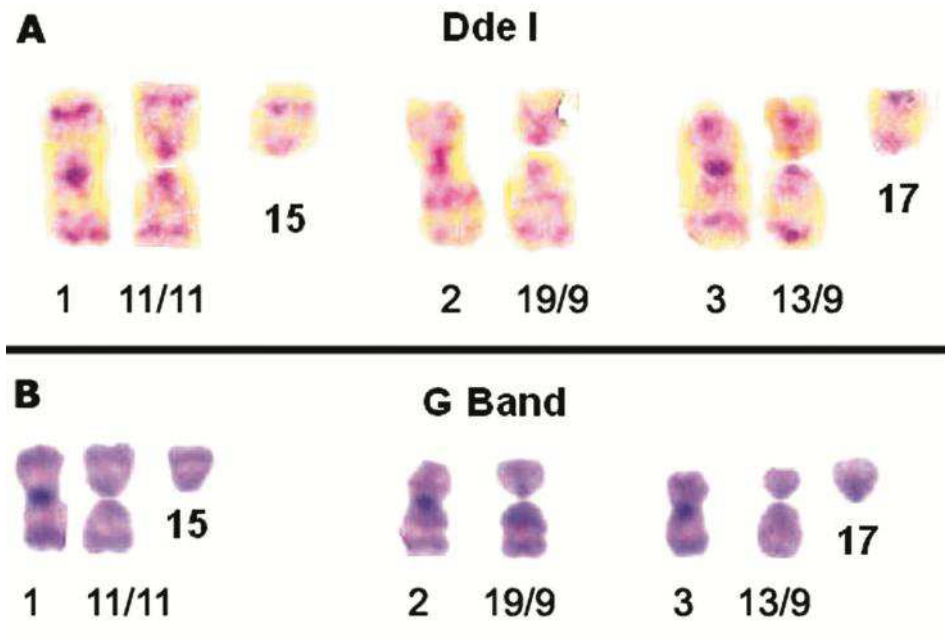

Figure 9. Translocations involved in origin of metacentric marker chromosomes of TG180 cell line. A TG180 chromosomes treated with *Dde* I. **B** TG180 chromosomes submitted to G-banding.

The structural alterations observed in TG180 were also observed in haematological cancers[39, 40], solid tumors[41], at the onset of acute myelogenous leukemia[42], and in another murine sarcoma cell line[43]. Many chromosome translocations of tumors have been studied and their gene fusion products identified[44]. So, it is possible that the Robertsonian translocation observed in TG180 may have caused fusion of some genes, producing chimeric proteins that may have activated cell proliferation, inactivated tumor suppressor genes, or affected DNA repair[45]. Paradoxically, an explanation for gene mutation can be offered by the chromosome theory of cancer, suggesting the interdependence of these events.

Despite the presence of chromosomal rearrangements and evident aneuploidy and numerical heterogeneity, some specific chromosomes have conserved their ploidy. Whereas the third chromosome of the complement presented diploid, triploid and tetraploid forms, the first chromosome of the complement showed conserved diploidy in all analyzed metaphases, which may be a required characteristic for tumor cell survival. In order to verify this

hypothetical benefit played by the conservation of some chromosomes, we carried out the NORs (nucleolus organizer regions) detection, since these regions are linked to high protein synthesis and, consequently, to the tumor aggressiveness turning interesting its conservation[46,47]. The silver nitrate impregnation revealed increased NORs activity in all TG180 cells. Mouse NORs in normal cells were located on chromosomes 12, 15, 16, 17, 18 and 19[48]; however, for tumor cells, in addition to the NORs-bearing chromosomes of normal cells, we also observed activation of NORs on chromosomes 2, 4, 8, 10 and 11, coinciding with the NORs described in mouse populations from different regions of the world[49]. Interestingly, we have observed activation of all rDNAs described for the mouse genome in the TG180 cell line, and seemed to be positively selected during tumor development.

The conservation of specific chromosomes in TG180 karyotype led us to investigate the inheritance patterns of chromosomes in a clonogenic assay. All 50 isolated TG180 cells individually propagated were not viable, except one that showed clonogenic features and constituted a new tumor cell population. This suggests that survival and clonal proliferation is not a frequent process, which under high selection pressure after crisis due to the extreme chromosomal instability resulted in an ideal chromosomal balance, enabling cell proliferation even under the aneuploidy status.

The resulting *in vitro* clonal expansion of a single-cell derived population showed 52% of heptaploid cells (7x) and a sub-population (32%) of near-tetraploid standard cytotype observed in the cell line (4x). Heptaploid cells were probably originated by endoreduplication during clonal expansion, since it was also observed many metaphases of TG180 with diplochromosomes in the clonal cell culture, corroborating with a study performed with a cell line derived from a primary gastric tumor[50].

Subsequently, the resulting cloned cells were inoculated in animals and, after 10 days of tumor development, cytogenetic analysis showed that most cells (91.2%) had returned to a near-tetraploid form, as usually observed in the original cell line. Probably the near-tetraploid karyotypical arrangement presented a suitable chromosomal combination adapted to proliferate *in vivo,* while the heptaploid cells were only viable in cell culture, showing the importance of the microenvironment on tumor development. Once culture

medium has very different conditions when compared with animal physiology[29], cells exposed to this condition are subject to different selective pressure, which directly influences its chromosome organization. Our hypothesis is that in TG180, tumor proliferative cells present near-tetraploidy formation, and only those chromosomes that are able to support *in vivo* growth, and changes in tumor microenvironment may influence the chromosomal architecture of these cells.

One of the most relevant characteristics of a proliferative and immortalized tumor cell is the telomerase activation or over-expression[51, 52]. A strong characteristic of very proliferative cells is the telomeric erosion that results in a crisis state[53]. Some cytogenetic studies and comparative genomic hybridization in epithelial tumors of mice with telomere dysfunction revealed a high rate of genomic aberrations among them; some non-reciprocal translocations, regional amplifications and deletions. These changes are not frequent in tumors of mice that have intact telomere function[54]. Therefore, it is clear the importance of telomerase expression to overcome crisis barrier and keep chromosomes integrity.

Although basal levels of telomerase expression are detected in mouse cells, differences can be observed in cells from distinct tissues[55]. Normal tissues with same embryonic origin of TG180, such as mesentery, peritoneal, and blood cells showed very low levels of Tert mRNA, even in high proliferative cells, such as spermatogonia, which did not reach the levels of telomerase expression of TG180. Thus, telomerase overexpression possibly plays an important role in the proliferative potential of the cell line, maintaining the integrity of telomeres, and conserving the stability of the ideal chromosomal balance. High telomerase activity is correlated with fewer aberrations, ploidy regulation and high telomere signal intensity, indicating its importance to keep genoma stability[56]. We believe that genetic instability generates a crisis process in which most cells, even the ones with an ideal chromosome balance, undergo apoptosis due to telomere erosion, and just rare cells will adapt and keep telomere integrity, as telomerase over-expression, enabling proliferation and promoting tumor progression, as proposed elsewhere[57].

The present cytogenetic and molecular data from TG180 allowed the proposal of a hypothesis for the evolution of TG180 chromosomes, which may

be extrapolated to other tumors. We hypothesize that a normal mouse cell that had faulty mechanisms of replication or checkpoint controls, due to physiological or genetic factors, may become polyploid through endoreduplication. After several rounds of mitotic cycles these cells may be recognized by the immune system, which causes an increasing in free radicals at tumor site, among other effects. As a result of the oxidative stress, DSBs may occur and, chromosomes may become destabilized, suffering several structural alterations, such as fusions, bridges and chromosome breakages, formation of microchromosomes, similar to those observed in TG180 cell culture, which are ubiquitous to cells with a near-tetraploid karyotype. Polyploidy certainly occurred before cell malignization, once that metacentric and micro-chromosomes, are present exclusively as single copies.

We believe that after chromosomal stabilization by telomerase activity, cells might have become immortal and proliferative, establishing a new tumor cell line. During cell line evolution, many changes may have occurred and only the advantageous configurations were positively selected. Although there is a cellular heterogeneity in TG180, only cells that have the ideal chromosome combination are responsible for the perpetuation of the cell line.

5. Conclusion

Polyploidy via endoreduplication and aneuploidy during cancer evolution are common events during TG180 sarcoma development, but by subjecting the cell line to a high selection pressure and to different environments, we have revealed specific conserved chromosomal architecture, which may have promoted an advantageous configuration. Clonal survival and expansion of tumor cells will be perpetuated will by the up-regulation of telomerase activity. This is a demonstration of interdependency between chromosome and gene theories for tumorigenesis, which may explain chromosome alterations, adaptation, and expansion.

6. Acknowledgments

We are grateful to the Laboratory of Animal Cytogenetics and the Laboratory of Nanobiotechnology of the Institute of Genetics and Biochemistry, Federal University of Uberlândia (UFU) for supporting this study, and to the Laboratory of Immunoparasitology (UFU) for providing the cell line and the use

of the *in vitro* culture facility. This work was also supported by the Brazilian funding agencies: Coordenação de Aperfeiçoamento de Pessoal de Nível Superior (CAPES), Conselho Nacional de Desenvolvimento Científico e Tecnológico (CNPq), and Fundação de Amparo à Pesquisa de Minas Gerais (FAPEMIG). We would also like to thank Dr. Sumathi Sankaran-Walters (University of California Davis) for her critical reading and suggestions, and English corrections.

7. Authors Disclosure Statement

The authors declare no competing financial interests.

8. References

1. Hanahan, D. & Weinberg, R.A. Hallmarks of cancer: the next generation. *Cell* **144**, 646-674 (2011).
2. Kroemer, G. & Pouyssegur, J. Tumor cell metabolism: cancer's Achilles' heel. *Cancer cell* **13**, 472-482 (2008).
3. Luo, J., Solimini, N.L. & Elledge, S.J. Principles of Cancer Therapy: Oncogene and Non-oncogene Addiction. *Cell* **136**, 823-837 (2009).
4. Negrini, S., Gorgoulis, V.G. & Halazonetis, T.D. Genomic instability - an evolving hallmark of cancer. *Nat Rev Mol Cell Bio* **11**, 220-228 (2010).
5. Beerenwinkel, N. et al. Genetic progression and the waiting time to cancer. *PLoS computational biology* **3**, e225 (2007).
6. Chen, K.G. et al. Genetic and epigenetic modeling of the origins of multidrug-resistant cells in a human sarcoma cell line. *Cancer Res* **65**, 9388-9397 (2005).
7. Roberti, A., La Sala, D. & Cinti, C. Multiple genetic and epigenetic interacting mechanisms contribute to clonally selection of drug-resistant tumors: current views and new therapeutic prospective. *J Cell Physiol* **207**, 571-581 (2006).
8. Stock, R.P. & Bialy, H. The sigmoidal curve of cancer. *Nat Biotechnol* **21**, 13-14 (2003).
9. Davoli, T., Denchi, E.L. & de Lange, T. Persistent telomere damage induces bypass of mitosis and tetraploidy. *Cell* **141**, 81-93 (2010).
10. Pihan, G. & Doxsey, S.J. Mutations and aneuploidy: co-conspirators in cancer? *Cancer cell* **4**, 89-94 (2003).
11. Hanahan, D. & Weinberg, R.A. The hallmarks of cancer. *Cell* **100**, 57-70 (2000).
12. Bertrand, V., Couturier-Turpin, M.H., Louvel, A., Panis, Y. & Couturier, D. Relation between cytogenetic characteristics of two human colonic adenocarcinoma cell lines and their ability to grow locally or metastasize or both: an experimental study in the nude mouse. *Cancer Genet Cytogenet* **113**, 36-44 (1999).

13. Chang, S., Khoo, C. & DePinho, R.A. Modeling chromosomal instability and epithelial carcinogenesis in the telomerase-deficient mouse. *Seminars in cancer biology* **11**, 227-239 (2001).
14. Chang, M.W. et al. Comparison of early passage, senescent and hTERT immortalized endothelial cells. *Experimental cell research* **309**, 121-136 (2005).
15. Guerra, M. & Souza, M.J. Como observar cromossomos - Um Guia de Técnicas em Citogenética Vegetal, Animal e Humana. (FUNPEC - Editora, Ribeirão Preto, SP, Brazil; 2002).
16. Sumner, A.T. A simple technique for demonstrating centromeric heterochromatin. *Experimental cell research* **75**, 304-306 (1972).
17. Verma, R.S. & Babu, A. Human chromosomes: Principles and techniques, Edn. 2nd. (Mac Graw-Hill Inc., New York, NY, USA; 1995).
18. Fagundes, V., Vianna-Morgante, A.M. & Yonenaga-Yassuda, Y. Telomeric sequences localization and G-banding patterns in the identification of a polymorphic chromosomal rearrangement in the rodent Akodon cursor (2n=14,15 and 16). *Chromosome research : an international journal on the molecular, supramolecular and evolutionary aspects of chromosome biology* **5**, 228-232 (1997).
19. Schmid, M. & de Almeida, C.G. Chromosome banding in Amphibia. XII. Restriction endonuclease banding. *Chromosoma* **96**, 283-290 (1988).
20. Howell, W.M. & Black, D.A. Controlled silver-staining of nucleolus organizer regions with a protective colloidal developer: a 1-step method. *Experientia* **36**, 1014-1015 (1980).
21. Levan, A., Fredga, K. & Sandberg, A.A. Nomenclature for Centromeric Position on Chromosomes. *Hereditas-Genetisk A* **52**, 201-& (1964).
22. Krishan, A. Rapid flow cytofluorometric analysis of mammalian cell cycle by propidium iodide staining. *J Cell Biol* **66**, 188-193 (1975).
23. Strober, W. Trypan blue exclusion test of cell viability. *Current protocols in immunology / edited by John E. Coligan ... [et al.]* **Appendix 3**, Appendix 3B (2001).
24. Duesberg, P., Li, R., Fabarius, A. & Hehlmann, R. The chromosomal basis of cancer. *Cellular oncology : the official journal of the International Society for Cellular Oncology* **27**, 293-318 (2005).

25. Gordon, D.J., Resio, B. & Pellman, D. Causes and consequences of aneuploidy in cancer. *Nature reviews. Genetics* **13**, 189-203 (2012).
26. Saunders, W.S. et al. Chromosomal instability and cytoskeletal defects in oral cancer cells. *Proceedings of the National Academy of Sciences of the United States of America* **97**, 303-308 (2000).
27. Cheung, A.L. & Deng, W. Telomere dysfunction, genome instability and cancer. *Frontiers in bioscience : a journal and virtual library* **13**, 2075-2090 (2008).
28. Visvader, J.E. Cells of origin in cancer. *Nature* **469**, 314-322 (2011).
29. Halliwell, B. Oxidative stress in cell culture: an under-appreciated problem? *FEBS letters* **540**, 3-6 (2003).
30. Storchova, Z. & Pellman, D. From polyploidy to aneuploidy, genome instability and cancer. *Nature reviews. Molecular cell biology* **5**, 45-54 (2004).
31. Stephens, P.J. et al. Massive genomic rearrangement acquired in a single catastrophic event during cancer development. *Cell* **144**, 27-40 (2011).
32. Galipeau, P.C. et al. 17p (p53) allelic losses, 4N (G2/tetraploid) populations, and progression to aneuploidy in Barrett's esophagus. *Proceedings of the National Academy of Sciences of the United States of America* **93**, 7081-7084 (1996).
33. Olaharski, A.J. et al. Tetraploidy and chromosomal instability are early events during cervical carcinogenesis. *Carcinogenesis* **27**, 337-343 (2006).
34. Rajagopalan, H. & Lengauer, C. Aneuploidy and cancer. *Nature* **432**, 338-341 (2004).
35. Larizza, L. & Schirrmacher, V. Somatic-Cell Fusion as a Source of Genetic Rearrangement Leading to Metastatic Variants. *Cancer Metast Rev* **3**, 193-222 (1984).
36. Larkins, B.A. et al. Investigating the hows and whys of DNA endoreduplication. *Journal of experimental botany* **52**, 183-192 (2001).
37. Jackson, S.P. Sensing and repairing DNA double-strand breaks. *Carcinogenesis* **23**, 687-696 (2002).

38. Khanna, K.K. & Jackson, S.P. DNA double-strand breaks: signaling, repair and the cancer connection. *Nature genetics* **27**, 247-254 (2001).
39. Qian, J. et al. Constitutional Robertsonian translocations in (9;22)-positive chronic myelogenous leukemia. *Cancer Genet Cytogenet* **132**, 79-80 (2002).
40. Welborn, J. Acquired Robertsonian translocations are not rare events in acute leukemia and lymphoma. *Cancer Genet Cytogenet* **151**, 14-35 (2004).
41. Bayani, J. et al. Spectral karyotyping identifies recurrent complex rearrangements of chromosomes 8, 17, and 20 in osteosarcomas. *Genes, chromosomes & cancer* **36**, 7-16 (2003).
42. Padilla-Nash, H.M. et al. Jumping translocations are common in solid tumor cell lines and result in recurrent fusions of whole chromosome arms. *Gene Chromosome Canc* **30**, 349-363 (2001).
43. Ghosh, S. & Chaudhuri, A. Analysis of three whole-arm translocations in a mouse sarcoma cell line. *Cytogenetics and cell genetics* **38**, 161-164 (1984).
44. Fletcher, J.A. Molecular biology and cytogenetics of soft tissue sarcomas: relevance for targeted therapies. *Cancer treatment and research* **120**, 99-116 (2004).
45. Rabbitts, T.H. et al. Mouse models of human chromosomal translocations and approaches to cancer therapy. *Blood Cells Mol Dis* **27**, 249-259 (2001).
46. Ishida, T. et al. Proliferating Cell Nuclear Antigen Expression and Argyrophilic Nucleolar Organizer Regions as Factors Influencing Prognosis of Surgically Treated Lung-Cancer Patients. *Cancer Research* **53**, 5000-5003 (1993).
47. Kaneko, S., Ishida, T., Sugio, K., Yokoyama, H. & Sugimachi, K. Nucleolar Organizer Regions as a Prognostic Indicator for Stage-I Non-Small-Cell Lung-Cancer. *Cancer Research* **51**, 4008-4011 (1991).
48. Dev, V.G., Tantravahi, R., Miller, D.A. & Miller, O.J. Nucleolus organizers in Mus musculus subspecies and in the RAG mouse cell line. *Genetics* **86**, 389-398 (1977).

49. Suzuki, H., Kurihara, Y., Kanehisa, T. & Moriwaki, K. Variation in the distribution of silver-staining nucleolar organizer regions on the chromosomes of the wild mouse, Mus musculus. *Molecular biology and evolution* **7**, 271-282 (1990).
50. Lima, E.M. et al. Conventional cytogenetic characterization of a new cell line, ACP01, established from a primary human gastric tumor. *Braz J Med Biol Res* **37**, 1831-1838 (2004).
51. Kim, N.W. et al. Specific association of human telomerase activity with immortal cells and cancer. *Science* **266**, 2011-2015 (1994).
52. Blasco, M.A. et al. Telomere shortening and tumor formation by mouse cells lacking telomerase RNA. *Cell* **91**, 25-34 (1997).
53. Gilley, D., Tanaka, H. & Herbert, B.S. Telomere dysfunction in aging and cancer. *The international journal of biochemistry & cell biology* **37**, 1000-1013 (2005).
54. Maser, R.S. & DePinho, R.A. Connecting chromosomes, crisis, and cancer. *Science* **297**, 565-569 (2002).
55. Prowse, K.R. & Greider, C.W. Developmental and tissue-specific regulation of mouse telomerase and telomere length. *Proceedings of the National Academy of Sciences of the United States of America* **92**, 4818-4822 (1995).
56. Izumi, H. et al. High telomerase activity correlates with the stabilities of genome and DNA ploidy in renal cell carcinoma. *Neoplasia* **4**, 103-111 (2002).
57. Shay, J.W. & Wright, W.E. Role of telomeres and telomerase in cancer. *Seminars in cancer biology* **21**, 349-353 (2011).

Capítulo 4

“Poliploidy and aneuploidy is ubiquitous in five immortalized murine cell lines and tetraploidization of normal cells leads to aneuploidy and malignant phenotype.”

Artigo formatado de acordo com a revista Cancer Cell International

Poliploidy and aneuploidy is ubiquitous in five immortalized murine cell lines and tetraploidization of normal cells leads to aneuploidy and malignant phenotype.

Oliveira-Júnior, RJ[1]; Antunes-Miranda, S[1]; Machado, PHA[1]; Almeida-Silva, M[1]; Alves, PT[1]; Luiz R. Goulart[1,2]; Morelli, S[1].

1 Institute of Genetics and Biochemistry, Federal University of Uberlândia, Uberlândia, MG, Brazil; **2** Department of Medical Microbiology and Immunology, University of California Davis, Davis, CA, USA.

Abstract

Aneuploidy is considered a hallmark of cancer and plays an important role in cancer origin and progression. It is believed that aneuploid cells are derived from initial polyploidy, that can occurs spontaneously or induced by environment agents or chemical compounds, and the genetic instability observed in polyploidy cells leads to chromosome losses or rearrangements resulting in variable and aberrant karyotypes. Two conflicting visions on tumorigenesis are widely discussed the the gene-mutation hypothesis and aneuploidy hypothesis of cancer. The first says that gene specific mutations start and maintain the altered phenotype of tumor cells and the second says that aneuploidy is necessary and sufficient for the initiation and progression of malignant transformation. Here we analyzed the chromosome composition of five murine cell lines in order to fully understand the role of aneuploidy in immortalized cells. All analyzed cell lines, both, tumoral and non-tumoral, showed a very similar pattern of chromosome reorganization. All cell lines are aneuploid and present structural alterations responsible for the emergence of different types of marker chromosomes. We also induced the polyploidization of normal cells and observed a marked state of chromosome intability that gave rises to a new cell line with a similar karyotype pattern observed in commercial cell lines. Both, the five analyzed cells and this new described cell line, presented important alterations in the expression profile of genes involved in cancer progression. We believe that aneuploidy is an essential step in cell transformation and that it is the easier way to promote hundreds or thousands of gene alterations, due to genetic instability generated by aneuploid state.

Keywords: Chromosome instability; cancer; P53; BRAF; TERT.

1. Introduction

Compared to normal cells, numerical and structural chromosome abnormalities are a most obvious and most distinguishing characteristics of cancer genomes [1]. Polyploidy, a state in which cells possess more than two sets of homologous chromosomes, occurs frequently in nature, although eukaryotic organisms generally have a diploid number of chromosomes. Moreover, the chromosome complement may differ within the same organism, depending on the cell type and in cancer cells, it is widely described higher ploidy than normal cells in a variety of tumor [2][3].

Tumor cells frequently have higher gene dosage than the original cells. As example, increasing in DNA ploidy influences positively cell proliferation of breast carcinoma and subset of patients with DNA multiploid/hypertetraploid tumours had the worst clinical outcome, with a relative risk of cancer related death [4]. The acquisition of a large chromosome number observed in tumor cells may be the result of endoreduplication [2][5]. The process of endoreduplication results in diplochromsomes, consisting of four chromatids grouped side by side, instead two. Endoreduplication occurs when the cells go through two rounds of DNA replication without the chromatid separation [6].

Most human cancers, noted for their rapid growth, also display various levels of aneuploidy, defined as a karyotype that is not a multiple of the haploid complement. This cell event results in an unbalanced genome with different copy numbers for genes on different chromosomes [7]. Many evidences support the idea of tetraploidy as a link to aneuploidy. Several tetraploid or near-tetraploid cells have been described in the premalignant condition (Barrett's oesophagus) [8], early-stage (cervix) [9], and even some mature cancers have near-tetraploid karyotypes [10].

Here we describe karyotypical abnormalities found in five different murine tumoral and non-tumoral immortalized cell lines. In order to verify influences of tetraploidy in cell phenotype, it was also performed a poliploidization with colcemid, generatind a new cell line that is described in the present work. The expression of three genes involved in tumor progression was also analyzed in order to verify influences of chromosomal abnormalities in expression profile.

2. Material and Methods

2.1 Animals, Cells and culture conditions

TG180 cells were purchased from American Type Culture Collection (ATCC, Manassas, USA). B16F10 and NIH-3T3 was kindly provided by Profa. Dra. Enilza Maria Espreafico (USP-FMRP). MEF cells were kindly provided by Prof. Dr. Cláudio Vieira da Silva (UFU-PPIPA). S180 cells were kindly provided by MSc. João Carlos Lima Rodrigues Pita (UFPB). Cells were grown using RPMI-1640 medium, with 10% fetal calf serum (FCS), 25 mM HEPES, 1% penicillin-streptomycin, and 2 mM L-glutamine. Animals were kept in the Animal Experimentation Laboratory (LEA) of the Federal University of Uberlândia under controlled conditions. Animals were housed under standard conditions (22±1^{o}C, humidity 60±5%, 12 h light/12 h dark cycle) with food and water *ad libitum*. All procedures for the handling, use and euthanasia of these animals followed the resolutions proposed by the Brazilian Society of Science in Laboratory Animals, was approved by the Ethics Committee in Animal Research of the Federal University of Uberlândia, Brazil (Permit Number: CEUA/UFU 039/09) and every effort was made to minimize suffering.

2.2 Colcemid polyploidization

Mouse fibroblasts were obtained from foreskin biopsies and grown 24h *in vitro* using RPMI-1640 medium with 10% fetal calf serum (FCS), 25 mM HEPES, 1% penicillin-streptomycin, and 2 mM L-glutamine. Then, non-aderent cells were washed and after growing for a week, an aliquot of fibroblast cells were frozen and after another week, the confluent culture were treated with colcemid 10µg/mL for 24h. Cells were washed and allowed to grow for 3 months. During cell passages, aliquots of cells were frozen with 10% of dimethylsulfoxide (DMSO) in fetal calf serum. First cytogenetic analyses were performed when cells acquired the third confluence (approximately after a month of cell culture).

2.3 Cell line cytogenetic characterization

Karyotypic analysis of cells was conducted in the animal cytogenetic laboratory of the Federal University of Uberlândia. The mitotic chromosomes

were obtained using the method described by Guerra (2002) [11]. The constitutive heterochromatin was revealed using the C-Band [12] and the staining with the fluorochromes chromomycin A3 and Hoechst 33258 [13]. It was obtained transversal marks in the chromosomes using the G-band method according to routine techniques [14] and digesting the chromosomes with the restriction enzyme *Dde* I [15]. The Nucleolus Organizing Regions were detected by the Ag-NOR impregnation [16]. The chromosomes characterizations were performed according to [17]. It was used conventional optical microscopes, epifluorescence microscope and AMG EVOS® fl Digital Inverted Fluorescence Microscope.

2.4 RNA preparation, cDNA synthesis and quantitative real-time RT-PCR

RNA was extracted from tumor tissues using the Trizol reagent (Invitrogen) and RNA mass was determined on a NanoDrop™ 1000 spectrophotometer (Thermo Scientific). cDNA synthesis was carried out using SuperScript II First-Strand Synthesis System for RT-PCR using oligo(dT) primer (Invitrogen) using 1µg of total RNA. The amplification of fragments corresponding to each gene was performed using the following primers: telomerase-F: 5'-TGGCTTGCTGCTGGACACTC-3' and telomerase-R: 5'-TGAGGCTCGTCTTAATTGAGGTCTG-3'; P53-F:5'-TGGAAGACTCCAGTGGGAAC-3' and P53-R:5'-TCTTCTGTACGGCGGTCTCT-3'; Braf-F: 5'-CATCTTCTTCCTCATCCTCG-3' and Bra-f-R: 5'-TTCAACATTTTCACTGCCAC-3'. GAPDH was amplified with primers: 5'-GCACAGTCAAGGCCGAGAAT-3’ (forward) and 5'-GCCTTCTCCATGGTGGTGAA-3' (reverse) and served as an internal control to normalize expression data and to verify integrity of the cDNA. In order to evaluate similar PCR amplification efficiencies of target genes and GAPDH genes, a serial dilution analysis was performed using cDNA synthesized from total RNA from normal and tumor cell lines.

All quantitative real time PCR (qRT-PCR) reactions were conducted using the SYBR Green detection reagent (Applied Biosystems). Conditions for PCR amplication of target genes were: 50 °C for 2 min and 94 °C for 5 min, followed by 10 cycles of 94 °C for 30 s, primer annealing (P53, BRAF, NANOG: 59ºC for 2 minutes; TERT: 57ºC for 2 minutes) and 72°C for 90 s. At the end of

each cycle the temperature decreased 0.5C, followed by 30 cycles of 94°C for 30 s, 50°C for 30 s and 72°C for 90 s, ending the reaction with 72C for 15 min. A melting curve analysis was generated to determine amplification efficiency and specificity (60–90°C with a heating rate of 0.2°C/s and continuous fluorescence measurement). Product purity, size and absence of primer dimmers were confirmed by the DNA melting curve analysis and by agarose gel electrophoresis. Relative gene expression of the target gene was calculated by using the ΔΔCT method. GAPDH amplification was used as normalization control for genes expression transcription level evaluation and Whole blood RNA was used as calibration group.

2.5 Statistical analysis

The statistical analysis concerning the distribution of chromosome number was performed by using a confidence interval for proportions by Student *t* test. All statistical analyses were conducted by the statistical program GraphPad Prism 5 for windows, version 5.00. Comparisons among groups of data were made using Two-way analysis of variance (ANOVA), followed by the Bonferroni posttest. *P* value <0.05 was considered statistically significant. All results were presented as mean ± SD unless otherwise noted.

3. Results and discussion

3.1 S180 sarcoma cell line

The S180 cell line, also known as Swiss Webster sarcoma is deposited in the ATCC cell bank under number TIB-66. This cell line is widely used and gave rise to many others cells lines. In the present report S180 cell line presents a modal number of 63 chromosomes (33 % of the analyzed metaphases). Chromosome number ranged from 29 to 67 chromosomes with higher frequency of metaphases showing hipertriploid/near-tetraploid cells that represent 84,7% of analyzed metaphases (Figure 1A). It was observed the presence of metaphases with diplochromosomes, indicating the occurrence of endoreduplication in this cell line.

S180 cells showed many chromosome aberrations, such as metacentric, submetacentric, microchromosomes and dicentric chromosomes (Figure B-E). G-banding karyotype of S180 cells revealed chromosomes present in pairs,

trissomy and tetrassomy, confirming the tetraploid origin of this cell line (Figure 1F). The different types of chromosome abnormalities observed in S180, as the dicentric chromosome, can be seen in metaphase of figure 1G. Chakrabarti et al. (1978) also described a stable and transmissible dicentric chromosome and a near-tetraploidy state [18]. The dicentric chromosome, a marker also found in the present study, probably is an important chromosome to cell line, once that it was identified in 1978 year and still remains present in the cell line.

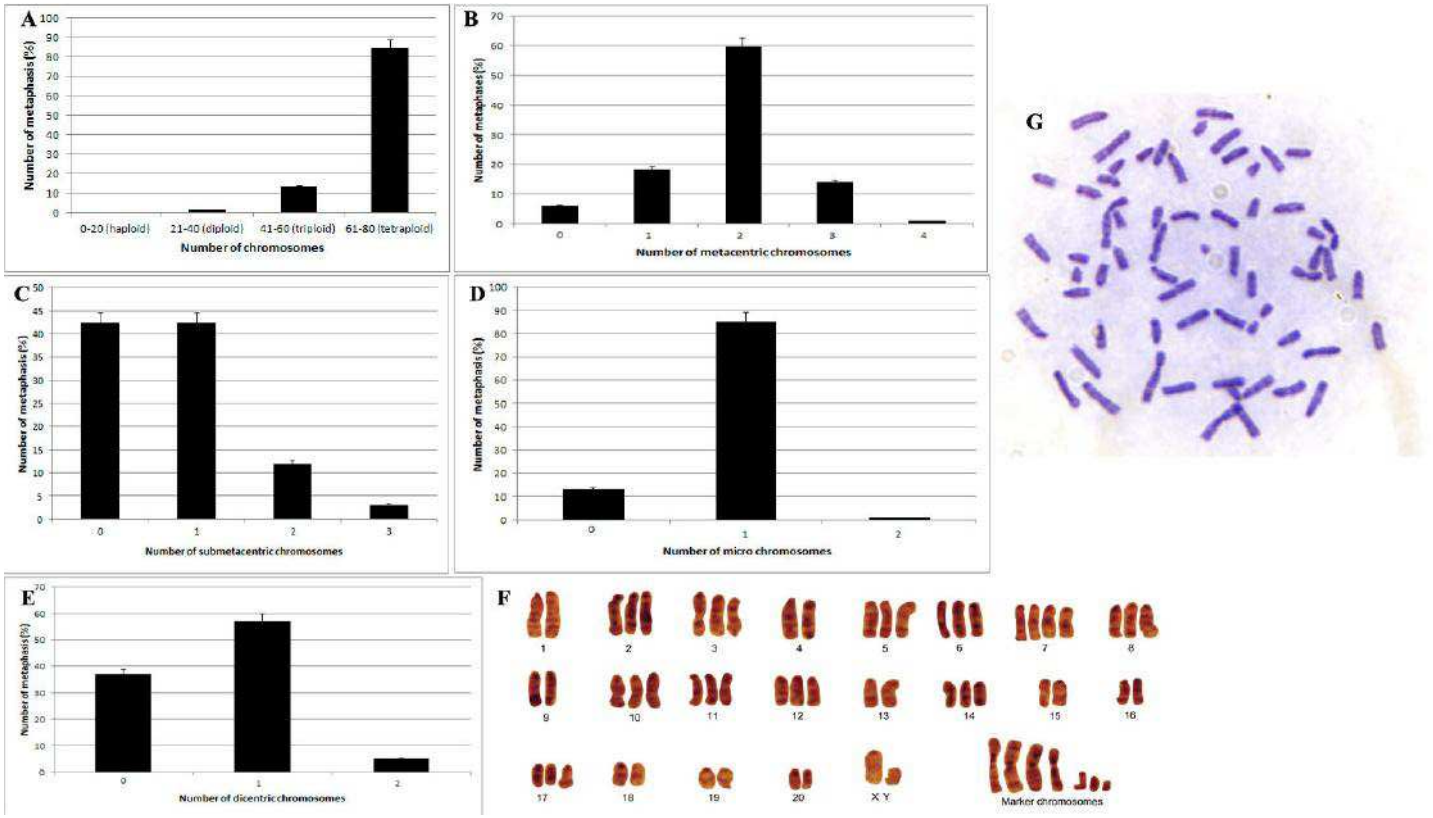

Figure 1 – Graphical representations and photomicrography of S180 cell line A) Chromosome distribution showing a higher number of metaphasis in a near tetraploid state. B) Frequency of the number of metacentric chromosomes per metaphase. C) Frequency of the number of submetacentric chromosomes per metaphase. D) Frequency of the number of microchromosomes per metaphase. E) Frequency of the number of the dicentric marker chromosome F) S180 G-banded karyotype showing the presence of tetrasomy in some chromosomes, indicating the tetraploid origin of this cell line. G) Metaphase presenting different structural alterations found in S180.

3.2 B16F10 tumoral cell line

Metastatic melanoma is one of the most aggressive cancers, whose development and progression are affected by many factors as ultraviolet rays and genotype. Melanoma has a high metastasis capacity, even in early stage of development, reaching mainly the central nervous system and lung. Several cell lines of murine melanoma were established and their classification was based on their properties of metastasis emission, in which B16F1 have less metastatic potential, while B16F10 (Code ATCC: CRL-6475) has a higher potential of metastasis emission. B16F10 is a poorly immunogenic cell line and can be grown *in vitro* or maintained in mice (*in vivo*) [19] [20] [21]. The present study performed chromosome counting and G-banding karyotype to monitor chromosome composition

B16F10 cell line metaphasis presented chromosome numbers ranged from 50 to 99, with 81.3% of metaphasis showing a hipertriploid/near tetraploid complement (ranging from 68 to 75 chromosomes) and modal number of 73 chromosomes (Figure 2A). Many structural alterations were also found in this melanoma cell line, as can be seen in the graphical representations and metaphase image (Figure 2 B-F). We found the emergence of metacentric and submetacentric chromosomes, resulting from Robertsonian translocations. We also observed a long acrocentric chromosome, whose banding patterns indicate that they are resulting from repeated tandem translocations, which usually involves two chromosomes attaching to each other at the telomeric regions. Karyotype assembly (Figure 2E) revealed a near-tetraploid or hiper-triploid complement. Previous reports have also described an aneuploid karyotype, with chromosome numbers ranging between 68 and 75, and modal number of 73 chromosomes [22] [23] [24].

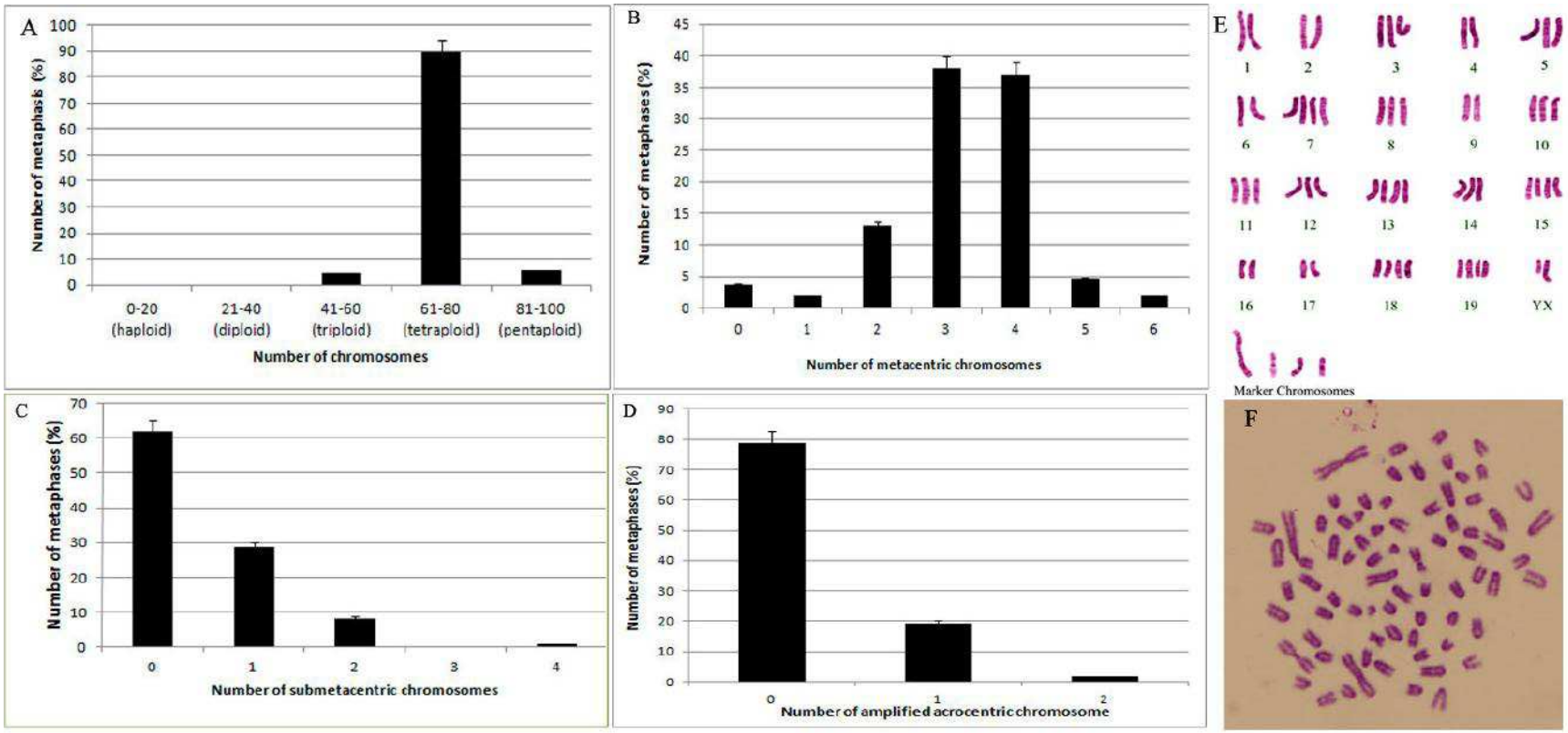

Figure 2 – Graphical representations and photomicrography of B16F10 cell line A) Chromosome distribution showing a higher number of metaphasis in a near tetraploid state. B) Frequency of the number of metacentric chromosomes per metaphase. C) Frequency of the number of submetacentric chromosomes per metaphase. D) Frequency of the number of the amplified acrocentric chromosome marker per metaphase. E) B16F10 G-banded karyotype showing the presence of tetrasomy in some chromosomes, indicating the tetraploid origin of this cell line. F) Metaphase presenting different structural alterations found in B16F10.

3.3 J774-1 cell line

This tumoral cell line is derived from a reticulum cell sarcoma and presents various characteristics of primary macrophages as synthesis and lysozyme secretion, phagocytosis, Fc receptor expression [25] [26]. This cell line is deposited in the American Type Culture Collection cell bank (www.atcc.org) under the number TIB-67. According to ATCC bank, the tumor is adherent and was originally isolated from a female.

Cytogenetic analysis of J774-1 cells showed that its metaphasis presented chromosome numbers ranged from 30 to 77, with 85,05% of metaphasis showing (ranging from 62 to 77 chromosomes) and modal number of 73 chromosomes (Figure 3A). This cell line also showed many structural rearrangements, such as metacentric chromosomes, submetacentric, subtelocentric and micro-chromosomes as showed in graphical (Figure 3B-E). Karyotype (Figure 3F) also revealed a hipertriploid/near-tetraploid complement. Different chromosomal aberrations can be visualized in J774-1 metaphasis (Figure 3G). J774-1 also showed endoreduplicated metaphases.

Using conventional karyotype coupled to Multicolor FISH (mFISH), Marquez et al (2011) also showed that the wild-type J774 cell line was characterized by a near-triploid karyotype and found a marker chromosome derivatived of Chr 14, characterized by the replacement of its telomeric end by a part of Chr 3 [27]. We have found up to three metacentric chromosomes and probably, one of them is the chromosome marker previously described. The difference in the number of chromosome markers indicates that J774 shows chromosome instability and is subjected to chromosome alterations during cell culture passages.

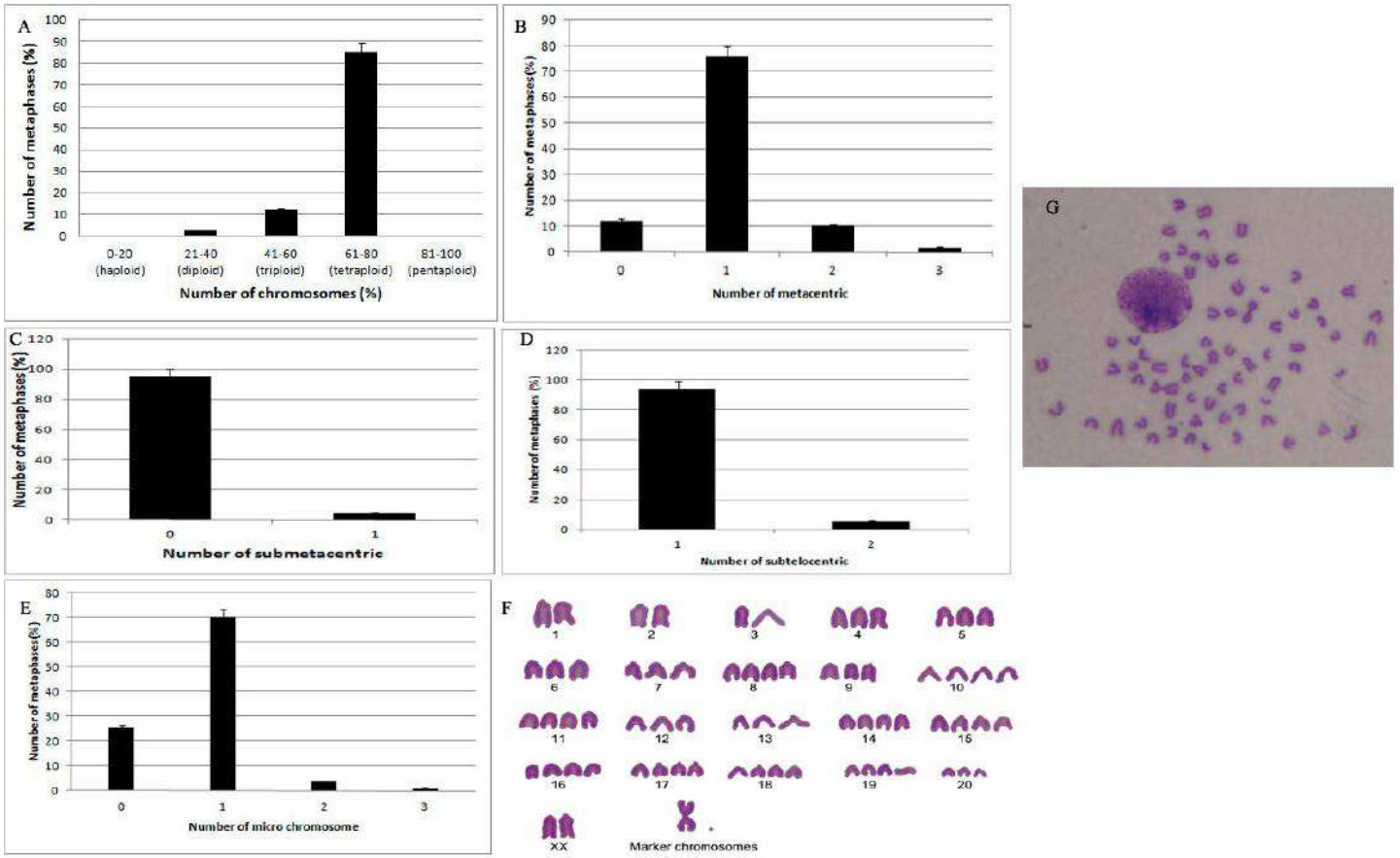

Figure 3 – Graphical representations and photomicrography of J774-1 cell line. A) Chromosome distribution showing a higher number of metaphasis in a near tetraploid state. B) Frequency of the number of metacentric chromosomes per metaphase. C) Frequency of the number of submetacentric chromosomes per metaphase. D) Frequency of the number of subtelocentric chromosomes per metaphase. E) Frequency of the number of microchromosomes per metaphase. F) J774-1 G-banded karyotype showing the presence of tetrasomy in some chromosomes, indicating the tetraploid origin of this cell line. G) Metaphase presenting different structural alterat

3.4 Mouse embryonic Fibroblast – MEF PS1

MEF are non-tumoral mouse cells frequently used as "feeder cells" in human embryonic stem cell research and as negative control cells. Many murine cell lines are used as models in an attempt to understand cancer biology. Cytogenetic characterization of these cell lines is important to demonstrate the role of chromosomal anomalies in the process of its immortalization. The Murine Embryonic Fibroblasts (MEF) has a variable Hayflick limit and may proliferate indefinitely, generating an undetermined mitotic potential, which makes it suitable for studying immortalization [28] [29].

In the present study we have characterized the karyotype of MEF-PS1 cell line. Chromosome counting presented numbers ranging from 40 to 85, with 81.3% of metaphasis showing a near tetraploid chromosome number (61-80 chromosomes) and modal number of 68 chromosomes (Figure 4 A). While in a normal murine cell all chromosomes are acrocentric, metaphasis of MEF showed many structural rearrangements, such as metacentric chromosomes, submetacentric, subtelocentric and micro-chromosomes as showed in graphical (Figure 4 B-E). G-banded karyotype (Figure 4 F) indicates a hiper-triploid/near-tetraploid complement and chromosome aberrations can be better visualized in the metaphase from figure 4 G.

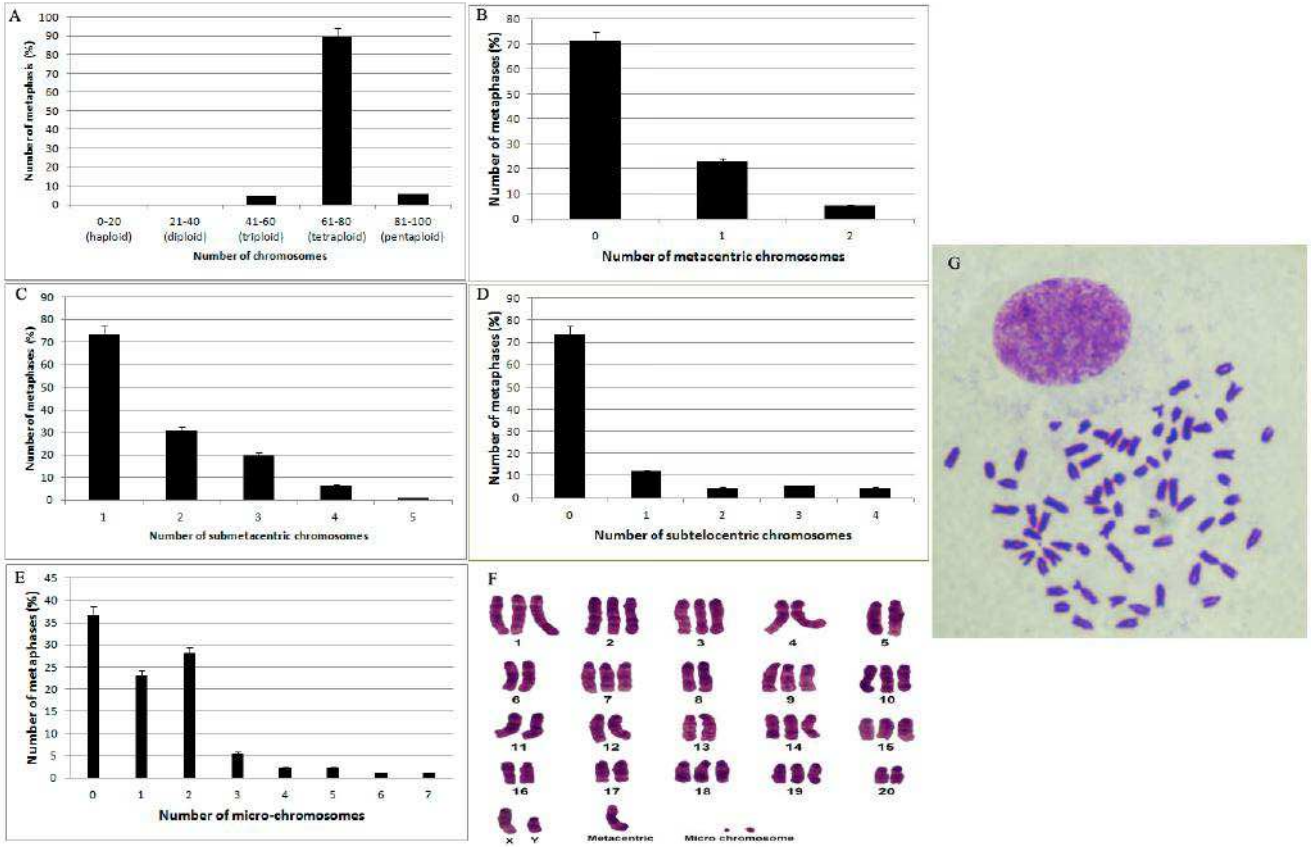

Figure 4 – Graphical representations and photomicrography of MEF PS1 cell line. A) Chromosome distribution showing a higher number of metaphasis in a near tetraploid state. B) Frequency of the number of metacentric chromosomes per metaphase. C) Frequency of the number of submetacentric chromosomes per metaphase. D) Frequency of the number of subtelocentric chromosomes per metaphase. E) Frequency of the number of microchromosomes per metaphase. F) MEF PS1 G-banded karyotype showing the presence of tetrasomy in some chromosomes, indicating the tetraploid origin of this cell line. G) Metaphase presenting different structural alterations found in MEF PS1.

3.5 NIH-3T3 cells

NIH-3T3 is an immortalized mouse embryonic fibroblasts cell line, originally isolated in 1962 at New York University School of Medicine, Department of Pathology [30]. This cell line has been used since then to various biomedical studies. Once that these cells have an indefinite mitotic capacity they are an excellent model for understanding the kinetics of cancer. In order to monitor the chromosome composition of NIH-3T3, the present work performed classic cytogenetic characterization.

Concerning to chromosome number, NIH-3T3 cell line presented a modal number of 41 chromosomes (Figure 5 A). The chromosome number of NIH-3T3 has been described by other authors also as a hyperdiploid, with an approximately equal number of unstable chromosome forms as 2 tri-radial, 1 metacentric, 2 quadri-radial, 2 chromosome gaps and did not observed any endoreduplication event [31]. In relation to chromosome structure, it was observed a high index of chromosomal abnormalities as dicentric chromosomes, micro-chromosomes, many metacentric chromosomes (ranging from 8 to 30), submetacentric and subtelocentric chromosomes (Figure 5 B-c).

In the present work we observed a much higher number of metacentric chromosomes than previously described in the inicial cell line. We also observed many metaphasis showing endoreduplication, indicating that this event can be involved in the chromosome alterations observed in the cell line. The increasing in the two arms chromosomes is probably due by non-reciprocal translocations and chromosome fusions. It explains the decreasing in the number of chromosomes per metaphase, indicating that cell line is undergoing to karyotype reorganization after initial tetraploidy.

The maintenance of the fundamental number (number of chromosome arms) near to the tetraploid complement (modal number of 64), prove the original tetraploidy of this cell line and the hiperdiploid number obtained by chromosome counting is resulting from chromosome fusions (robertsonian translocations).

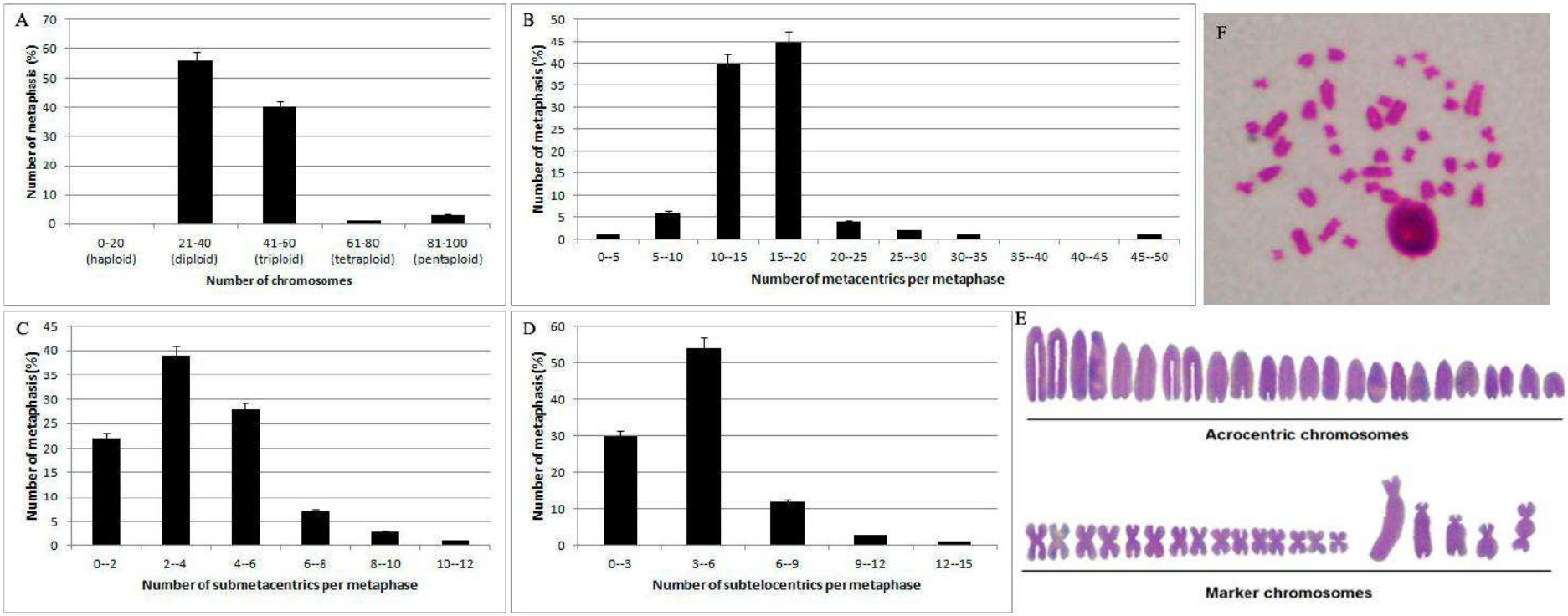

Figure 5 – Graphical representations and photomicrography of NIH-3T3 cell line. A) Chromosome distribution showing a higher number of metaphasis in a near tetraploid state. B) Frequency of the number of metacentric chromosomes per metaphase. C) Frequency of the number of submetacentric chromosomes per metaphase. D) Frequency of the number of subtelocentric chromosomes per metaphase. E) NIH-3T3 G-banded karyotype showing the presence of tetrasomy in some chromosomes, indicating the tetraploid origin of this cell line. F) Metaphase presenting different structural alterations found in NIH-3T3.

3.6 A new hipertriploid/near-tetraploid cell line induced through colcemid polyploidization

Due to the constant presence of polyploidy and aneuploidy in immortalized cell lines, we decided to verify the effects of polyploidy in cell proliferation and chromosome inheritance, using colcemid to generate tetraploid cells from mouse normal fibroblasts. Before polyploidization, fibroblasts had a very slow cell doubling, taking over a week to get confluent. After colcemid treatment, cells got confluent each three days. A month after colcemid treatment cells start to lose contact inhibition, a characteristic of malignization (Figure 6). Cytogenetic analysis revealed that colcemid treatment really induced polyploidization, once that most cells presented a near tetraploid complement (Figure 7 A and F). Beyond numerical alteration, we also observed many structural alterations in the chromosomes of this new cell line, such as the emergence of metacentric chromosomes, submetacentric, subtelocentric and microcromosomes (Figure 7 B-E). Metaphasis also showed many chromosome breaks and gaps (Figure G). This new obtained cell line was named JP.

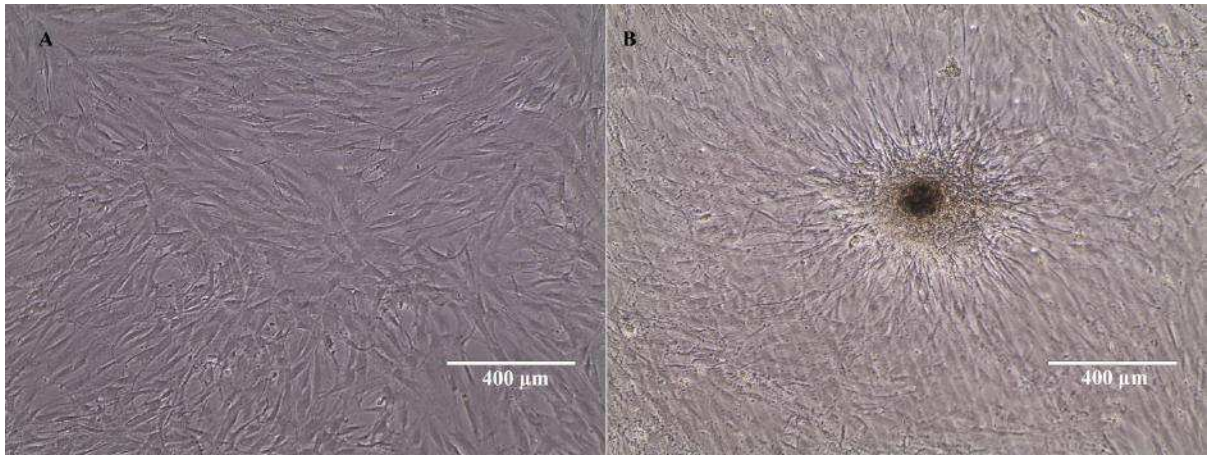

Figure 6 – Photomicrography of JP cells. A) Cells forming monolayers before reaching complete confluence. B) - Loss of contact inhibition. The cells continue to proliferate after reaching confluence, causing them to pile on top of each other, forming cell aggregates.

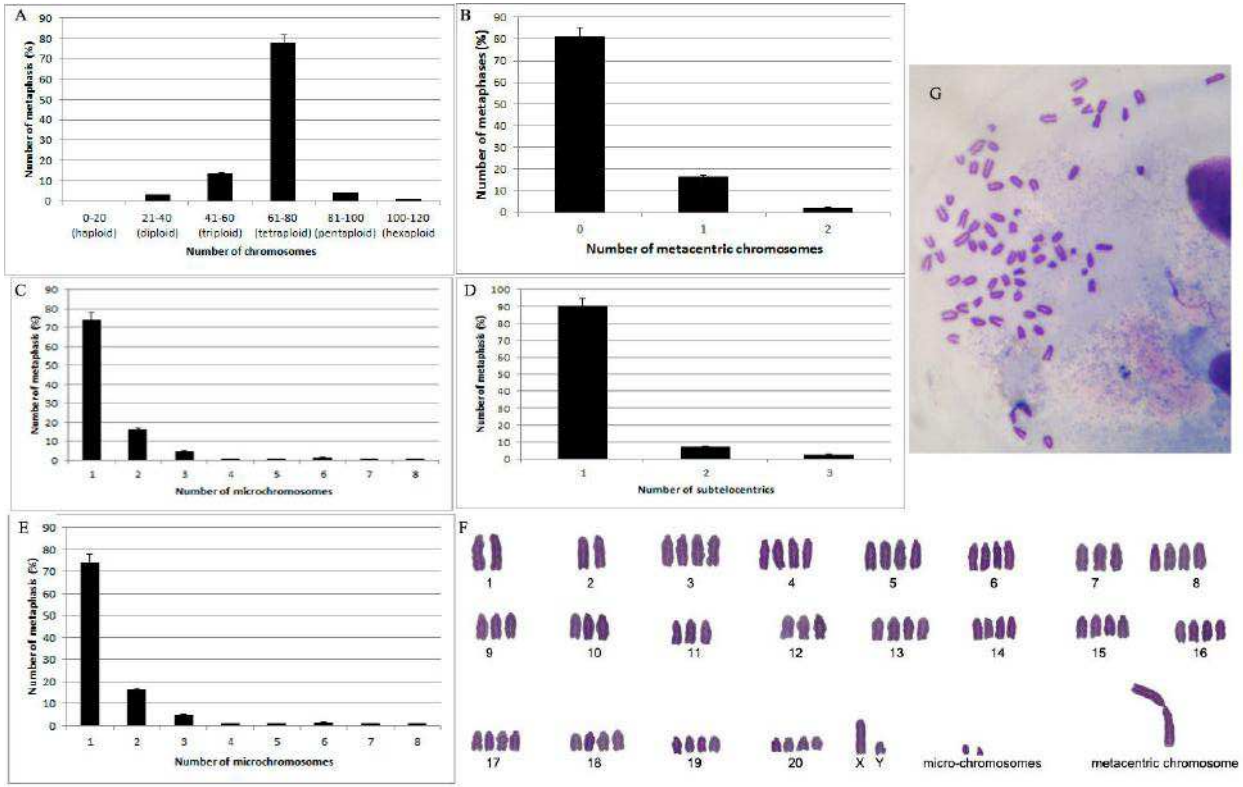

Figure 7 – Graphical representations and photomicrography of JP cell line. A) Chromosome distribution showing a higher number of metaphasis in a near tetraploid state. B) Frequency of the number of metacentric chromosomes per metaphase. C) Frequency of the number of microchromosomes per metaphase D) Frequency of the number of subtelocentric chromosomes per metaphase. F) JP G-banded karyotype showing the presence of tetrasomy in some chromosomes, indicating the tetraploid origin of this cell line. G) Metaphase presenting different structural alterations found in JP cell line.

The chromosome aberrations observed in JP cell line indicates that induction of polyploidy by colcemid generated chromosome instability, which promoted aneuploidy, chromosome breaks, associations and karyotype reorganization. Phenotype alterations, as increasing in cell doubling and loss of contact inhibition, can be a consequence of chromosome alterations, and it is an indicative that polyploidization started neoplastic transformation in the initial normal cells.

In a previous work, syrian hamster embryo cells in culture were treated with colcemid, resulting in morphological and neoplastic transformation of the cells. The group did not find any measurable induction of gene mutations and structural chromosome aberrations, but numerical chromosome changes were observed. It was observed an increase in the number of aneuploid cells and both chromosome loss and gain were induced. Their results are consistent with a role of carcinogen-induced chromosome non-disjunction and polyploidy in carcinogenesis [32]. Lanni et al. (2003) also observed an hyperproliferative status and cell hypertrophy in a culture of myofibroblast which presented spontaneous polyploidization. These characteristics became progressively more prominent in long-passage samples in parallel polyploidization increasing [33].

According to Ganem et al. (2007) polyploid cells are genetically unstable and can act as intermediates on the road to aneuploidy and, ultimately, cancer [3]. In this context, our group also believes that polyploidy is an essential event in carcinogenesis of solid tumors and in some cell line immortalization and that it promotes aneuploidy, an important hallmark of cancer cells. Many works suggest that aneuploidy is required for carcinogenesis in mice and that it can work with intra-genic mutations during tumorigenesis. The genomic plasticity provided by aneuploidy could facilitate, much more efficiently than punctual genic mutation, changes in gene dosage that would promote tumorigenesis and accelerate the oncogenes accumulation and the loss of tumor suppressor genes [34] [35] [36].

Getting a new cell line with neoplastic characteristics through the induction of plolyploidization with colcemid proved the importance of this event during carcinogenesis. The chromosomal alterations observed in the described cell line enhances the idea that polyploidization per se gives rise to genetic instability, generating aberrant karyotypes during cell culture passages.

3.7 Expression analyzes of genes evolved in tumoral progression

In order to verify the influence of karyotypical changes observed in JP cell line in comparison with the other analyzed cells, we performed real time PCR experiments to quantify levels of expression of the following classes of genes: (A)- Genes responsible to promoting cell proliferation as BRAF and Telomerase (TERT); (B)- The P53 gene responsible by tumor suppressing.

In all analyzed cell lines, BRAF gene (Figure 8 A) was more expressed than control group, however JP polyploid cell line and NIH-3T3 showed the lowest expression levels in relation to the other cell lines. All tumoral cells showed high levels of BRAF expression but, surprisingly MEF cell line showed the highest level of BRAF expression, being more expressed even than tumor cells. BRAF gene encodes a serine/threonine-specific kinase that is a key intracellular signaling component of the RAS/RAF/mitogenactivated protein/extracellular signal-regulated kinase (MEK)/ERK cascade and its over-expression leading to an increase in cell proliferation, cell survival, transformation, tumorigenicity, invasion and vascular development [37][37].

The high level of BRAF expression in MEF PS1 and tumor cell lines explains its immortalization and high proliferation index. Although also immortalized, NIH-3T3 did not show over-expression of BRAF, so its immortalization is probably due to another pathway. As JP polyploidy is a newly established cell line, it may not have acquired mutational events that lead to BRAF deregulation.

TERT gene (Figure 8B) was extremely over-expressed by tumoral cell line S180 in comparison to other cell lines. S180 is an extremely aggressive sarcoma, in comparison to its similar cell line TG180, that also over-expresses TERT, but in lower levels. JP polyploidy cell line expressed higher levels of telomerase than the tumoral cells J774-1 and B16F10. Telomerase over-expression in JP cell line is further evidence that these cells underwent transformation. One of the most relevant characteristics of a proliferative and immortalized tumor cell is the telomerase activation or over-expression. Beyond keeping telomere integrity, permitting limitless replication, telomerase confers additional functions that are required for tumorigenesis [38][39];[40]; [41].

P53 gene presented low levels of expression in S180, B16F10, NIH-3T3 and JP cells (Figure 8D), however in macrophage J774-1 and MEF it present

elevated expression in relation to control and other cell lines. The p53 tumor suppressor gene plays an important role in preventing tumor development, once that p53 protein interacts with other p53 signal pathway members to control cell proliferation [42]. High P53 expression was not expected in tumor or immortalized cells, once that its role is proliferation inhibition, but according to Campsi (2005), even presenting intact function of tumor suppressors as P16 and P53 cells can acquire immortalized phenotype having an indefinite proliferation potential [29]. Romanov et al (2001) also demonstrated that normal human breast epithelial cells in culture, continue to proliferate in the presence of elevated p53 and p21, suggesting that escape senescence process is associated with genomic changes that may lead to neoplastic transformation [43].

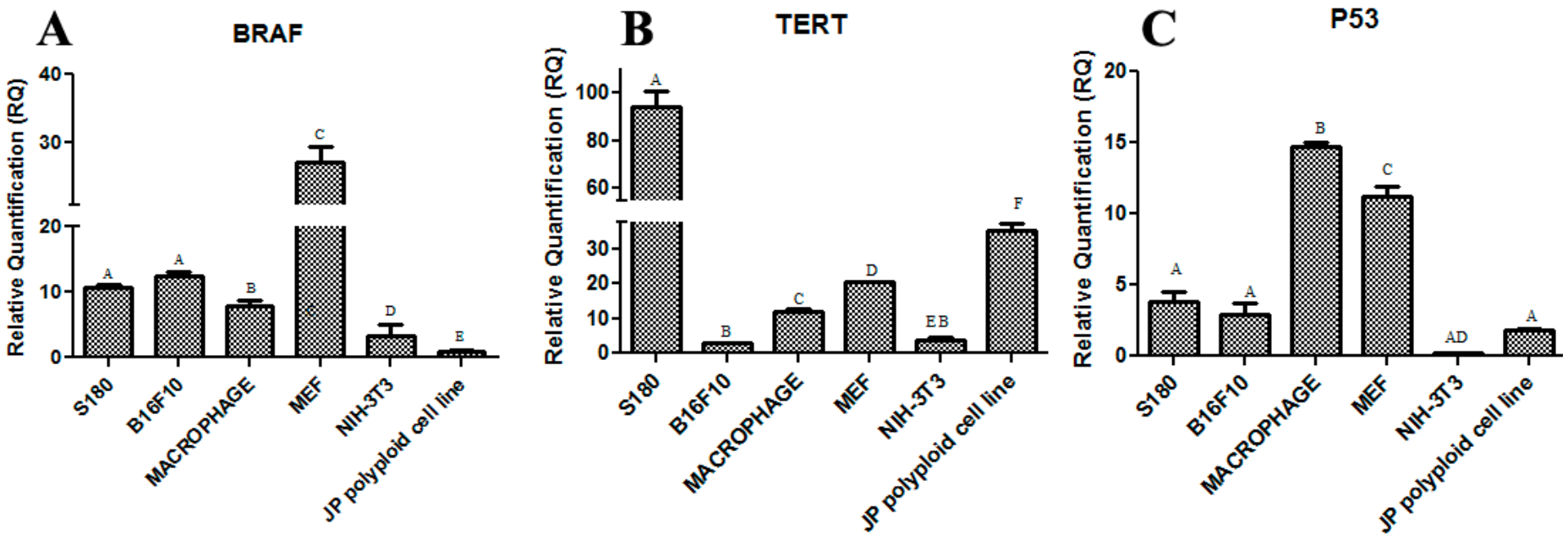

Figure 8 – Graphic representation of the relative quantification of expression levels. A) BRAF gene; B) Telomerase (TERT) gene; C) P53 gene. Columns with the same letter did not show statistical diference. P value < 0,05.

4. Conclusion

The ubiquitous presence of aneuploidy in human solid tumors associated to the results obtained from the present chromosomal analyzes enforces the essential role played by polyploidy driving aneuploidy in cell transformation and that aneuploidy is an easier way to promote hundreds or thousands of gene alterations, due to genetic instability generated by this karyotypical state.

5. References

1. Gordon DJ, Resio B, Pellman D: **Causes and consequences of aneuploidy in cancer.** *Nature reviews. Genetics* 2012, **13**:189–203.

2. Storchova Z, Pellman D: **From polyploidy to aneuploidy, genome instability and cancer**. *Molecular cell biology* 2004, **5**:45–54.

3. Ganem NJ, Storchova Z, Pellman D: **Tetraploidy , aneuploidy and cancer**. *Current Opinion in Genetics & Development* 2007, **17**:157–162.

4. Pinto AE, Andre S, Soares J: **Short term significance of DNA ploidy and cell proliferation in breast carcinoma : a multivariate analysis of prognostic markers in a series of 308 patients**. *Journal of Clinical Pathology* 1999, **52**:604–611.

5. Heselmeyer K, Macville M, Schrock E, Blegen H, Hellstrom AC, Shah K, Auer G, Ried T: **Advanced-stage cervical carcinomas are defined by a recurrent pattern of chromosomal aberrations revealing high genetic instability and a consistent gain of chromosome arm 3q**. *Genes Chromosomes Cancer* 1997, **19**:233–240.

6. Sumner AT: **Induction of diplochromosomes in mammalian cells by inhibitors of topo II**. *Chromosoma* 1998, **107**:486–490.

7. Siegel JJ, Amon A: **New Insights into the Troubles of Aneuploidy**. *Annual review of cell and developmental biology* 2012, **28**:189–214.

8. Galipeau PC et al.: **17p (p53) allelic losses, 4N (G2/tetraploid) populations, and progression to aneuploidy in Barrett's esophagus.**

Proceedings of the National Academy of Sciences of the United States of America 1996, **93**:7081–7084.

9. Olaharski AJ et al.: **Tetraploidy and chromosomal instability are early events during cervical carcinogenesis**. *Carcinogenesis* 2006, **27**:337–343.

10. Rajagopalan H, Lengauer CA: **Aneuploidy and cancer**. *Nature* 2004:338–341.

11. Guerra M, Souza MJ: *Como observar cromossomos - Um Guia de Técnicas em Citogenética Vegetal, Animal e Humana*. Editora, Ribeirão Preto, SP, Brazil: FUNPEC; 2002:184.

12. Sumner AT: **A simple technique for demonstrating centromeric heterochromatin**. *Experimental cell research* 1972, **75**:304–306.

13. Verma RS, Babu A: *Human chromosomes: Principles and techniques*. 2nd edition. New York, NY, USA: Mac Graw-Hill Inc.; 1995:419.

14. Fagundes V, Vianna-Morgante AM, Yonenaga-Yassuda Y: **Telomeric sequences localization and G-banding patterns in the identification of a polymorphic chromosomal rearrangement in the rodent Akodon cursor (2n=14,15 and 16).** 1997, **5**:228–232.

15. Schmid M, de Almeida CG: **Chromosome banding in Amphibia. XII. Restriction endonuclease banding**. *Chromosoma* 1988, **96**:283–290.

16. Howell WM, Black DA: **Controlled silver-staining of nucleolus organizer regions with a protective colloidal developer: a 1-step method.** *Experientia* 1980, **36**:1014–1015.

17. Levan A, Fredga K, Sandberg AA: **Nomenclature for Centromeric Position on Chromosomes**. *Hereditas-Genetics* 1964, **52**:201–208.

18. Chakrabarti S, Chakrabarti A: **Stable and transmissible dicentric chromosome with terminal centromeres in ascites cells of mouse**

sarcoma 180. *CELLULAR AND MOLECULAR LIFESCIENCES* 1978, **34**:1271–1273.

19. Lahn M, Sundell KL: **The role of protein kinase C-alpha (PKC-) in melanoma**. *Melanoma Res* 2004, **14**:85–89.

20. Golumbek PT, Azhari R, Jaffee EM, Levitsky HI, Lazenby A, Leong K, Pardoll DM: **Controlled Release, Biodegradable Cytokine Depots: A New Approach in Cancer Vaccine Design. v., p., .** *Cancer research* 1993, **53**:5841–5844.

21. Fidler IJ: **Biological behavior of malignant melanoma cells correlated to their survival in vivo.** *Cancer research* 1975, **35**:218–224.

22. Paszter L, F. H, RL. W: **Distinctive C-bands as identification markers for B16 melanoma lines**. *Pigment Cell* 1976, **2**:59–68.

23. Hu F, Wang YR, Hsu T.C.: **Clonal origin of metastasis in B16 murine melanoma: A cytogenetic study. :, .** *J Natl Cancer Inst* 1987, **78**:155–163.

24. Wang RY, Hsu TC, Kendal WS: **Repeated Tandem Translocations in a Clone and Subclones of B16-F10 Murine Melanoma**. *Cancer Genet Cytogenet* 1987, **29**:81–89.

25. Ralph P, Prichard J, Cohn M: **Reticulum cell sarcoma: an effector cell in antibody-dependent cell-mediated**. *immunity. J. Immuno* 1975, **114**:898.

26. Ralph P, Nakoinz I: **Phagocytosis and cytolysis by a macrophage tumour and its cloned cell line**. *Nature* 1975, **257**:393.

27. Marquez B, Ameye G, Vallet CM, Tulkens PM, Poirel H a, Van Bambeke F: **Characterization of Abcc4 gene amplification in stepwise-selected mouse J774 macrophages resistant to the topoisomerase II inhibitor ciprofloxacin.** *PloS one* 2011, **6**:e28368.

28. Serrano M, Gomez-Lahoz E, DePinho RA, Beach D, BarSagi D: **Inhibition of ras-induced proliferation and cellular transformation by p16 INK4**. *Science* 1995, **267**:249–252.

29. Campisi J: **Senescent Cells, Tumor Suppression, and Organismal Aging: Good Citizens, Bad Neighbors**. *Cell* 2005, **120**:513–52.

30. Todaro GJ, Green H: **Quantitative studies of the growth of mouse embryo cells in culture and their development into established lines**. *The journal of cell biology* 1963:299–313.

31. Thorgeirsson UP, Williams JE, Heilman CA, Talmadge JE, Liotta LA: **express the metastatic phenotype in nude NIH / 3T3 Cells Transfected with Human Tumor DNA Containing Activated ras Oncogenes Express the Metastatic Phenotype in Nude Mice**. *Molecular and cellular biology* 1985, **5**:3–7.

32. Tsutsui T, Maizumi H, Barrett JC: **Colcemid-induced neoplastic transformation and aneuploidy in Syrian hamster embryo cells Carcinogenesis**. *Carcinogenesis* 1984, **5**:89–93.

33. Lanni C, Bottone MG, Bardoni a, Dyne K, Soldani C, Pellicciari C, Caporali R, Montecucco C: **Proliferation characteristics and polyploidization of cultured myofibroblasts from a patient with fibroblastic rheumatism.** *European journal of histochemistry : EJH* 2003, **47**:257–62.

34. Pihan G, Doxsey SJ: **Mutations and aneuploidy: Co-conspirators in cancer?** *Cancer cell* 2003, **4**:89–94.

35. Pfau SJ, Amon A: **Chromosomal instability and aneuploidy in cancer: from yeast to man**. *EMBO reports* 2012, **13**:515 – 527.

36. Andrew J Holland, Cleveland DW: **Losing balance: the origin and impact of aneuploidy in cancer**. *EMBO reports* 2012, **13**:501 – 514.

37. Pritchard C, Carragher L, Aldridge V, Giblett S, Jin H, Foster C, Andreadi C: **UKPMC Funders Group Mouse models for BRAF-induced cancers**. *Biochem Soc Trans* 2009, **35**:1329–1333.

38. Kim NW, Piatyszek MA, Prowse KR, Harley CB, West MD: **Specific association of human telomerase activity with immortal cells and cancer**. *Science* 1994, **266**:2011–2015.

39. Blasco MA, Lee HW, Hande MP, Samper E, Lansdorp PM: **Telomere shortening and tumor formation by mouse cells lacking telomerase RNA**. *Cell* 1997, **91**:25–34.

40. Stewart S a, Hahn WC, O'Connor BF, Banner EN, Lundberg AS, Modha P, Mizuno H, Brooks MW, Fleming M, Zimonjic DB, Popescu NC, Weinberg R a: **Telomerase contributes to tumorigenesis by a telomere length-independent mechanism.** *Proceedings of the National Academy of Sciences of the United States of America* 2002, **99**:12606–11.

41. Shay JW, Wright WE: **Role of telomeres and telomerase in cancer**. *Seminars in cancer biology* 2011, **21**:349–353.

42. Isin M, Yenerel M, Aktan M, Buyru N, Dalay N: **Analysis of p53 tumor suppressor pathway genes in chronic lymphocytic leukemia.** *DNA and cell biology* 2012, **31**:777–82.

43. Romanov SR, Kozakiewicz BK, Holst CR, Stampfer MR, Haupt L. ., Tlsty TD, TD..: **Normal human mammary epithelial cells spontaneously escape senescence and acquire genomic changes**. *Nature* 2001, **409**:633–637.

Capítulo 5

“Specific recombinant peptides to the tg180 sarcoma tumor cell line for drug delivery and imaging applications”

Artigo formatado de acordo com a revista Molecules

SPECIFIC RECOMBINANT PEPTIDES TO THE TG180 SARCOMA TUMOR CELL LINE FOR DRUG DELIVERY AND IMAGING APPLICATIONS

Oliveira-Júnior, RJ[1]; Santos, FAA[1]; Fujimura, PT[1]; Ueira-Vieira, C[1]; Goulart, LR[1]; Morelli, S[1].

[1]Instituto de Genética e Bioquímica, Universidade Federal de Uberlândia, MG; robson_junr@yahoo.com.br

Abstract

Therapy and diagnosis of cancer are major goals of many research centers around the world. Among available strategies, the phage display subtractive proteomic technology has provided important information for putative therapeutic and diagnostic targets. The technology involves the screening of ligands randomly displayed in the surface bacteriophage libraries, which consists of successive cycles of selection, washing, elution and amplification, resulting in high affinity peptide/antibody markers to any given target. These ligands can be used to recognize specific cancer markers or cells, either as direct therapeutic molecules to malignant cells or as sensing molecules for imaging analysis. The present work used a murine tumor cell line (TG180) as a model to select peptides capable of binding to these cells aiming tumor-target applications as proof-of-concept. We have used two commercial phage display libraries, a linear and a conformational, *Ph.D.12 and Ph.D.C7C*, respectively *(New England Biolabs).* We have performed validation assays by using whole cell ELISA, immunocytochemistry, immunohistochemistry, and flow cytometry. Three cycles of selection were used with two subtraction (elution) strategiesvto eliminate those phage clones that bind to normal cells: (A) a pool of different normal tissue cells from mice (muscle, heart, whole blood, bone marrow, spleen, liver, lung and brain) and (B) muscle tissue and total blood for negative elution. After selection, 96 clones for each strategy were randomly amplified, and the DNA was sequenced, translated, submitted to validation. Fourty four valid sequences from strategy 1 and thirty nine valid sequences from strategy 2 were produced. For strategy A, one sequence was predominant and repeated 21 times while in strategy B all sequences were different. From the preliminary validation with ELISA assays against whole tumor cells, four clones with the highest reactivity were selected for additional analyses. Results based on immunocytochemistry, immunohistochemistry, flow cytometry and *in vivo* imaging confirmed the specificity of the selected peptides, which demonstrated to be strong ligands of tumor cells only, without any recognition of normal cells. Mass spectrometry (LC-MS/MS) analyses suggest that clones bind to vimentin, an important tumor marker. Our results suggest that the new ligands can be used either as drug delivery molecules or as imaging probes for *in vivo* or *in vitro* diagnostics.

Keywords: Phage-Display; Flow-cytometry; immunocytochemistry; immunohistochemistry; *in vivo* imaging; vimentin.

1. Introduction

Phage display, a subtractive proteomic technology, has provided important information for putative therapeutic and diagnostic targets. It is a powerful technology for identifying and engineering polypeptides with novel functions that bind to other molecules and it has had a major impact on immunology, cell biology, drug discovery and pharmacology. Its utility lies principally in generating molecular probes against specific targets and for the analysis and manipulation of protein/ligand interactions. Peptides selected by phage display are being explored in vaccine development, enzyme inhibition, inflammation, plant pathology, cardiovascular disease, cancer, etc. [1][2][3].

Peptides selected by phage display are capable of binding their target proteins with high affinity and unsurpassed specificity, and are thus attracting increasing attention as therapeutics and imaging diagnosis, once that early evaluation of cancer response to a therapeutic regimen can increase the effectiveness of treatment schemes and, by enabling early termination of ineffective treatments, minimize toxicity, and reduce expenses [4][5].

New peptide-based probes to facilitate the molecular imaging of disease are rapidly evolving due to implementation of combinatorial chemistry and bacteriophage (phage) display [2]. The use of phage as self-replicating biological nanoparticles is a very safe, simple and attractive solution for the development and implementation of peptides that can be used for *in vivo* imaging [6].

Many bioactive peptides have been selected by phage display for molecular imaging purposes. An example is the 12-mer peptide called bevacizumab-responsive peptide (BRP), a potentially useful pre-clinically and clinically for monitoring treatment response, that predicts tumor early response to antiangiogenic drugs [5]. Sun et al (2012) also have selected a peptide called OSP-1 which is able to bind specifically to an osteosarcoma cell line and according to the authors, OSP-1 peptide can be labeled to serve as a probe for osteosarcoma imaging *in vivo* and *in vitro.* [7].

The poor selectivity of chemotherapeutic drugs for neoplastic cells can cause dose-limiting side effects that compromise clinical outcome [8]. In this context, phage display can also be a tool for selection of peptides having the ability of direct chemotherapy or other molecules, such as oligonucleotides,

specifically to tumor cells, once that peptides can recognize relevant sites on the surface of the target protein, which can be present or over-expressed just in tumor cells [9]. Du et al. (2012), for example, designed and synthesized a hepatocarcinoma-binding peptide and coupled it into micelles for targeting therapy of doxorubicin suppressing both, *in vitro* and *in vivo* tumor growth [10].

A growing list of peptides selected by phage display used to delivery antisense oligonucleotides and siRNAs has also been identified. Lundberg et al. (2007), established a endosomolytic cell penetrating peptide called EB to deliver siRNA and induce gene silencing. This peptide is much more effective in forming complexes and transporting biologically active siRNA than its parent peptide penetratin [11]. According to Fougerolles (2008), complexation of siRNA with positively charged peptides has been an approach successfully used by several laboratories to obtain an specific delivery of silencing agents [12].

Here, we use *in vitro* phage display selection to identify targeting peptides selective for TG180 sarcoma cell line. The possible target of two peptides was identified and we demonstrate their selectivity for the tumor cells and perspectives of utility in tumor homing and imaging strategies. In a previous work, our group has demonstrated that TG180 cells over-expresses telomerase and that the silencing of this protein inhibits *in vitro* cell proliferation. Thus, the finding of peptides able to target TG180 cells performed in the present work can be a useful tool to deliver siRNAs specifically against telomerase gene of tumor cells, avoiding telomerase silencing in normal cells, such as stem cells and germinative cells. Our group has also discovered a Diterpene from the plant *Xylopia langsdorffiana,* named Trachylobane-360, which exhibits both, *In Vitro* and *in Vivo* Antitumor Effect in TG180 cells [13]. Thus, the complexing of this phytotherapeutic compound to tumor homing peptides is also a good strategy to avoid side effects of chemotherapy.

2. Material and Methods

2.1 Animals, Cells and culture conditions

TG180 sarcoma cell line were purchased from American Type Culture Collection (ATCC, Manassas, USA) and grown *in vitro* using RPMI-1640 medium, with 10% fetal calf serum (FCS), 25 mM HEPES, 1% penicillin-

streptomycin, and 2 mM L-glutamine. The *in vivo* maintenance of the cells was done by the inoculation of 300 µL of cells (1.0 x 10^7 cells cells) in the peritoneum of three Balb-c male mice, weighting ± 20 grams. Animals were kept in the Animal Experimentation Laboratory (LEA) of the Federal University of Uberlândia under controlled conditions. Animals were housed under standard conditions (22±1°C, humidity 60±5%, 12 h light/12 h dark cycle) with food and water *ad libitum*. All procedures for the handling, use and euthanasia of these animals followed the rules of the Brazilian Society for Laboratory Animals Science, and was approved by the Ethics Committee in Animal Research of the Federal University of Uberlândia, Brazil (CEUA/UFU N. 039/09), and every effort was made to minimize suffering.

2.2 Peptide selection through phage display (Biopanning)

For the peptide screening, a PhD.-12 and a Ph.D.-C7C phage library (New England Biolabs, Beverly, MA, USA) were used. The PhD.-12 and Ph.D.-C7C are random peptide libraries with 12-mer and 7-mer, respectively, fused to the minor coat protein (pIII) of the M13 bacteriophage, with a peptide diversity of 1.9×10^9. Peptides from PhD.-12 are linear while the randomized segment of the Ph.D.-C7C library is flanked by a pair of cysteine residues, which are oxidized during phage assembly to a disulfide linkage, resulting in the displayed peptides being presented to the target as loops. A sample from both libraries containing 2×10^{11} infectious phage particles was subjected to three rounds of selection and amplification. TG180 cells were taken as the target cells, as well as normal tissue cells from mouse (cells from kidney, liver, heart, whole blood, bone marrow, brain, spleen and muscle) were used as the absorber cells for whole-cell subtractive screening from the phage display libraries. It was performed two distinct subtractive screening strategies in parallel, one using all tissues cited above (Strategy A) and another one using just muscle and whole blood cells (Strategy B). The positive selection was carried out using 1,0 x 10^7 TG180 cell line suspended in PBS 1X. Cells were blocked with BSA 5% at 4°C for 1h and washed three times with PBS 1X. Meanwhile, cells were incubated with 2×10^{11} phage particles from libraries in 200 µL of PBS 1X at 4°C for 1h. After incubation the unbound phage particles were discarded, followed by elution of

bound phages with 1 mL of elution buffer (0.2 M Glicine-HCl, pH 2.2 and BSA 1 mg/mL) for 10 min at room temperature. After elution, the solution was centrifuged at 4000 rpm and 4°C for 1 min and the supernatant transferred to a new microtube containing 150 µL of 1 M Tris-HCl (pH 9.1) for neutralization. The eluted phages were amplified in *E. coli* ER2738 strain (New England Biolabs, Beverly, MA, USA), purified using PEG-NaCl precipitation and after each of the three rounds of biopanning, individual bacterial colonies containing amplified phage clones were grown in a microtiter plate and titrated essentially as described [14].

2.3 Bioinformatic analysis

Phage DNA was isolated from 1 mL overnight cultures and the sequencing reactions were carried out by using the DyEnamic ET Dye Terminator Cycle Sequencing Kit (GE Healthcare) with the primer -96 M13 (5'-CCCTCATTAGTTAGCGCGTAACG-3'), according to the manufacturer's instructions, and detection was performed in a MegaBace 1000 Genetic Analyzer (Amersham Biosciences) automatic capillary sequencer. Amino acid sequences were deduced according to the nucleotide sequences and analyzed using ExPASy (the Expert Protein Analysis System) World Wide Web server (http://web.expasy.org/translate/). The sequence alignment with ClustalW2 software (http://www.ebi.ac.uk/Tools/ msa/clustalw2/). The peptides alignment to target protein were performed using the program Pepsurf, a program for mapping a set of peptides, affinity selected against a probe molecule, onto a three dimensional structure of a target protein (http://pepitope.tau.ac.il/sources.html). The protein sequences used forAlignments were obtained from the RCSB PDB - Protein Data Bank (http://www.rcsb.org/pdb/home/home.do). 3D structures of peptides were determined using the program Molegro Molecular Viewer MMV 2011.2.2.0 (www.molegro.com).

2.4 Cell-based ELISA with phage

To test specific binding of these peptides to TG180 cells, it was performed Cell-based phage-ELISA experiments. Initially it was performed a pre-screening experiment to chose the most reactive clones. A ninety-sixwell

MaxisorpTM microtiter plate (NUNC, NY, USA) was seeded with 1,0 x 10^6 TG180 cells in 200 µL of carbonate buffer (0.1 M $NaHCO_3$, pH 8.6) overnight at 4 ºC. Cells were previously neutralized to endogenous peroxidase with 0,3% H_2O_2. The wells were washed with PBS (phosphate-buffered saline) and then blocked for 1 h at 37ºC with 5% BSA in PBS (BSA/PBS). The plate was washed twice with PBS and incubated with culture supernatant containing amplified phage particles (~10^{10} pfu/mL) for 2 h at 37ºC. The wells were washed four times with PBS-T followed by incubation with HRP-conjugated mouse anti-M13 (GE Healthcare Bio-Sciences) diluted (1:5000) in BSA/PBS for 1 h at 37ºC. The plate was washed five times in PBS 1X and the reaction was revealed by the addition of 0.03% H_2O_2 and 1 mg/mL o-phenylenediamine dihydrochloride (OPD, Sigma-Aldrich) in 0.1 M citrate-phosphate, pH 5.0. The reaction was interrupted by adding sulphuric acid (2 N) and the optical density (OD) was determined by spectrophotometry at 492 nm (Titertek Multiskan Plus, Flow Laboratories, USA).

After initial prescreening, the best clones were selected, amplified and quantified using spectrophotometry on the absorbance of 269 and 320 nanometers as described [14]. The pre-selected clones were used in a cell-based ELISA using TG180 cell line, another murine tumoral cell line called J774-1 (derived from macrophage) and Mouse Embryonic fibroblast (MEF, non tumoral cell line). J774-1 and MEF were used to test the specificity of selected clones to TG180 cell line. ELISA experiments were performed in triplicate using 1,0 X 10^{11} pfu/well.

2.5 Immunohistochemistry

TG180 cells were inoculated into gastrocnemius muscle of balb-c mice and after growing, solid tumors were fixed in 10% neutral buffer formalin, embedded in paraffin and sectioned at 5.0 µm for immunohistochemical studies. Staining was performed in three different sets to confirm the results. Sections were dewaxed in xylene series, rehydrated through a graded series of ethanol washes, washed in distilled water and PBS, then blocked for endogenous peroxidase activity by three incubation with 3% H_2O_2 in H_2O_2 for 5 min each one and washed in PBS 1X. The sections were subjected to antigen retrieval

procedure by microwaving in 0.01 M sodium citrate buffer pH 6.0. After washing in PBS, the non-specific binding was blocked using 2% normal goat serum in PBS 1X for 30 minutes at 37ºC. The sections were then incubated overnight at 4 °C with the selected phage clones (2,0 X 10^{11} pfu/section). The negative control sections were obtained by the addition of PBS 1X in place of the phage particles. Wild-type phages and a phage which expresses an irrelevant peptide also were used as controls. The sections were then incubated with HRP anti-M13 Monoclonal Conjugate antibody (GE Healthcare Bio-Sciences) diluted in PBS 2% normal goat serum for 1h at 37ºC. To visualize the immunoreaction, sections were immersed diaminobenzidine (Liquid DAB + substrate, Chromogen System, DAKO - USA). Finally, sections were counterstained with Mayer's hematoxylin, differentiated with ammonia water solution, dehydrated in ethanol, cleared in xylene and mounted with entelan [15].

2.6 Immunofluorescent image analysis by flow cytometry and microscopy

For the screening of phages binding to TG180 cell line, immunofluorescence staining was performed and cells were analyzed under flow cytometry, epifluorescence microscopy and confocal microscopy. About 1 × 10^6 cells were washed with icecold PBS and then blocked with BSA 5% for 30 min at 4 °C. TG180 cells were incubated with 1,0 x 10^{11} pfu diluted in BSA 5% 1h at 4 °C. After washing three times with PBS, mouse anti-M13 antibody (GE Healthcare Bio-Sciences) diluted in BSA 5% was added to cells and incubated for 1h at 4 °C. After washing three times with PBS again, fluorescein isothiocyanate (FITC)-conjugated goat anti mouse antibody (Sigma-Aldrich) was added to the cells for the detection of bound phages. After 1h incubation at 4 °C, the cells were washed five times and resuspended in PBS. Flow cytometry analyses were performed with AccuriC6 flow cytometer, using the optical filter FL1 533/30 nm, FITC/GFP (BD Biosciences, San Diego, CA). Cells were also mounted on individual slides to microscopy analyzes. Conventional epifluorescence images were taken using the microscopy AMG EVOS® fl Digital Inverted Fluorescence Microscope and confocal images were captured in an excitation wavelength at 488 nm with magnification of 40x, using a confocal laser scanning microscope (Carl Zeiss LSM 510 META, Jena,

Germany). The images obtained by a CLSM were converted to digital image and merged together using the Zeiss LSM Image Browser.

2.7 In vivo imaging

The tumor models were established by intramuscular injection of TG180 cells (1,0 x 10^7 cells) in 300 µL of PBS 1X in the gastrocnemius of mice. After 2 weeks of tumor inoculation, animals received 1,0 x 10^{12} pfu intravenously in the dorsal penile vein. Thirty minutes after phage administration, animals received mouse anti-M13 antibody (GE Healthcare Bio-Sciences) and Anti-Mouse IgG - Atto 647N (Sigma-Aldrich). The animal was successively subjected to fluorescence imaging (NIR) and X-ray imaging (X-ray) with the Kodak In-Vivo Imaging System FX Pro and the two images were merged for tumor localization.

2.8 Immobilization of phage expressing peptides on magnetic beads and protein immunoprecipitation

Total proteins of TG180 tumor cell line were extracted using the Complete Lysis-M EDTA-free kit (Roche Applied Science). Proteins which bind specifically to selected clones were isolated using magnetic separation. 10^7 magnetic beads (Dynabeads M-270 Epoxy – Dynal) were washed three times with sodium phosphate buffer 0.1 M and pH 7.4. Magnetic beads were then mixed with approximately 2,4.10^{11} viral particles in 75uL of 3M ammonium sulfate buffer pH = 7.4 and 25uL of sodium phosphate buffer 1.2 M pH 10.2. The magnetic beads/phages conjugated were incubated under agitation for 16 hours at 37 ° C. After incubation period, the beads were washed 3x with PBS and then incubated with 200ul of tumor protein extract for 4 hours at 4 ° C. The beads were washed 5 times with PBS, and protein was eluted with 0.2 M glycine pH = 2.5.

2.9 Mass spectrometry analyzes

2.9.1 Protein Digestion and Liquid Chromatography Tandem Mass Spectrometry (LC-MS/MS)

Protein samples were precipitated using ProteoExtract Protein Precipitation Kit (Calbiochem, Darmstadt, Germany) and enzymatically digested using trypsin in a solution of 10% actonitrile and 50mM ammonium bicarbonate

overnight at 37C. Protein sulfhydryl groups were reduced with TCEP bondbreaker (Pierce Biochemical, Rockford, IL) and alkylated using iodoacetamide. Digested proteins were then acidified with 5% (v/v) formic acid and cleaned up using Aspire RP30 desalting tips (Thermo Scientific). Digested peptides were then dried down by vacuum centrifugation.

LC-MS/MS analysis was performed using a standard top 15 method on Thermo Scientific Q-Exactive orbitrap mass spectrometer in conjunction with a Proxeon Easy-nLC II HPLC (Thermo Scientific) and Proxeon nanospray source. The digested peptides were reconstituted in 2% acetonitrile /0.1% trifluoroacetic acid and loaded onto a 100 micron x 25 mm reverse phase trap (Magic C18 100Å 5U trap) where they were desalted online before being separated using a 75 micron x 150 mm reverse phase column(Magic C18 200Å 3U). Data dependent MS/MS data was collected using higher energy collision dissociation (HCD). Peptides were eluted using a gradient of 0.1% formic acid (A) and 100% acetonitrile (B). A 65 minute gradient was ran with 5% to 35% B over 50 minutes, 35% to 80% B over 3 minutes, 80% B for 1 minute, 80% to 5% B over 1 minute, and finally held at 5% B for 10 minutes.

2.9.2 Data Analysis

2.9.2.1 Database Searching

Tandem mass spectra were extracted and charge states deconvoluted and deisotoped. All MS/MS samples were analyzed using X! Tandem (The GPM, thegpm.org; version TORNADO (2010.01.01.4)). X! Tandem was set up to search the Uniprot complete mouse proteome database (October 2012; 76,151 entries) and the Uniprot complete human proteome database (October 2012; 71,825 entries) plus an equal number of reverse sequences and 115 common laboratory contaminant proteins for the mouse database, and 47 common laboratory contaminant proteins for the common laboratory contaminant proteins for the human database(www.gpm.org/crap/), assuming the digestion enzyme trypsin. X! Tandem was searched with a fragment ion mass tolerance of 20 PPM and a parent ion tolerance of 10 PPM. Iodoacetamide derivative of cysteine was specified in X! Tandem as a fixed modification. Deamidation of asparagine and glutamine, oxidation of methionine and tryptophan, sulphone of methionine, tryptophan oxidation to

formylkynurenin of tryptophan and acetylation of the n-terminus were specified in X! Tandem as variable modifications.

2.9.2.2 Criteria For Protein Identification

Scaffold (version Scaffold_3.5.1, Proteome Software Inc., Portland, OR) was used to validate MS/MS based peptide and protein identifications. Peptide identifications were accepted if they could be established with an X!Tandem score greater than 1.8. Protein identifications were accepted if they could be established at greater than 50.0% probability and contained at least 1 identified peptide. Protein probabilities were assigned by the Protein Prophet algorithm (Nesvizhskii, AI Anal Chem. 2003 Sep 1;75 (17):4646-58). Proteins that contained similar peptides and could not be differentiated based on MS/MS analysis alone were grouped to satisfy the principles of parsimony. Using these parameters, a false discovery rate was calculated as 0% on the peptide level and 0% on the protein level for samples searched against the mouse and human database.

2.10 Statistical analysis

All statistical analyses were conducted by the statistical program GraphPad Prism 5 for windows, version 5.00. Comparisons among groups of data were made using Two-way analysis of variance (ANOVA), followed by the Bonferroni posttest. *P* value <0.05 was considered statistically significant. All results were presented as mean ± SD unless otherwise noted.

3. Results and discussion

3.1 Peptide library screening

The identification of molecules that binds specifically to tumor cells brings many biotechnological applications, mainly related to drug delivery and imaging used to diagnosis and treatment prognosis. Here, we have used TG180 tumor cell line as a target cancer model to select specific sarcoma binding peptides. This will allow for the discovery of peptides that specifically recognize molecular markers expressed by these tumor cells. In order to obtain ligand peptides, phages expressing 12mer and 7mer peptides on their surface were applied to *ex vivo* selection rounds on cultured TG 180 cells. Mouse normal cells were

used for negative control selection. In each round, the bound phages were rescued and amplified in E. coli for the following round of panning, while the unbound phages were removed by washing with PBS 1X.

Isolated phage colonies derived from the third round elution were amplified in 96 wells plates and single-stranded DNA was extracted and sequenced. We obtained 68 DNA sequences from phages selected by strategy A (pool of cells as subtract selection). However, only 39 sequences were considered valid, presenting the number of nucleotides corresponding to the number of expected aminoacids. For selection strategy B (muscle/blood subtracting selection) it was obtained 44 valid sequences from 89 DNA sequences. For sequences translation we used Expert Protein Analysis System World Wide Web server and the peptides were aligned using the ClustalW2 software (Figure 1).

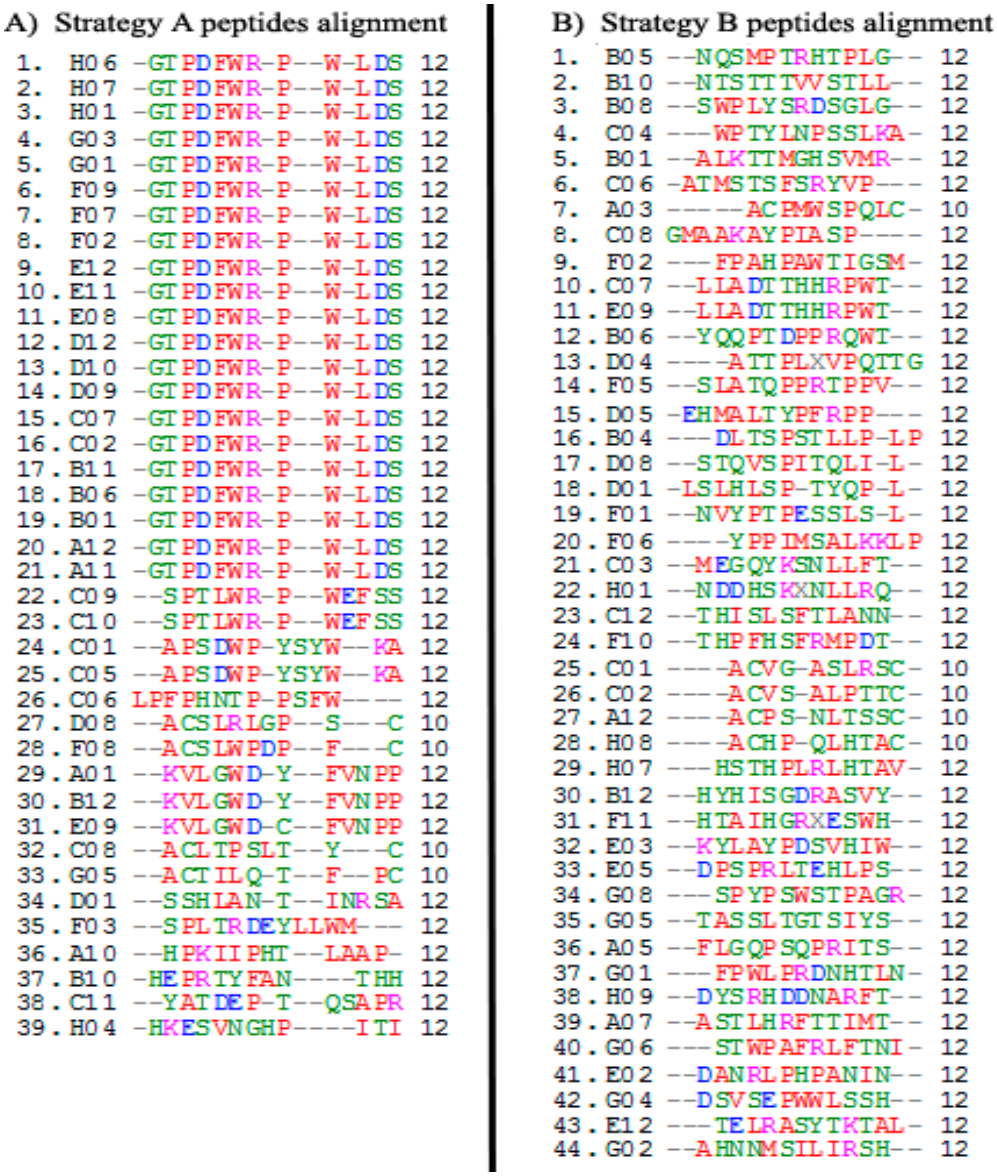

Figure 1 – Alignment of peptides obtained through biopanning strategy A and B using ClustalW program.

The obtained sequences were analyzed using the program WebLogo3 (http://weblogo.berkeley.edu/) and a graphical representation of the sequences did not indicate a conserved sequence between the aligned peptides. From the 39 valid sequences obtained from selection strategy A, a peptide named PF2 showed a higher frequency (53,84%). The graphical representation using the program WebLogo3 (Figure 2) considering all 21 sequences of PF2 and the other 18 sequences indicates the prevalence of this clone.

Figure 2 - Graphical representation of the sequence logo of PF2 peptide, generated by WebLogo3 (http://weblogo.berkeley.edu/).

3.2 Cell-based ELISA pre-screening

Cell-based ELISA assays were performed to identify clones that bind to TG180 antigens. The pre-screening allowed the selection of best clones. The three best clones from selection strategy A (Figure 3) and selection strategy B (Figure 4), the ones which showed higher absorbances, were select to perform subsequent experiments.

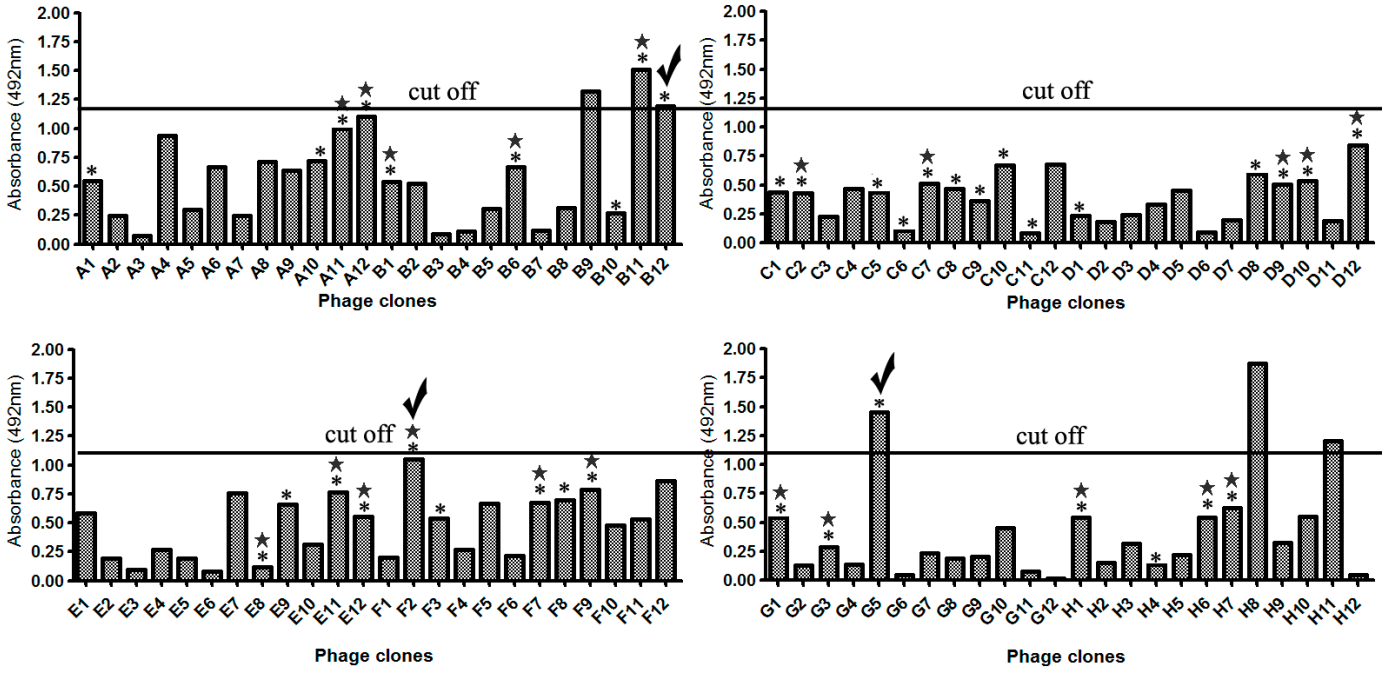

Figure 3 - Evaluation of the binding selectivity for the 96 phage clones of selection strategy A using a phage cell-ELISA. It was seeded $1x10^6$ cells/well in 96-well plates. Approximated 1×10^{10} pfu phages were added to each well at 4ºC for 1 h. A HRP-conjugated mouse anti-M13 was added in turn. An OD450

was obtained after the reaction blocking. *means valid sequences and ★means clones with the same peptide sequence.

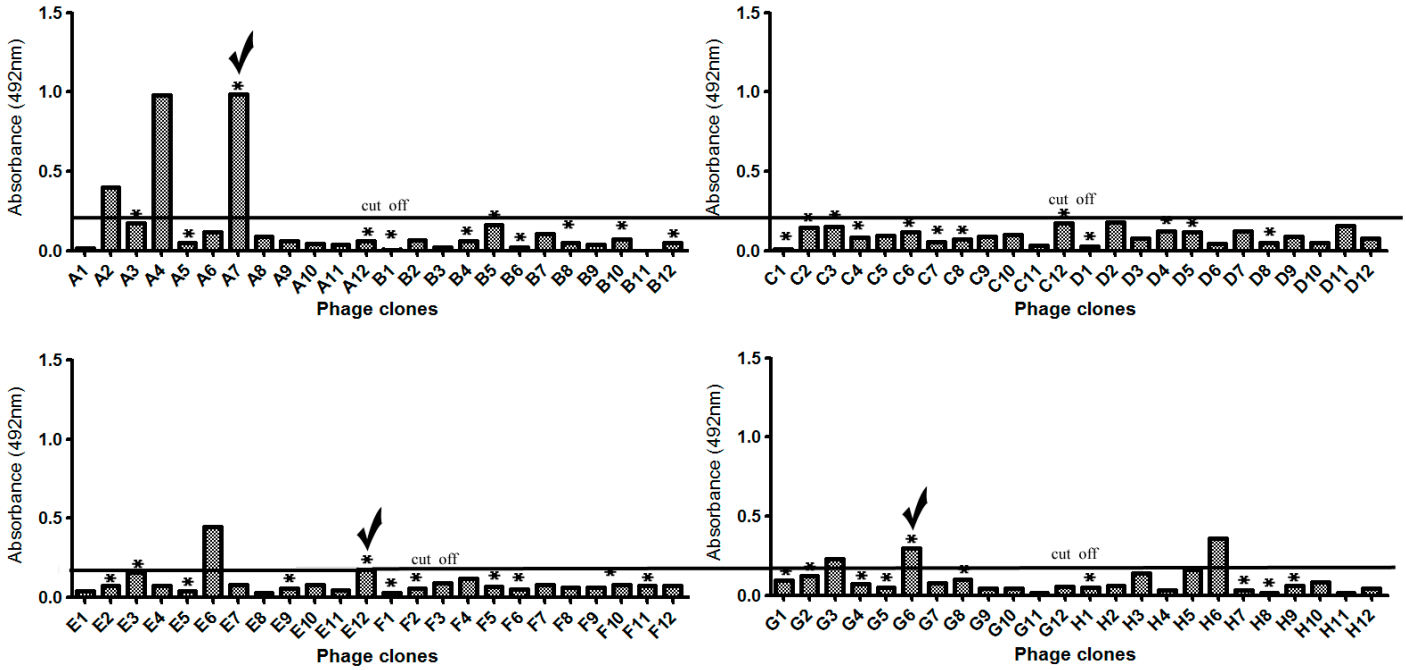

Figure 4 - Evaluation of the binding selectivity for the 96 phage clones of selection strategy B using a phage cell-ELISA. It was seeded 1x10^6 cells/well in 96-well plates. Approximated 1 x 10^{10} pfu phages were added to each well at 4ºC for 1 h. A HRP-conjugated mouse anti-M13 was added in turn. An OD450 was obtained after the reaction blocking. *means valid sequences.

3.3 Cell based ELISA in normal and tumoral cells and Fluorescence-Activated Cell Sorting (FACS)

The six pre-selected clones were amplified and quantified to be used in a cell based ELISA (Figure 5). Normal fibroblast cell line MEF and macrophage tumoral cell line J774-1 were used as negative control to figure out clones selectivity. Four clones (PF2, PB12, MA7 and ME12, Table 1) presented had higher specificity and afinity to TG180 cells and clones PG5 and MG6 demonstrated low specificity and low affinity, respectively. According to Zang et al. (2009), specific ligants that bind to tumor biomarkers is essential to increase the selectivity of cancer therapy and can helps in cancer detection [16]. The use of normal cells and other tumor cells during subtractive screening is a crucial step for select target tumor-specific antigens that are absent or differently expressed compared to non-tumoral condition. This assay allowed the choice of the best candidate phage clones with the highest specificity.

Table 1: Name and sequence of the selected clones, which presented higher affinity and specificity to TG180 cell line.

Selected clone	sequence
PF2	GTPDFWRPWLDS
PB12	KVLGWDYFVNPP
MA7	ASTLHRFTTIMT
ME12	TELRASYTKTAL

Furthermore, the sequences obtained in the present study do not exist in the current version of the MimoDB database. MimoDB is a database collecting peptides that have been selected from random libraries based on their ability to bind small compounds, nucleic acids, proteins, cells, tissues, organs, and even entire organisms through phage display and other surface display technologies. Using MimoDB, experimental scientists can search their peptides against all peptides in the MimoDB database in batches to verify if each peptide has been reported by other groups with different targets [17][18].

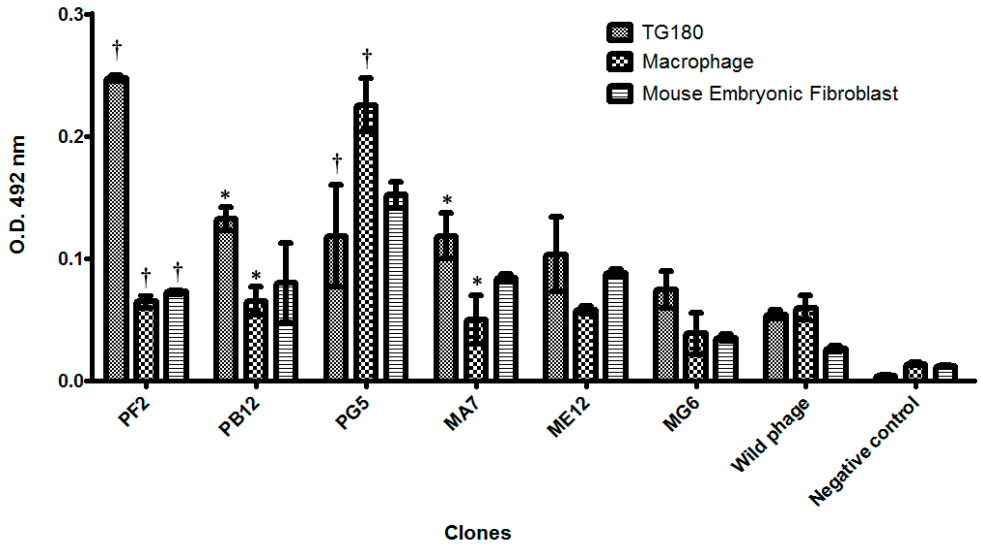

Figure 5 - Cell-ELISA evaluation of the binding selectivity for the 6 phage clones selected by strategies A and B. It was seeded $1x10^6$ cells/well in 96-well plates. Approximated 1×10^{10} pfu phages were added to each well at 4ºC for 1 h. A HRP-conjugated mouse anti-M13 were added in turn. An OD450 was obtained after the reaction blocking. It was compared TG180xMacrophage and TG180xMEF. *P <0.05, †P <0.001.

Flow cytometry was also used in order to verify the efficiency of the six initially selected clones in binding to TG180 cell line. FACS results corroborated with cell-based ELISA results, evidencing a better binding efficiency of the four clones PF2, PB12, MA7 and ME12 (Figure 6), which were chosen to perform subsequent experiments to confirm its effectiveness.

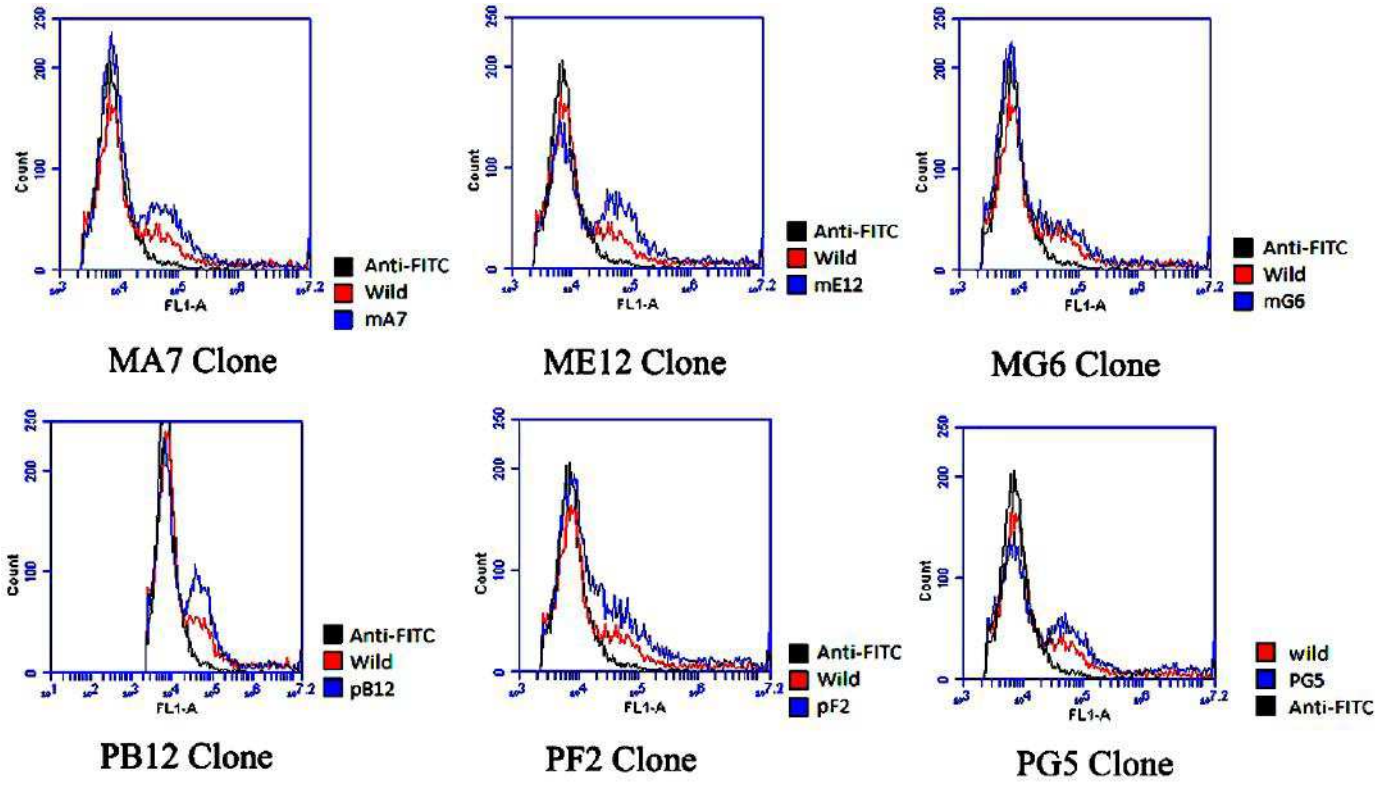

Figure 6 - Fluorescence-Activated Cell Sorting (FACS) analysis of phage clones efficiency in binding to TG180 cells. Negative controls are represented in a black line as cells incubated just with the FITC labeled antibody and red line represents cells incubated with the wild type phage. The selected clones are represented in the blue line.

3.4 Tumor specific binding analysis of clones by immunohistochemistry

Tissue slides from TG180 solid tumor induced in mouse gastrocnemius were prepared to evaluate specific binding of the selected clones (PF2, PB12, MA7 and ME12). From the results shown in Figure 7, all clones demonstrate specific binding to cytoplasmatic region of sarcoma TG180 cells. In contrast, no staining was observed in normal tissue (muscle and inflammatory cells) and in tissues incubated with phages expressing an irrelevant peptide. A weak staining was present with the wild-type phage. In the analyzed slides, the positive area (dark brown) was located at the cytoplasm of cancer cells,

indicating that peptides expressed by phages recognize biomarker molecules located at this region of tumor cells.

The immunohistochemistry results indicate that the biopanning strategy using subtractive selection rounds was successful in selecting clones without cross reaction with normal tissues. This specificity in phage binding is certain due to the peptide expressed in the pIII protein of bacteriophages, once that irrelevant phage didn´t show any reactivity and wild-type phage presented just a weak binding. The discovery of peptides that binds to cancer-specific receptors can be used to pursue the selective addressing of neoplasms. This strategy can eliminate or decrease the non-specific toxicity of most anticancer agents against normal cells, avoiding the side-effects observed in classic chemotherapy, once that it is well described the differential expression of several biomarkers in cancer cells. When compared to macromolecular compounds, as monoclonal antibodies, an expanding class of drugs for treating cancer, bioactive peptides display advantages as faster blood clearance, rapid tissue penetration, easy incorporation to delivery materials and drugs and low immunogenicity [19].

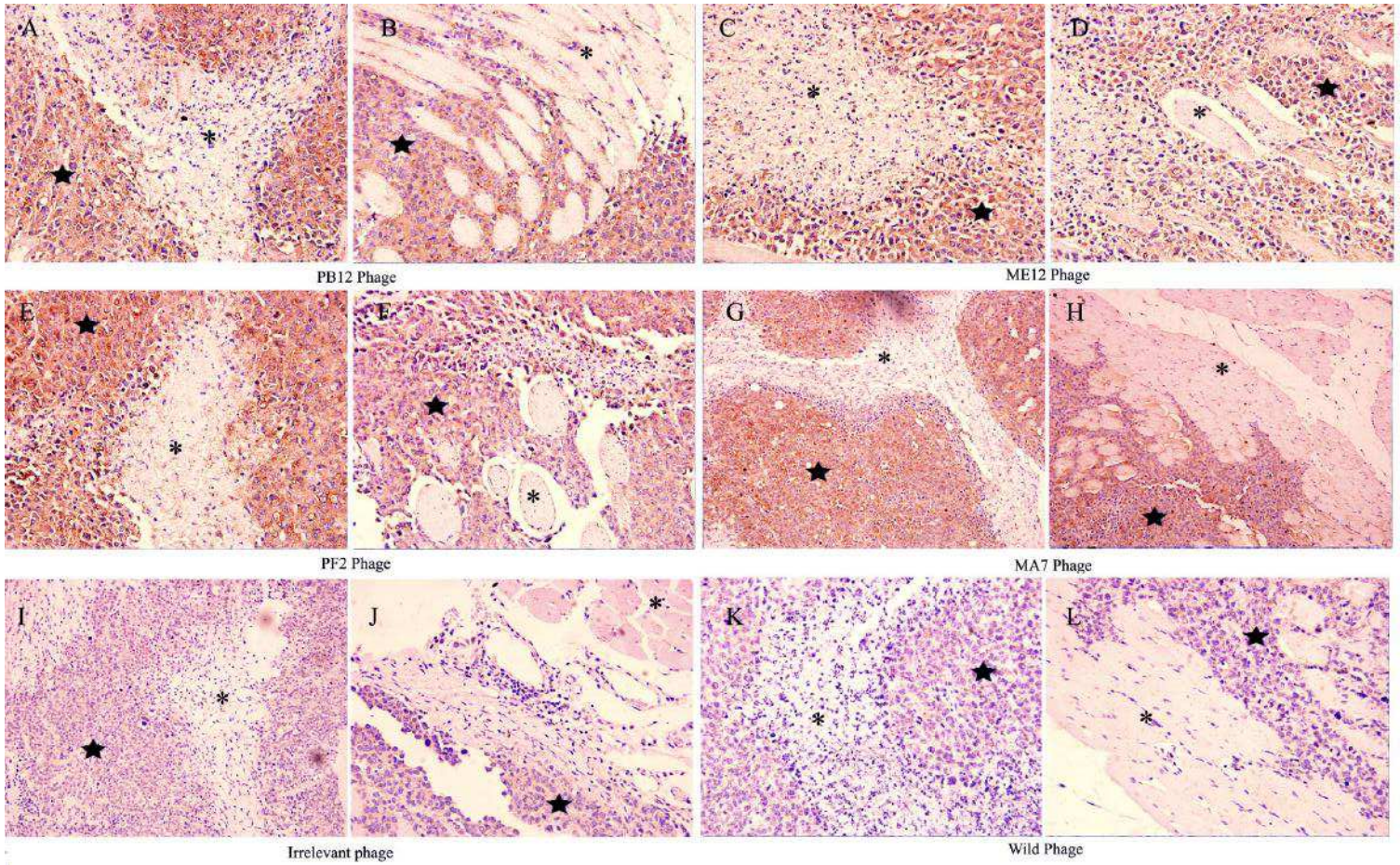

Figure 7 - Binding analysis of selected phage clones by immunohistochemistry. The results demonstrate that all selected clones showed a specific binding affinity to tumor cells (PB12:A and B; ME12: C and D; PF2: E and F; MA7: G and H). In contrast, no positive staining was observed in tumors treated with an irrelevant phage (I and J) and wild-type phage (K and L). ★ indicates tumor tissue and * indicates normal tissues.

3.5 Immunofluorescence microscopy analysis demonstrates the binding of clones to TG180 cells

Binding of selected clones were analyzed by epifluorescence and confocal microscopy. TG180 cells were treated and tested using the same methods and conditions as those used for FACS. Results from epifluorescence microscopy indicate that all four selected clones (PB12, PF2, MA7 and ME12) could bind to TG180 cells (Figure 8), while negative controls represented by the incubation with anti-mouse labeled with FITC and wild-type phage did not show any staining.

Immunofluorescence images of the clones PF2 (Figure 9), PB12 (Figure 10) and wild-type phage (figure 11) were also acquired with a confocal laser scanning microscope. The results confirm the binding properties of clones and confocal images indicate that phages bind in all extension of cell membrane and cytoplasm. Overlapping of slices achieved by confocal microcopy and 3D videos are presented in supplemental data, that show the binding of clones PF2, PB12 and wild-type phage in a TG 180 cell.

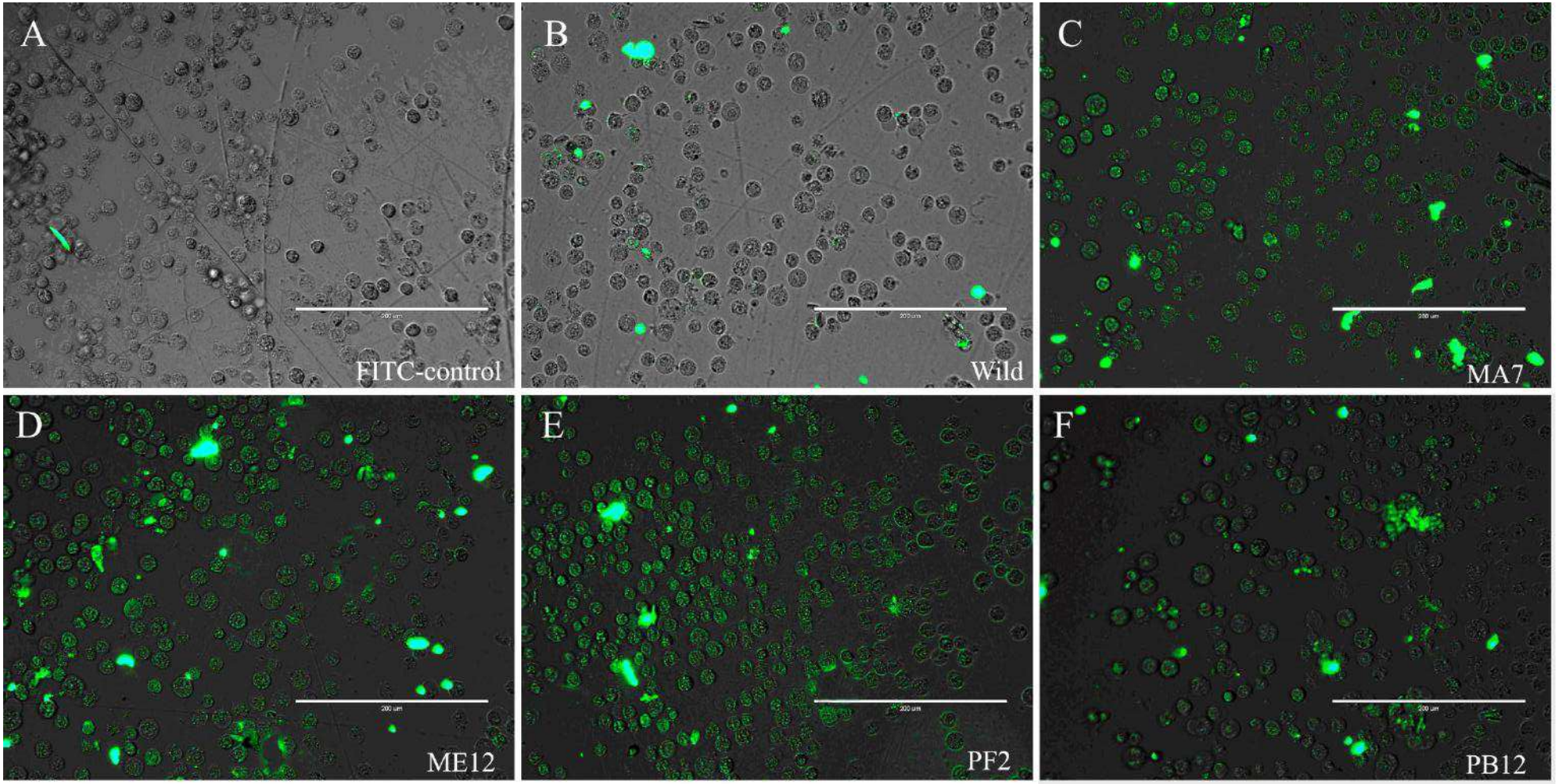

Figure 8 - The binding of the selected phage clones to TG180 cells. Cells were incubated witg phage particles, mouse anti-M13 antibody and than immunostained with a gota anti-mouse FITC labeled antibody. (A) Cells without any phage particle, just incubated with the FITC labeled antibody. (B) Cells incubated with wild type phage. (C) Cells incubated with clone MA7. (D) Cells incubated with clone ME12. (E) Cells incubated with clone PF2. (F) Cells incubated with clone PB12.

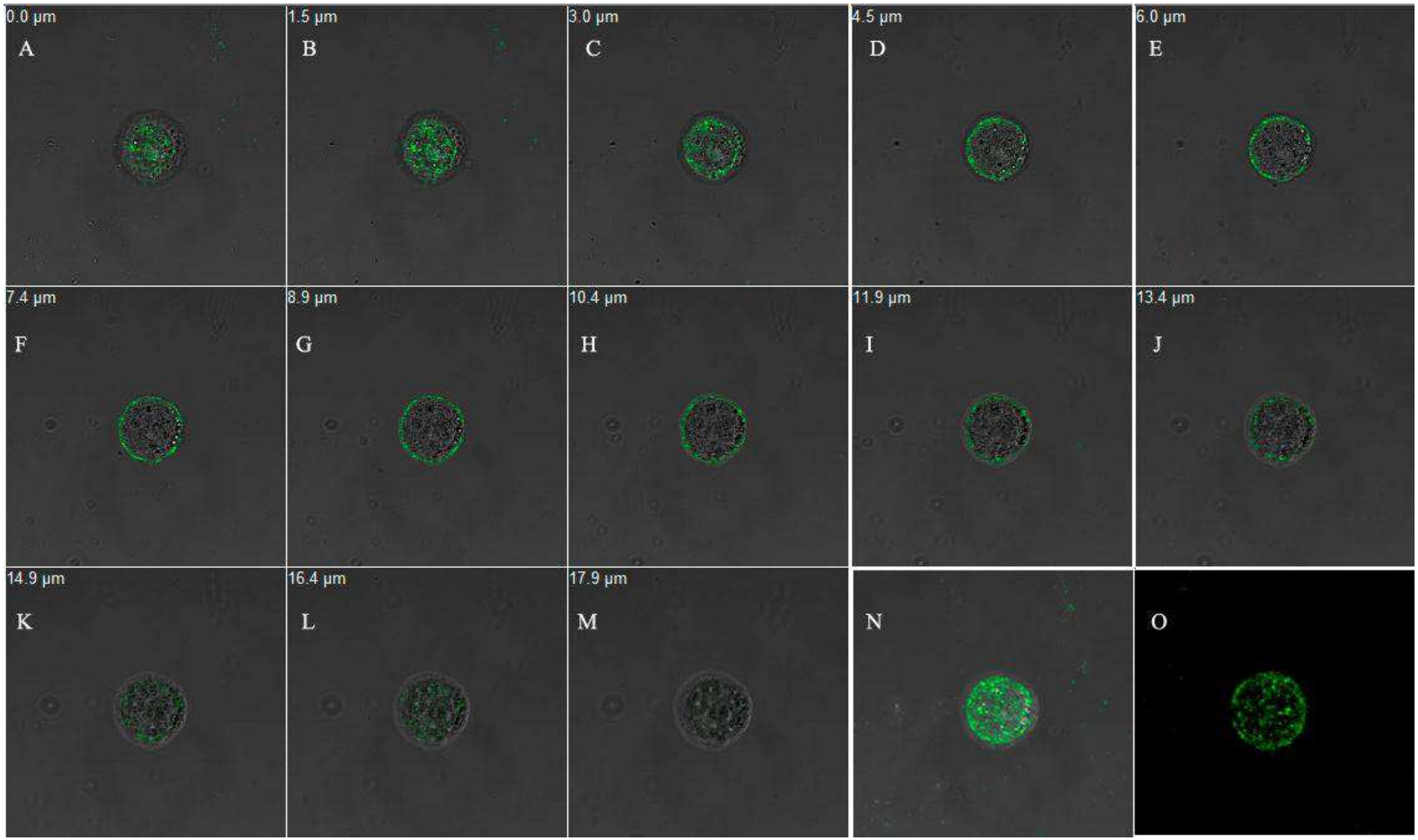

Figure 9 – Confocal images with slices in different focal planes (z Axis) showing the binding of PF2 clone in all extension of cell membrane and cytoplasm. Images were captured in phase contrast and in an excitation wavelength of 488 nm (FITC excitation) with magnification of 40x. Images from **A** to **M** are resulting from the overlap of fluorescence image and phase contrast. Image **N** is resulting from the merging of images **A** to **M**. Image **M** is resulting from the merging of images **A** to **M** using just the fluorescent capture.

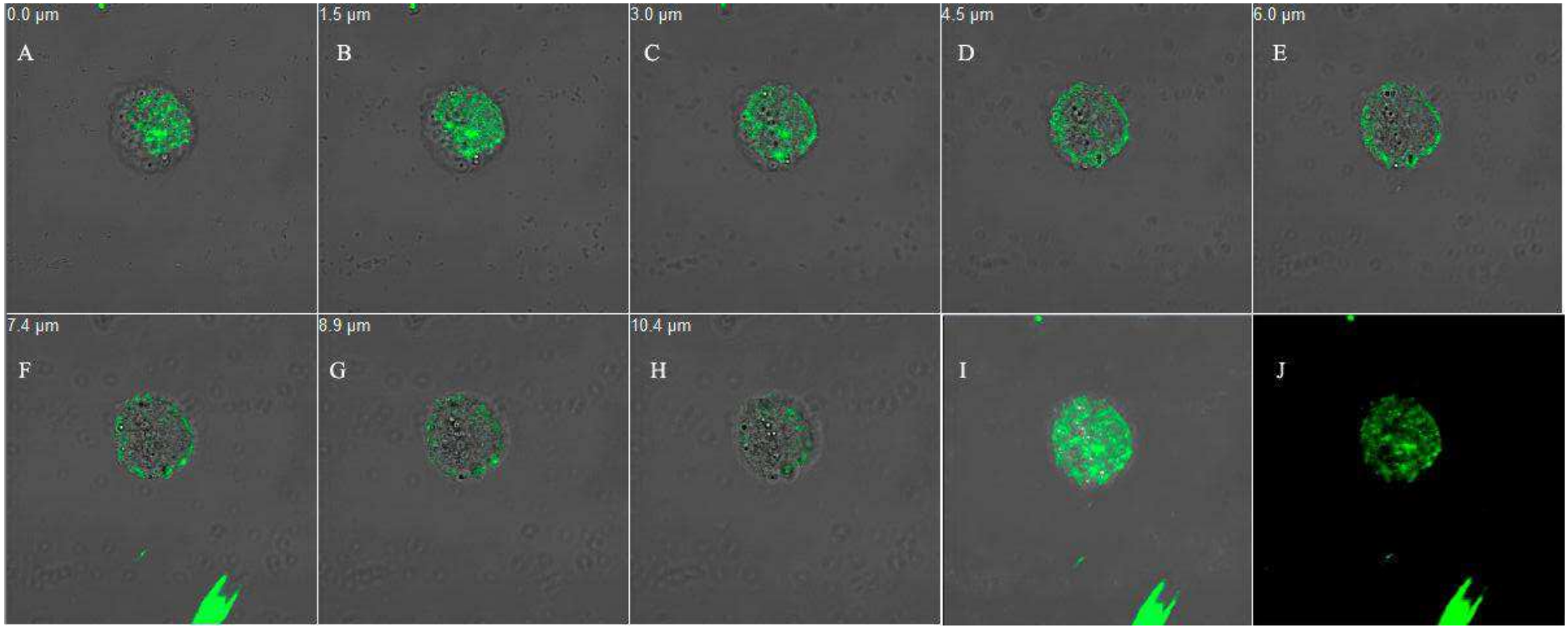

Figure 10 – Confocal images with slices in different focal planes (z Axis) showing the binding of PB12 clone in all extension of cell membrane and cytoplasm. Images were captured in phase contrast and in an excitation wavelength of 488 nm (FITC excitation) with magnification of 40x. Images from **A** to **H** are resulting from the overlap of fluorescence image and phase contrast. Image **I** is resulting from the merging of images **A** to **H**. Image **J** is resulting from the merging of images **A** to **H** using just the fluorescent capture.

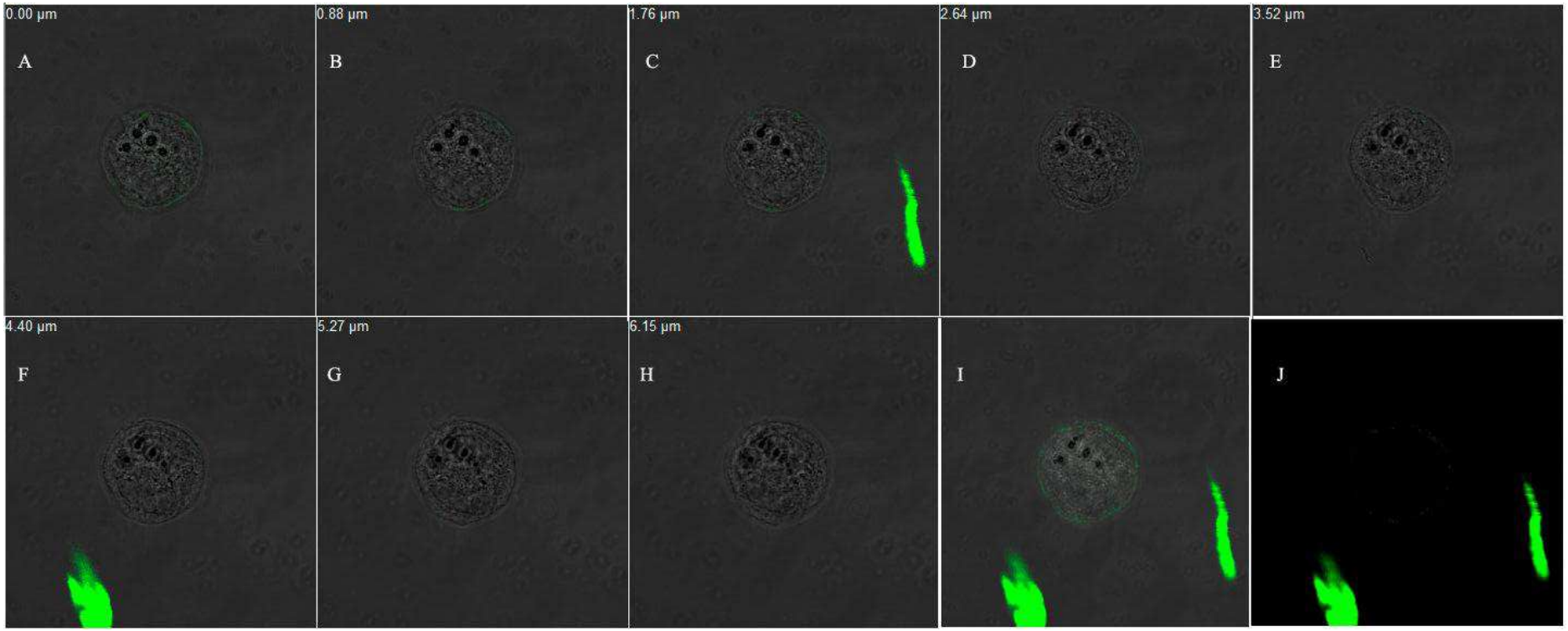

Figure 11 – Confocal images with slices in different focal planes (z Axis) showing the binding of wild-type phage in all extension of cell membrane and cytoplasm. Images were captured in phase contrast and in an excitation wavelength of 488 nm (FITC excitation) with magnification of 40x. Images from **A** to **H** are resulting from the overlap of fluorescence image and phase contrast. Image **I** is resulting from the merging of images **A** to **H**. Image **J** is resulting from the merging of images **A** to **H** using just the fluorescent capture.

3.6 *In vivo* imaging of PF2 clone indicates that the expressed peptide homes to tumor site

In order to confirm the tumor targeting ability of PF2 selected clone, an *in vivo* imaging experiment was performed. Comparing the in vivo imaging obtained with wild-type phage (Figure 12A) and PF2 clone (Figure 12B), it was verified a greater concentration of fluorescent particles in the tumor site (red circle) of PF2 treated mouse. The other markings observed out of tumor site are due to autofluorescence of some organs like intestine and testis, also observed in untreated animals. Results indicate that PF2 clone is able to target specifically tumor cells when administrated in the blood stream.

Molecules able to target drug delivery has raised much attention, once that it can direct the treatment specifically to tumor site, decreasing or inhibiting deleterious side-effects [20][21][3][22]. Some phage display selected peptides has already been conjugated to imaging agents, nanoparticles, oligonucleotides (siRNAs and antisenseRNA) and liposomes to target different tumor types and deliver molecules used in the therapeutic or imaging of tumors [23][24] [25][26][2][4][27]. In this paper, we have reported for the first time peptides ligand to TG180 cells. These peptides can be used to different biotechnological applications, once that this cell line is broadly used in biomedical research. The applications can achieve since tumor imaging or molecules delivery to the development of strategies to test the antitumoral activity of chemical compounds. For example, mice can be inoculated with TG180 cells and the development of solid tumors can be monitored during the treatment using labeled peptides. The peptides found in the present study can even be used in immunohistochemistry analyses of TG180 histological slides, allowing the differentiation of normal and tumoral cells. Furthermore, the described peptides can be evaluated in human sarcomas to verify the possibility of binding.

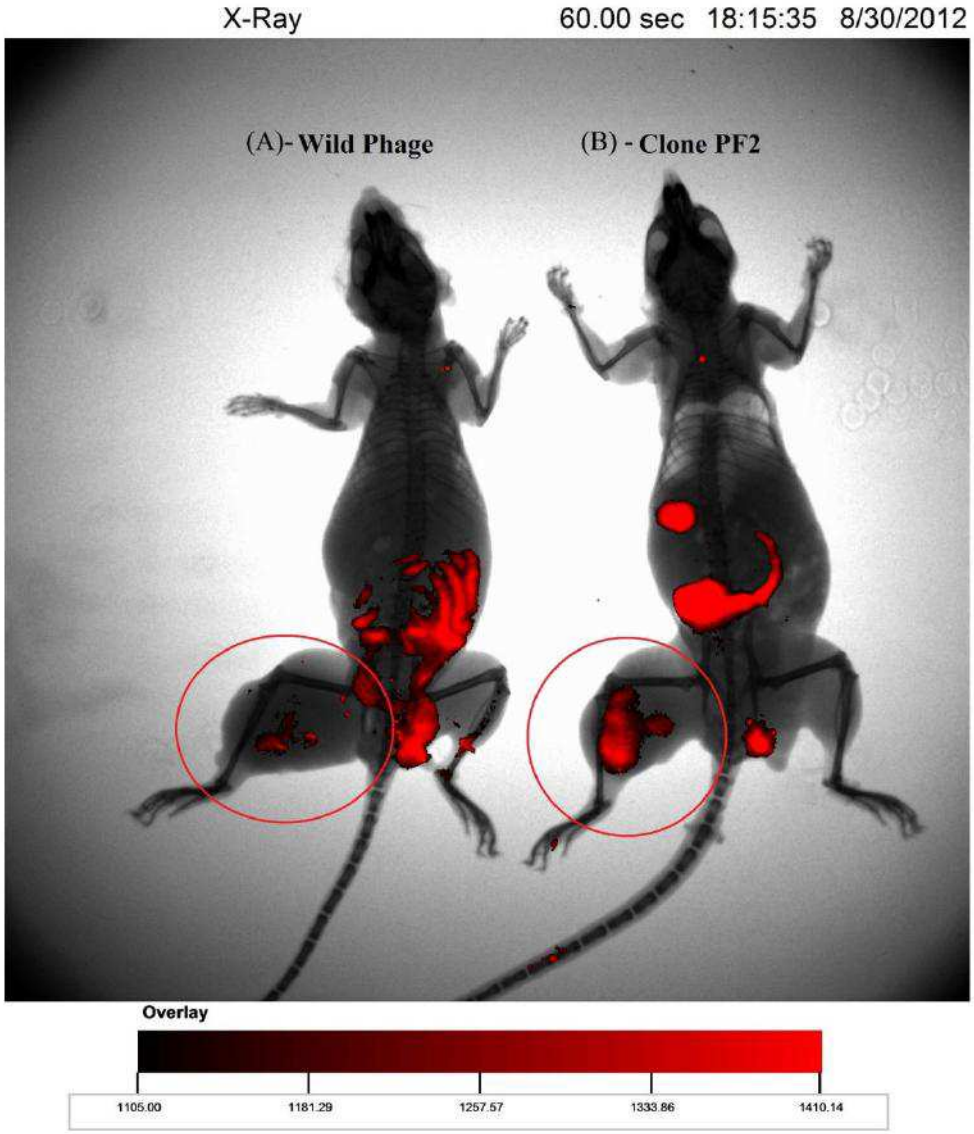

Figure 12 – In vivo imaging of tumors. Tumor bearing mice received intravenously 1,0 x 10^{12} pfu, mouse anti-M13 antibody and anti-Mouse IgG - Atto 647N (red fluorescence). The animal was subjected to fluorescence and X-ray imaging with the Kodak In-Vivo Imaging System FX Pro and the two images were merged for tumor localization. The red circles indicate tumor sites and the greater fluorescence observed in mouse that received PF2 clone in comparison to wild-type phage, shows the active targeting capability of the PF2 clone.

3.7 Liquid Chromatography Tandem Mass Spectrometry (LC-MS/MS) identifies the protein vimentin as the target molecule of phage clones

Phage clones expressing the selected peptides were immobilized on the surface of magnetic beads to perform immunoprecipitation of proteins with affinity to them. Beads-phage complexes were incubated with TG180 total

protein extract, submitted to immobilization in a magnetic apparatus and washed. Proteins which bound to phages were eluted, lyophilized and sequenced.

The LC-MS/MS analyzes has identified a total of twenty different proteins (Figure 13), among which just eight were derived from mouse. The presence of proteins from other species, like human cytokeratins and other proteins, probably is resulting from sample contamination during spectrometry or protein extraction protocols. Within mouse proteins, just vimentin showed a number of signed spectra in which 2 peptides derived from vimentin were identified in sample selected by the clone PF2 (Figure 14), 4 peptides in PB12 sample (figure 15) and no peptide derived from vimentin was identified in the sample selected by wild type phage (Figure 16). In the figure 13, the area marked in red represents the data from vimentin and it is possible to verify that both clones, PF2 and PB12, showed over than 95% of probability to have vimentin in the sequenced samples and this protein was not captured by wild-type phage. The other proteins did not achieved a conclusive number of valid spectra or, in the case of the protein named activated RNA polymerase II transcriptional coactivator p15, the number of spectra was very similar in all samples.

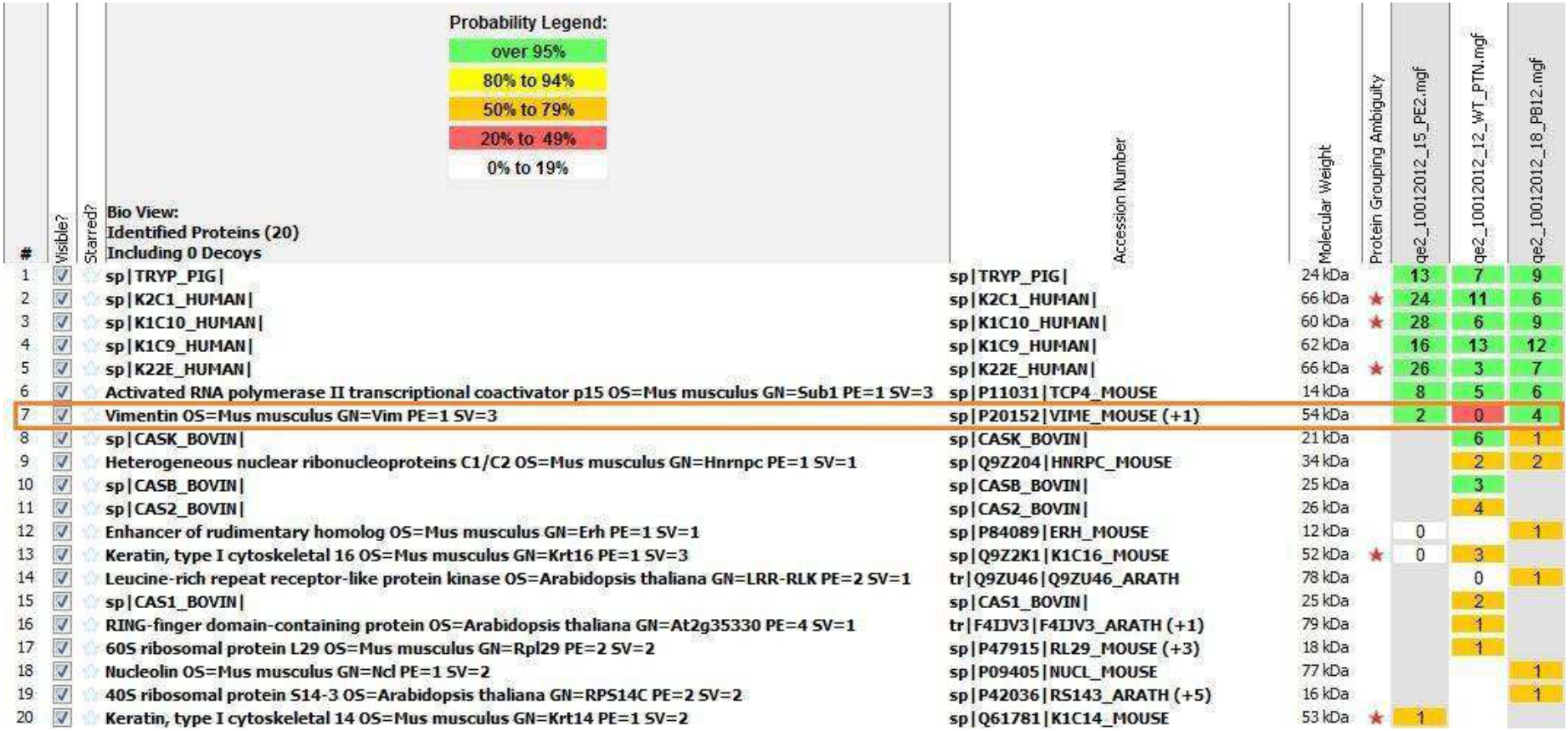

Probability Legend:

Probability
over 95%
80% to 94%
50% to 79%
20% to 49%
0% to 19%

#	Visible?	Starred?	Bio View: Identified Proteins (20) Including 0 Decoys	Accession Number	Molecular Weight	Protein Grouping Ambiguity	qe2_10012012_15_PE2.mgf	qe2_10012012_12_WT_PTN.mgf	qe2_10012012_18_PB12.mgf
1	☑	☆	sp|TRYP_PIG|	sp|TRYP_PIG|	24 kDa		13	7	9
2	☑	☆	sp|K2C1_HUMAN|	sp|K2C1_HUMAN|	66 kDa	★	24	11	6
3	☑	☆	sp|K1C10_HUMAN|	sp|K1C10_HUMAN|	60 kDa	★	28	6	9
4	☑	☆	sp|K1C9_HUMAN|	sp|K1C9_HUMAN|	62 kDa		16	13	12
5	☑	☆	sp|K22E_HUMAN|	sp|K22E_HUMAN|	66 kDa	★	26	3	7
6	☑	☆	Activated RNA polymerase II transcriptional coactivator p15 OS=Mus musculus GN=Sub1 PE=1 SV=3	sp|P11031|TCP4_MOUSE	14 kDa		8	5	6
7	☑	☆	Vimentin OS=Mus musculus GN=Vim PE=1 SV=3	sp|P20152|VIME_MOUSE (+1)	54 kDa		2	0	4
8	☑	☆	sp|CASK_BOVIN|	sp|CASK_BOVIN|	21 kDa			6	1
9	☑	☆	Heterogeneous nuclear ribonucleoproteins C1/C2 OS=Mus musculus GN=Hnrnpc PE=1 SV=1	sp|Q9Z204|HNRPC_MOUSE	34 kDa			2	2
10	☑	☆	sp|CASB_BOVIN|	sp|CASB_BOVIN|	25 kDa			3	
11	☑	☆	sp|CAS2_BOVIN|	sp|CAS2_BOVIN|	26 kDa			4	
12	☑	☆	Enhancer of rudimentary homolog OS=Mus musculus GN=Erh PE=1 SV=1	sp|P84089|ERH_MOUSE	12 kDa		0		1
13	☑	☆	Keratin, type I cytoskeletal 16 OS=Mus musculus GN=Krt16 PE=1 SV=3	sp|Q9Z2K1|K1C16_MOUSE	52 kDa	★	0	3	
14	☑	☆	Leucine-rich repeat receptor-like protein kinase OS=Arabidopsis thaliana GN=LRR-RLK PE=2 SV=1	tr|Q9ZU46|Q9ZU46_ARATH	78 kDa			0	1
15	☑	☆	sp|CAS1_BOVIN|	sp|CAS1_BOVIN|	25 kDa			2	
16	☑	☆	RING-finger domain-containing protein OS=Arabidopsis thaliana GN=At2g35330 PE=4 SV=1	tr|F4IJV3|F4IJV3_ARATH (+1)	79 kDa			1	
17	☑	☆	60S ribosomal protein L29 OS=Mus musculus GN=Rpl29 PE=2 SV=2	sp|P47915|RL29_MOUSE (+3)	18 kDa			1	
18	☑	☆	Nucleolin OS=Mus musculus GN=Ncl PE=1 SV=2	sp|P09405|NUCL_MOUSE	77 kDa				1
19	☑	☆	40S ribosomal protein S14-3 OS=Arabidopsis thaliana GN=RPS14C PE=2 SV=2	sp|P42036|RS143_ARATH (+5)	16 kDa				1
20	☑	☆	Keratin, type I cytoskeletal 14 OS=Mus musculus GN=Krt14 PE=1 SV=2	sp|Q61781|K1C14_MOUSE	53 kDa	★	1		

Figure 13 – Proteins identified by Liquid Chromatography Tandem Mass Spectrometry. Vimentin, the seventh protein marked in red is the unique to protein which presented a valid number of assigned spectra and was selected by PF2 and PB12 and was not selected by wild-type phage.

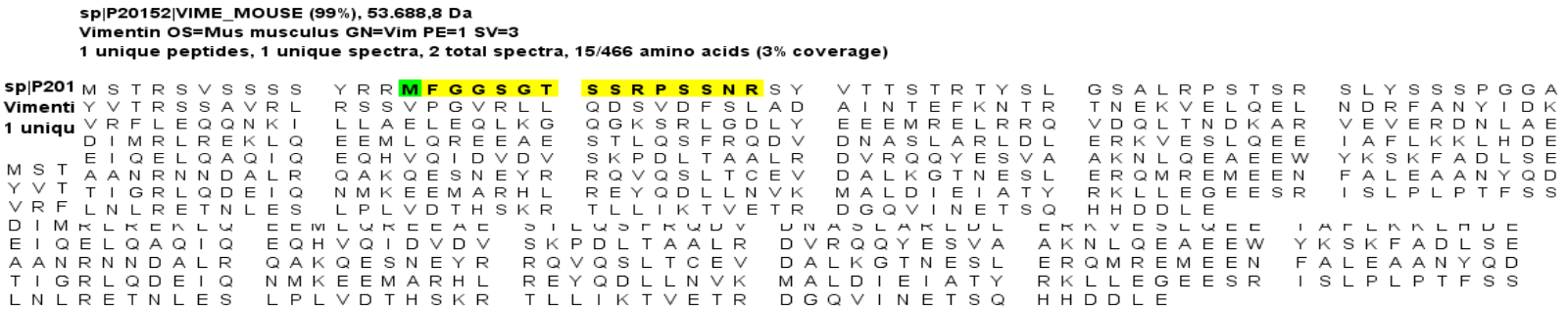

Figure 14 – Complete sequence of vimentin highlighting in yellow the sequence of peptides identified in the PF2 incubated sample.

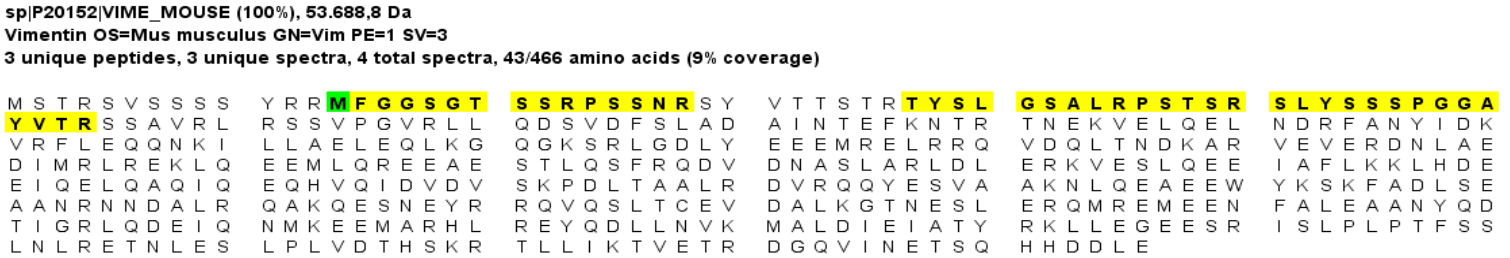

Figure 15 – Complete sequence of vimentin highlighting in yellow the sequence of peptides identified in the PB12 incubated sample.

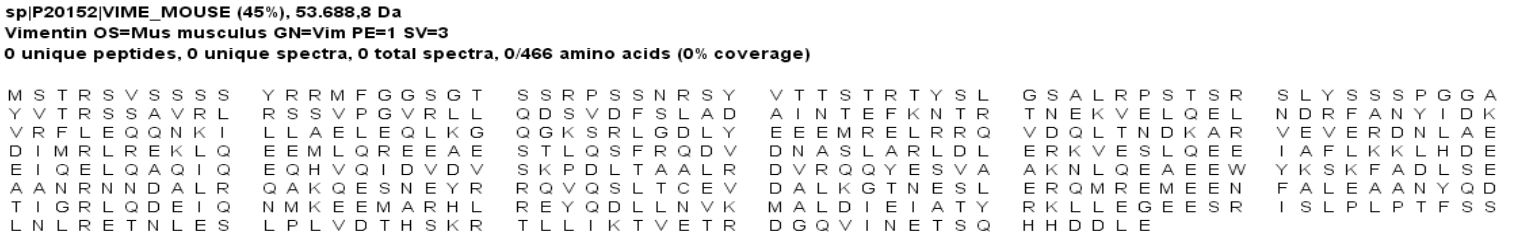

Figure 16 – Complete sequence of vimentin highlighting in yellow the sequence of peptides identified in the wild type phage incubated sample.

Vimentin is a type III intermediate filament that is ubiquitous in the cytoplasm of mesenchymal cells and is not usually expressed by epithelial cells. This intermediary filament is a cytosolic component responsible to many cellular functions as wound healing, cell–cell physical interactions, motility, contraction, migration, proliferation, protein synthesis, gene expression, apoptosis and signal transduction [28] [29] [30] [31]. Vimentin is considered as a specific marker for tumors of mesenchymal origin and is widely used as an immunohistochemical marker for sarcomas [32], once that soft tissue sarcomas express vimentin, but some epithelial cancers that exhibits epithelial to mesenchymal transition phenotypes also expresses this protein [31].

Vimentin expression has been evidenced in many tumors and it has been observed an association between vimentin expression and tumor development and progression. Vimentin has been identified as a key regulator and its over-expression has been associated with invasion and metastasis in a variety of human carcinomas as hepatocellular carcinoma cells, in prostate cancer, gastrointestinal tract cancers, breast cancer, Malignant melanoma, Central nervous system tumors, pancreatic ductal adenocarcinomas, lung cancer and other tumors [29][33][34][35][36].

Cytoskeletal proteins play essential roles in cancer cell proliferation, expansion, and metastasis. Thus, inhibiting the function of cytoskeletel proteins has become an important direction in research [32]. Vimentin, an important cytoskeletal constituent, has been considered a novel target to anticancer therapy and many anti-vimentin therapeutic approaches have been subject of many studies [31][32]. For example, Withaferin-A, a phytotherapic compound isolated from *Withania somnifera*, binds to vimentin, by covalently modifying its cysteine residue and induces inhibition of capillary growth in mouse model of corneal neovascularization and can be used for treating angioproliferative and malignant disease [37]. Silibinin, isolated from *Silybum marianum*, has shown strong anticancer efficacy against both androgen-dependent and androgen-independent prostate cancer. This phytochemical acts as an anti-metastatic agent via inhibiting invasion, motility and migration in novel, highly bone metastatic cells by down-regulating the vimentin and MMP-2 expression [38]

Many phage display peptides which bind to vimentin have already been described. Glaser-Gabay et al. (2011), identified a peptide with the sequence

SAHGTSTGVPWP that binds to vimentin and induces angiogenesis under hypoxic/ischemic conditions [39]. According to Satelli and Li, (2011) their group identified a novel linear peptide called comprehensive carcinoma homing peptide (CHP, sequence VNTANST) which binds to vimentin and possesses excellent targeting and homing properties, which make it a potentially useful tool in cancer treatment. They belive that vimentin is expressed on the surface of cancer cells and is internalized upon contact with specific ligands [36].

Vimentin is also a target to Human Immunodeficiency Virus (HIV) proteases. HIV-1 has been shown *in vitro* to cleave many cytoskeletal proteins during its cell infection, including vimentin, a known substrate for HIV-1 [40] [41]. The cleavage of vimentin by HIV-1 proteases is essential for inducing changes in chromatin organization and promotes distribution induced by HIV-1, turning this protein important in virus infection [42]. As in the present study it was observed that the selected peptides are able to bind to vimentin, future researches can be performed to verify if the binding of these peptides to vimentin affects anyway HIV infection.

The present work has also identified four promising peptides that target specifically murine sarcoma cells, in which two of them probably are vimentin ligands. Using immunofluorescence and immunohistochemistry techniques, it was possible to localize PF2 and PB12 peptides binding to the cell surface and to cell cytoplasm. As vimentin is an intermediate filament that composes the cytoskeleton, its location is expected to be restricted to the cytosolic portion of cells. However, vimentin has been shown to be a nuclear and extracellular protein, as well and although the mechanism of this transport remains unclear, there have been several reports of vimentin transport to the cell surface [36]. In epithelial malignant cells, immunohistochemistry technique has identified vimentin in the cytoplasm, perimembrane and membrane [35]. The exposed data support the vimentin marking pattern that was found in TG180 sarcoma cells.

Vimentin is known to interact with a large number of proteins and to participate in various cellular functions. Among proteins that interact with vimentin is the plectin, that promotes the integration of cytoplasm [43][36]. Plectin is a giant (500 kDa) multifunctional cytolinker that is abundantly expressed in a wide variety of mammalian cells and tissues, possessing a

vimentin-binding site [44]. As plectin is a ligand of vimentin, the peptides expressed by the two selected phage clones PF2 and PB12 were aligned to vimentin 3D-structure using the program Pepsurf (Figure 17 A and B). Both peptides aligned to the same domain of plectin in nearby regions (Figure 17 C). 3D structures of peptides expressed by PF2 (Figure 18) and PB12 (Figure 19) were determined using the program Molegro Molecular Viewer MMV 2011.2.2.0.

The peptide expressed by clone PF2 showed a perfect 3D alignment of seven from its twelve aminoacids, 1 showed mismatch and just 4 showed no match. PB12 peptide showed a perfect 3D alignment of eight from its twelve aminoacids, 4 showed mismatches and none showed no-match. Data obtained from alignment indicates that the surface characteristics of these peptides are equivalent to an epitope of plectin and the peptides can be mimetic to specific regions of this protein. The binding properties of peptides to vimentin can be resultant of the similarity found between plectin and the selected peptides. Computational docking simulations can elucidate the correct region where peptides are able to bind.

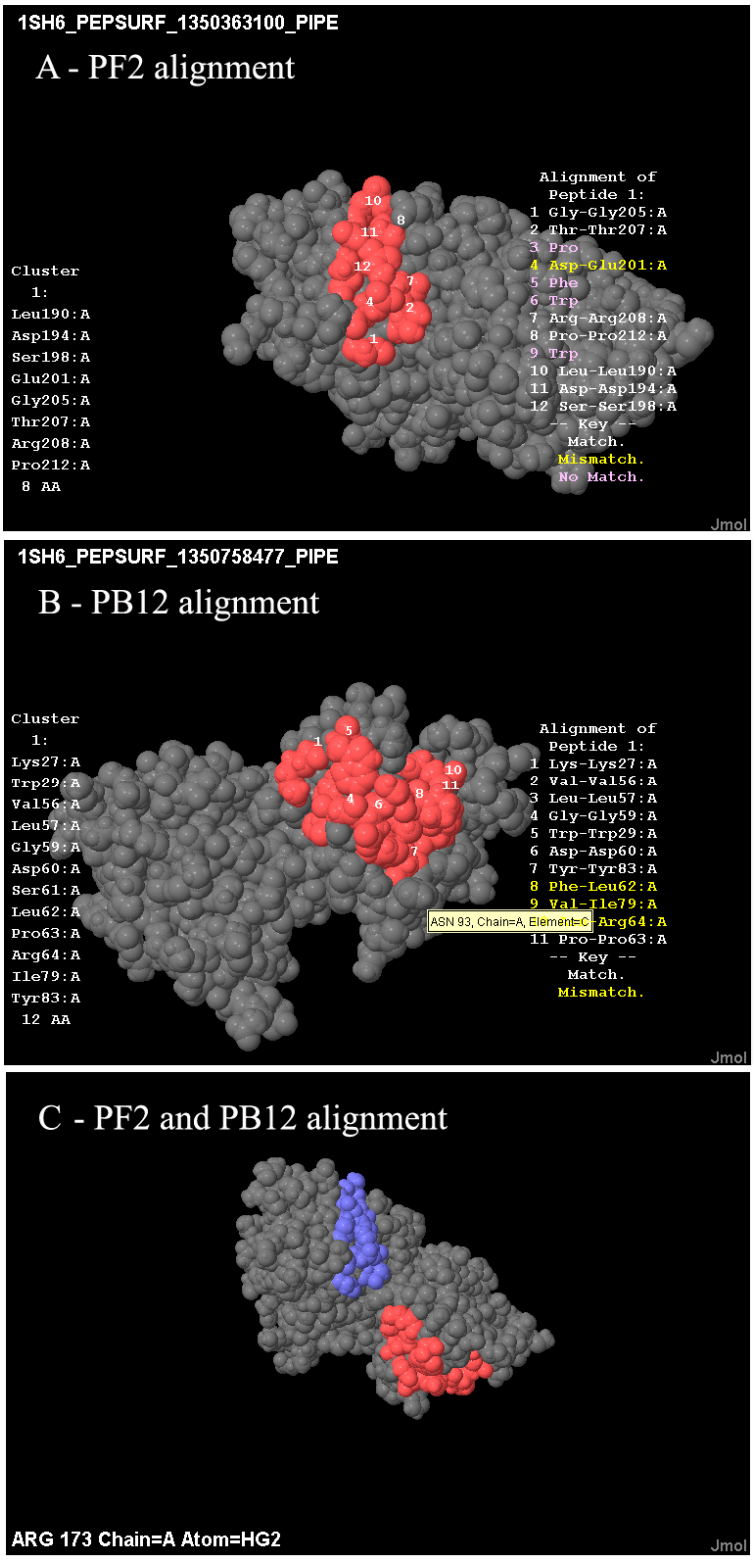

Figure 17 - Models of 3D structures predicted for the interaction between plectin and peptides expressed by PF2, PB12. A- PF2 peptide showing a perfect match of 7 aminoacids. B- PB12 peptide showing a perfect match of 8 aminoacids. C- Alignment of both peptides in plectin, showing the proximity between the aligned regions.

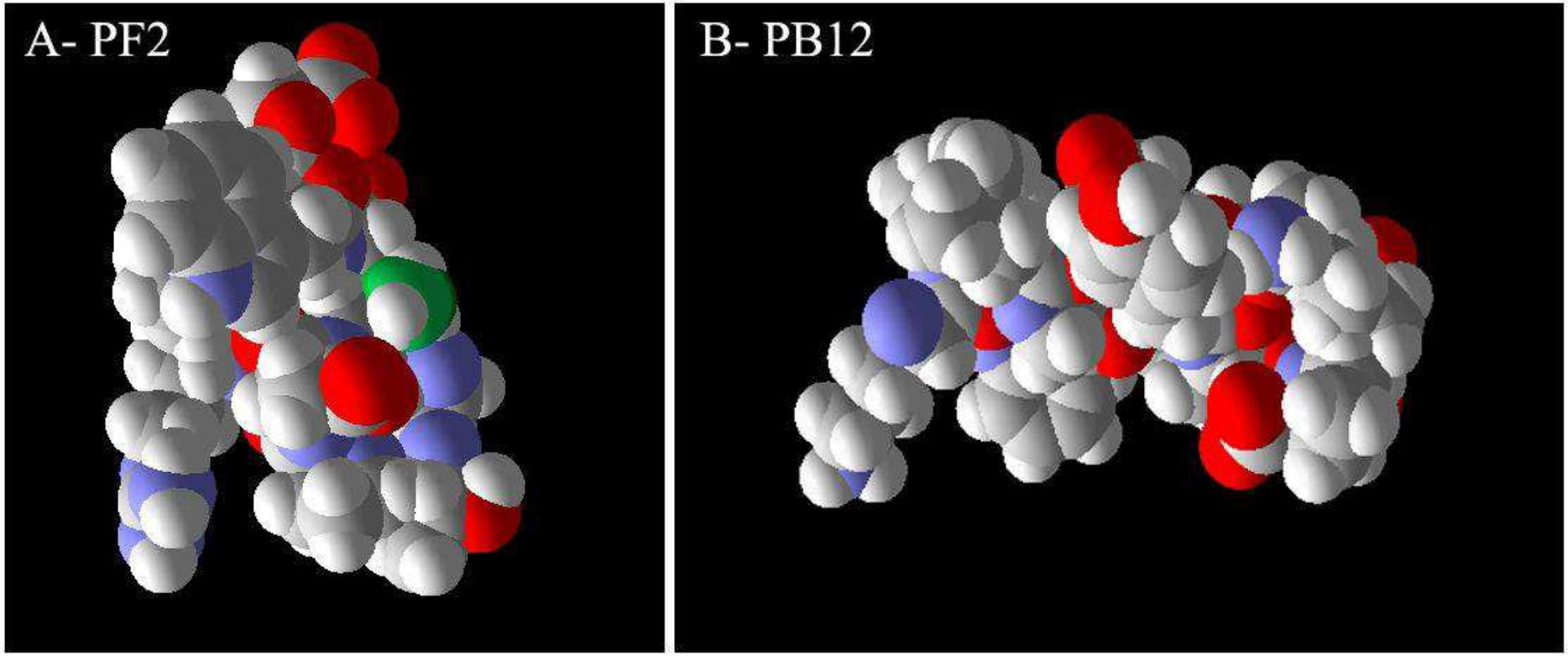

Figure 18 – Models of 3D structures predicted by the peptides PF2 (A) and PB12 (B) using the program Molegro Molecular Viewer.

4. Conclusions

Using an *in vitro* functional screening protocol we have isolated peptides that are selective for TG180 sarcoma cell line. We have demonstrated the ability of the PF2 and PB12 peptides to target solid tumors using *in vivo* imaging. It was also predicted the probable interaction between the selected clones and its target protein, vimentin, an important protein evolved in tumor progression. The peptides identified in the present study are promising in the development of tumor homing and imaging strategies.

5. References

1. Willats, W. G. T. Phage display: practicalities and prospects. *Plant molecular biology* **2002**, *50*, 837-54.

2. Deutscher, S. L. Phage Display in Molecular Imaging and Diagnosis of Cancer. **2011**, *110*, 3196-3211.

3. Francisco, S. S. Phage display in pharmaceutical biotechnology Sachdev S Sidhu. **2000**, 610-616.

4. Sun, N.; Aileen, S.; Willbold, D. Mirror image phage display – Generating stable therapeutically and diagnostically active peptides with biotechnological means. *Journal of Biotechnology* **2012**, *161*, 121-125.

5. Cao, Q.; Liu, S.; Niu, G.; Chen, K.; Yan, Y.; Liu, Z.; Chen, X. Phage display peptide probes for imaging early response to bevacizumab treatment. **2011**, 1103-1112.

6. Newton-Northup, J. R.; Figueroa, S. D.; Quinn, T. P.; Deutscher, S. L. Bifunctional phage-based pretargeted imaging of human prostate carcinoma. *Nuclear medicine and biology* **2009**, *36*, 789-800.

7. Sun, X.; Niu, G.; Yan, Y.; Yang, M.; Chen, K.; Ma, Y.; Chan, N. Phage Display − Derived Peptides for Osteosarcoma Imaging Phage Display – Derived Peptides for Osteosarcoma Imaging. *Clinical Cancer Research* **2010**, *16*, 4268-4277.

8. Corti, A.; Pastorino, F.; Curnis, F.; Arap, W.; Ponzoni, M.; Pasqualini, R. Targeted Drug Delivery and Penetration Into Solid Tumors. *molecules* **2011**, *16*, 857-887.

9. Molek, P.; Strukelj, B.; Bratkovic, T. Peptide Phage Display as a Tool for Drug Discovery: Targeting Membrane Receptors. **2011**, 857-887.

10. Du, Y.-zhong; Cai, L.-li; Liu, P.; You, J.; Yuan, H.; Hu, F.-qiang Biomaterials Tumor cells-specific targeting delivery achieved by A54 peptide functionalized polymeric micelles. *Biomaterials* **2012**, *33*, 8858-8867.

11. Lundberg, P.; Su, T.; Cpps, C.-penetrating Delivery of short interfering RNA using endosomolytic cell-penetrating peptides. *The FASEB Journal* **2007**, *21*, 2664-2971.

12. Fougerolles, A. R. D. E. Delivery Vehicles for Small Interfering RNA In Vivo. *HUMAN GENE THERAPY* **2008**, *132*, 125-132.

13. Pita, J. C. L. R.; Xavier, A. L.; de Sousa, T. K. G.; Mangueira, V. M.; Tavares, J. F.; de Oliveira Júnior, R. J.; Veras, R. C.; Pessoa, H. D. L. F.; da Silva, M. S.; Morelli, S.; Ávila, V. D. M. R.; da Silva, T. G.; Diniz, M. D. F. F. M.; Castello-Branco, M. V. S. In vitro and in vivo antitumor effect of trachylobane-360, a diterpene from Xylopia langsdorffiana. *Molecules (Basel, Switzerland)* **2012**, *17*, 9573-89.

14. Barbas, C. F. I.; Burton, D. R.; Scott, J. K.; Silverman, G. J. *Phage Display: A Laboratory Manual*; first.; Cold Spring Harbor Laboratory Press: New york, 2001; p. 736.

15. Ferro, E. a; Bevilacqua, E.; Favoreto-Junior, S.; Silva, D. a; Mortara, R. a; Mineo, J. R. Calomys callosus (Rodentia : Cricetidae) trophoblast cells as host cells to Toxoplasma gondii in early pregnancy. *Parasitology research* **1999**, *85*, 647-54.

16. Zang, L.; Shi, L.; Guo, J.; Pan, Q.; Wu, W.; Pan, X.; Wang, J. Screening and identification of a peptide specifically targeted to NCI-H1299 from a phage display peptide library. *Cancer letters* **2009**, *281*, 64-70.

17. Huang, J.; Ru, B.; Zhu, P.; Nie, F.; Yang, J.; Wang, X.; Dai, P.; Lin, H.; Guo, F.-B.; Rao, N. MimoDB 2.0: a mimotope database and beyond. *Nucleic acids research* **2012**, *40*, D271-7.

18. Ru, B.; Huang, J.; Dai, P.; Li, S.; Xia, Z.; Ding, H.; Lin, H.; Guo, F.; Wang, X. MimoDB: a new repository for mimotope data derived from phage display technology. *Molecules (Basel, Switzerland)* **2010**, *15*, 8279-88.

19. Langer M, B.-S. A. Peptides as carrier for tumor diagnosis and treatment. *Curr Med Chem Anticancer Agents* **2001**, *1*, 71-93.

20. Azzazy, H. M. E.; Highsmith, W. E. Phage display technology: clinical applications and recent innovations. *Clinical biochemistry* **2002**, *35*, 425-45.

21. Benhar, I. Biotechnological applications of phage and cell display. *Biotechnology advances* **2001**, *19*, 1-33.

22. Rosenkranz, B. Biomarkers and surrogate endpoints in clinical drug development. *APPLIED CLINICAL TRIALS* 30-35.

23. Key, J.; Dhawan, D.; Knapp, D. W.; Kim, K.; Kwon, I. C.; Choi, K.; Leary, J. F. Design of peptide-conjugated glycol chitosan nanoparticles for near infrared fluorescent (NIRF) in vivo imaging of bladder tumors. *Proc. of SPIE* **2012**, *8233*, 1-10.

24. Yi, H.; Ghosh, D.; Ham, M.-H.; Qi, J.; Barone, P. W.; Strano, M. S.; Belcher, A. M. M13 phage-functionalized single-walled carbon nanotubes as nanoprobes for second near-infrared window fluorescence imaging of targeted tumors. *Nano letters* **2012**, *12*, 1176-83.

25. Jeong, M.-H.; Kim, K.; Kim, E.-M.; Cheong, S.-J.; Lee, C.-M.; Jeong, H.-J.; Kim, D. W.; Lim, S. T.; Sohn, M.-H.; Chung, J. In vivo and in vitro evaluation of

Cy5.5 conjugated epidermal growth factor receptor binding peptide. *Nuclear medicine and biology* **2012**, *39*, 805-12.

26. Zhu, L.; Wang, H.; Wang, L.; Wang, Y.; Jiang, K.; Li, C.; Ma, Q.; Gao, S.; Wang, L.; Li, W.; Cai, M.; Wang, H.; Niu, G.; Lee, S.; Yang, W.; Fang, X.; Chen, X. High-affinity peptide against MT1-MMP for in vivo tumor imaging. *Journal of Controlled Release* **2011**, *150*, 248-255.

27. Svensen, N.; Walton, J. G. a; Bradley, M. Peptides for cell-selective drug delivery. *Trends in pharmacological sciences* **2012**, *33*, 186-92.

28. Steinmetz, N. F.; Cho, C.-F.; Ablack, A.; Lewis, J. D.; Manchester, M. Cowpea mosaic virus nanoparticles target surface vimentin on cancer cells. *Nanomedicine* **2012**, *6*, 351-364.

29. Iwatsuki, M.; Mimori, K.; Fukagawa, T.; Ishii, H.; Yokobori, T.; Sasako, M.; Baba, H.; Mori, M. The clinical significance of vimentin-expressing gastric cancer cells in bone marrow. *Annals of surgical oncology* **2010**, *17*, 2526-33.

30. Ivaska, J.; Pallari, H.-M.; Nevo, J.; Eriksson, J. E. Novel functions of vimentin in cell adhesion, migration, and signaling. *Experimental Cell Research* **2007**, *313*, 2050-2062.

31. Lahat, G.; Zhu, Q.-S.; Huang, K.-L.; Wang, S.; Bolshakov, S.; Liu, J.; Torres, K.; Langley, R. R.; Lazar, A. J.; Hung, M. C.; Lev, D. Vimentin is a novel anti-cancer therapeutic target; insights from in vitro and in vivo mice xenograft studies. *PloS one* **2010**, *5*, e10105.

32. Dong, B.; Zhu, Y. M. Molecular targeted therapy for cancer. *Chinese Journal of Cancer* **2010**, *29*, 340-345.

33. Pan, T.-L.; Wang, P.-W.; Huang, C.-C.; Yeh, C.-T.; Hu, T.-H.; Yu, J.-S. Network analysis and proteomic identification of vimentin as a key regulator associated with invasion and metastasis in human hepatocellular carcinoma cells. *Journal of proteomics* **2012**, *75*, 4676-92.

34. Wei, J.; Xu, G.; Wu, M.; Zhang, Y.; Li, Q.; Liu, P.; Zhu, T.; Song, A.; Zhao, L.; Han, Z.; Chen, G.; Wang, S.; Meng, L.; Zhou, J.; Lu, Y.; Ma, D. Overexpression of vimentin contributes to prostate cancer invasion and metastasis via src regulation. *Anticancer research* **2008**, *28*, 327-34.

35. Handra-Luca, a; Hong, S.-M.; Walter, K.; Wolfgang, C.; Hruban, R.; Goggins, M. Tumour epithelial vimentin expression and outcome of pancreatic ductal adenocarcinomas. *British journal of cancer* **2011**, *104*, 1296-302.

36. Satelli, A.; Li, S. Vimentin in cancer and its potential as a molecular target for cancer therapy. *Cellular and molecular life sciences : CMLS* **2011**, *68*, 3033-46.

37. Bargagna-Mohan, P.; Hamza, A.; Kim, Y.-eon; Khuan Abby Ho, Y.; Mor-Vaknin, N.; Wendschlag, N.; Liu, J.; Evans, R. M.; Markovitz, D. M.; Zhan, C.-G.; Kim, K. B.; Mohan, R. The tumor inhibitor and antiangiogenic agent withaferin A targets the intermediate filament protein vimentin. *Chemistry & biology* **2007**, *14*, 623-34.

38. Wu, K.-jie; Zeng, J.; Zhu, G.-dong; Zhang, L.-lin; Zhang, D.; Li, L.; Fan, J.-hai; Wang, X.-yang; He, D.-lin Silibinin inhibits prostate cancer invasion, motility and migration by suppressing vimentin and MMP-2 expression. *Acta pharmacologica Sinica* **2009**, *30*, 1162-8.

39. Glaser-Gabay, L.; Raiter, A.; Battler, A.; Hardy, B. Endothelial cell surface vimentin binding peptide induces angiogenesis under hypoxic/ischemic conditions. *Microvascular research* **2011**, *82*, 221-6.

40. Nkeze, J. Effects of HIV-1 protease on cellular functions and their potential applications in antiretroviral therapy. *Cell & Bioscience* **2012**, *2*, 1-19.

41. Snasel, J.; Shoeman, R.; Horejsı, M.; Hruskova-Heidingsfeldova, O.; Sedlacek, J.; Ruml, T.; Pichova, I. Cleavage of Vimentin by Different Retroviral Proteases. *Archives of Biochemistry and Biophysics* **2000**, *377*, 241–245.

42. Shoeman RL, Hüttermann C, Hartig R, T. P. Amino-terminal polypeptides of vimentin are responsible for the changes in nuclear architecture associated with

human immunodeficiency virus type 1 protease activity in tissue culture cells. *Mol Biol Cell* **2001**, *12*, 143–54.

43. Svitkina, T. M.; Verkhovsky, a B.; Borisy, G. G. Plectin sidearms mediate interaction of intermediate filaments with microtubules and other components of the cytoskeleton. *The Journal of cell biology* **1996**, *135*, 991-1007.

44. Winter, L.; Wiche, G. The many faces of plectin and plectinopathies: pathology and mechanisms. *Acta neuropathologica* **2012**.